Bachelor Thesis

Finite-Volume Methods for the Shallow-Water Equations

presented by
Leon Jakobi

supervised by
Prof. Dr. Christian Klingenberg

Julius-Maximilians-Universität Würzburg
Senior Professorship at the Institute of Mathematics
Mathematical Fluid Mechanics
Campus Hubland Nord
97074 Würzburg

Würzburg, June 2024

Contents

Abstract

The present thesis serves as an introduction to modeling with the shallow-water equations. Besides their derivation within the framework of fluid mechanics, the numerical solution is addressed. To this end, finite-volume methods are employed which will be introduced and discussed on the basis of said system of differential equations. Simulations of real-world applications (e. g. the propagation of earthquake-generated tsunami waves) help to illustrate the practical utility of the mathematical model.

Zusammenfassung

Die vorliegende Arbeit dient als Einführung in die Modellierung mit den Shallow-Water-Gleichungen. Neben deren Herleitung im Rahmen der Strömungsmechanik wird insbesondere auch die numerische Lösung thematisiert. Hierfür kommen Finite-Volumen-Verfahren zum Einsatz, die anhand ebenjenes Differentialgleichungssystems eingeführt und diskutiert werden. Simulationen von Anwendungsbeispielen (z. B. die Ausbreitung von durch Erdbeben verursachten Tsunamiwellen) illustrieren den praktischen Nutzen des mathematischen Modells.

Acknowledgments

It is my pleasure to thank all those who have helped me during the writing process of this thesis. First and foremost I must thank my supervisor Prof. Dr. Christian Klingenberg. He was the one who introduced me to the numerics of partial differential equations during a prior seminar. His trust and encouragement were important factors in the creation of this thesis.

I am also grateful to my parents who have supported me throughout my academic journey. They always left me the liberty to explore my own interests and were there for me when I needed them. An equal amount of gratitude goes to my friends and especially my girlfriend. It is their company that has kept me sane all these years. I am sure of it.

Finally, I must thank Lea Demmler who proofread this thesis. Its readability is owed in large parts to her invaluable notes.

Introduction

> *It must be [...] one of the race's most persistent and comforting hallucinations to trust that "it can't happen here" — that one's own time and place is beyond cataclysm.*
>
> John Wyndham, *The Day of the Triffids*

Solving a partial differential equation is one of the most common tasks in applied mathematics. The required numerical computations are therefore of great importance. This thesis is intended as a case study. It investigates one such model from start to finish — from its derivation to its theoretical analysis and its numerical solution. The shallow-water equations are a set of partial differential equations that govern the movement of certain types of waves. The flow of water is, generally speaking, a very difficult task to handle on a computer. In this context, the shallow-water framework provides practitioners with a relatively simple model which retains enough detail to produce viable results in many cases. Its applications are widespread, but among the most famous ones are the simulation of tsunami waves and the waves which result from the failure of a dam wall.

Tsunamis have plagued Japan more than any other country on earth. On March 11, 2011 a magnitude 9 earthquake was detected about 70 kilometers outside of the Oshika peninsula. The resulting flood wave displaced over 160 000 people and left over 2 000 dead. The "Great East Japan Earthquake" as it is called today also famously resulted in the Fukushima nuclear incident. The troubled relationship of the Japanese people with the sea is mirrored in many works of art. One of these is Hokusai's *The Great Wave off Kanagawa* which graces this thesis' cover [14].

In 1941, the Red Army blew up the strategically important Dnipro dam near Zaporizhzhia in Ukraine. The subsequent inundation was supposed to impede the advance of the German Wehrmacht. The flooding killed somewhere between 20 and 100 thousand people, mostly local civilians. Over 80 years later the destruction of dams is still an important part of military warfare. Recently the very same dam has come under fire again. This time by Russian forces as part of the Russo-Ukrainian War.

These disasters have shown the need for better preventative measures, the need for evacuation plans and inundation maps. With the help of modern-day processors, mathematical models can lead to simulations which aid in these tasks. It would be hubris, however, to assume that such calculations are all that it takes. Unpredictability will always remain a large part of our relationship with water. And we should not do ourselves the disservice of underestimating nature's power.

The structure of this thesis is as follows. It is split into three chapters and 13 sections. I have tried my best to write each section as independently of the rest as possible. The text should be accessible to all those with a strong background in linear algebra and multidimensional real analysis. What theoretical knowledge is required beyond that is collected in chapter I. The second chapter introduces the reader to the shallow-water equations. They are derived in detail, starting from the Euler equations. In addition, extensions to this model and real-world applications are discussed. Chapter III describes the numerical solution of conservation laws. It showcases the fundamental idea of finite-volume methods with Godunov flux, presents a simple approximate Riemann solver and treats the incorporation of source terms. The thesis concludes with numerical simulations.

Chapter I

Theoretical Background

This chapter briefly presents the necessary theoretical notions for the remainder of this thesis. We will assume that the reader is already somewhat familiar with most of these concepts. Should this not be the case, relevant literature will be referenced throughout.

Section 1 gives a short introduction to the class of problems at the heart of this thesis: differential equations. We then recall some fundamental facts and definitions from vector analysis in section 2, including but not limited to Gauss' integral theorem. The final section 3 discusses an important class of partial differential equations to which the titular shallow-water equations belong.

1 Differential Equations

Let us begin by recalling the standard terminology that is associated with differential equations. A more thorough exploration can be found in any introductory textbook on partial differential equations like that of Olver [25] or Evans [9].

A *differential equation* introduces a relationship between a function and its derivatives. Since the function itself is not known, the goal is to deduce it from the relation that the differential equation provides. This process of finding solution functions is what we refer to as *solving* the differential equation. For better illustration, we list some examples:

(a) $\dfrac{\mathrm{d}u}{\mathrm{d}t}(t) = u(t);$

(b) $\left[\dfrac{\mathrm{d}^2u}{\mathrm{d}t^2}(t)\right]^2 = 2t\dfrac{\mathrm{d}u}{\mathrm{d}t}(t) + \sin(t)u(t);$

(c) $\dfrac{\partial u}{\partial t}(x,t) + \dfrac{\partial u}{\partial x}(x,t) = 0;$

(d) $\dfrac{\partial u}{\partial t}(x,t) = \dfrac{\partial^2 u}{\partial x^2}(x,t) + \sin(t)\left[\dfrac{\partial^2 u}{\partial t \partial x}(x,t)\right]^2.$

In all of the examples above we are looking for functions u such that the corresponding relation is fulfilled for all t or (x,t) in a specified region, e. g. on $]0,\infty[$ for (a) and (b) or on $\mathbb{R}\times]0,\infty[$ for (c) and (d). So a clearer notation of (c) might be

$$\frac{\partial u}{\partial t}(x,t) + \frac{\partial u}{\partial x}(x,t) = 0 \qquad \text{for all } (x,t) \in \mathbb{R}\times]0,\infty[\,. \tag{1.1}$$

Obviously, the function u has to be defined in a way that this makes sense, e. g. $u : D \to \mathbb{R}$ for an open set $D \subseteq \mathbb{R}^2$ with $\mathbb{R}\times]0,\infty[\subseteq D$ for (1.1). This also includes the differentiability

of u to at least the degree that the differential equation requires. If the function u depends on just one variable (like in (a) and (b)), we call the differential equation *ordinary*, otherwise we speak of a *partial* differential equation. This thesis will focus almost exclusively on the latter type.

Writing down many and long differential equations becomes cumbersome very quickly and hence shorter notations have been developed: The variables that u depends on can almost always be inferred from the derivatives that appear, so we will usually omit them when no confusion is to be expected. The variable t will typically represent time while x, y, z will be stand-ins for space. With this convention (c) turns into

$$\frac{\partial u}{\partial t} + \frac{\partial u}{\partial x} = 0.$$

In addition, a more compact derivative notation is often employed where the subscript indicates the differentiation. With this notation (d) simplifies to

$$u_x = u_{xx} + \sin(t)(u_{xt})^2.$$

We will switch between these conventions as needed.

Differential equations are commonly classified by *order*, i. e., by the highest-order derivative that appears. Example (c) is of first and example (d) of second order. Most applications get by with orders one or two. Some problems may also require order three or four, but everything higher is quite rare.

When several differential equations for possibly several functions come together, we speak of a *system* of differential equations. In section 8 we will encounter the system ($(x,t) \in \mathbb{R} \times]0, \infty[$)

$$\begin{aligned} h_t + (hu)_x &= 0, \\ (hu)_t + (hu^2 + \tfrac{1}{2}gh^2)_x &= 0 \end{aligned} \tag{1.2}$$

for real-valued functions $(x,t) \mapsto h(x,t)$ and $(x,t) \mapsto u(x,t)$ where $g \in \mathbb{R}$ is a known constant. By introducing the right vectors, a system can usually be converted into a more simple vector-valued differential equation, if we differentiate vectors componentwise. In the case of the system (1.2) we could, for example, define two functions in $\mathbb{R}^2$ via

$$\boldsymbol{q}(x,t) := \begin{pmatrix} q_1(x,t) \\ q_2(x,t) \end{pmatrix} := \begin{pmatrix} h(x,t) \\ h(x,t)u(x,t) \end{pmatrix}$$

and

$$\boldsymbol{f}(\boldsymbol{q}) := \begin{pmatrix} f_1(q) \\ f_2(q) \end{pmatrix} := \begin{pmatrix} q_2 \\ \frac{(q_2)^2}{q_1} + \frac{1}{2}g(q_1)^2 \end{pmatrix} = \begin{pmatrix} h(x,t)u(x,t) \\ h(x,t)\left[u(x,t)\right]^2 + \frac{1}{2}g\left[h(x,t)\right]^2 \end{pmatrix}$$

to transform it into the system

$$\boldsymbol{q}_t + \boldsymbol{f}(\boldsymbol{q})_x = \boldsymbol{0}.$$

This is the standard form of a so-called *conservation law* which will be discussed in detail in section 3. Throughout this thesis vectors will be set in bold to distinguish them from their scalar counterparts.

Notice that a differential equation can be *linear*, i. e., the derivative functions all appear by themselves like in (c) instead of in products or more complicated combinations like in

(1.2). Otherwise they are called *nonlinear*. The benefit of linear differential equations is that a linear combination of two particular solution functions has to be a solution itself.

It is customary to group differential equations into three classes. This can be done for more general (nonlinear) systems, but we will illustrate the idea for a scalar linear second-order partial differential equation

$$au_{tt} + bu_{tx} + cu_{xx} + du_t + eu_x + fu = g, \tag{1.3}$$

where a, b, c, d, e, f and u are functions of x and t and so is g. If the so-called *forcing function* g vanishes, then the differential equation is called *homogeneous*. In order for (1.3) to actually be of second order at least one of the three functions a, b, c should not vanish everywhere. Now the so-called *discriminant*

$$\Delta := b^2 - 4ac$$

can be defined and with it we distinguish the following cases: The equation (1.3) at a point (x, t) is called

- *hyperbolic*, if $\Delta(x, t) > 0$,
- *parabolic*, if $\Delta(x, t) = 0$ with $a^2 + b^2 + c^2 \neq 0$, and
- *elliptic*, if $\Delta(x, t) < 0$.

The names arise by studying the related quadratic equation

$$ax^2 + bxy + cy^2 + dx + ex + fy + g = 0.$$

It is well-known that the resulting curves in the x-y-plane are conic sections and that for $\Delta > 0$ these are hyperbolas, for $\Delta = 0$ they are parabolas and for $\Delta < 0$ one finds ellipses. It should be clear that not all differential equations obey this sorting process, but most applications require one of these types. Since a, b and c will generally not be constant, it is possible for the type of a differential equation to change with position and time. However, this case is relatively uncommon. Typically, the motion of waves is modeled with hyperbolic systems, making them the focus of this thesis. The most famous parabolic equation is the *heat equation* which describes how bodies heat up and cool down. Elliptic problems arise, for example, in electrostatics in the form of the *Laplace* or the *Poisson equation*.

Notice that a differential equation by itself can have many solutions, e. g. it is easy to see that both $t \mapsto \exp(t)$ and $t \mapsto 2\exp(t)$ satisfy equation (a). This illustrates why one typically adds some initial or boundary values to (hopefully) force the solution to be unique. For example, if we add the initial condition

$$u(0) = 1$$

to (a), then $t \mapsto \exp(t)$ turns out to be the only solution (by the Picard-Lindelöf theorem). For partial differential equations this same idea is somewhat more complicated. Here the initial data naturally needs to be an entire function u_0, e. g.

$$u(x, 0) = u_0(x).$$

A differential equation together with an initial condition is called an *initial value problem* (or *Cauchy problem*). Boundary values will only play a role in this thesis for certain numerical considerations.

All of these discussions are in vain, if no solution(s) exists to begin with. The existence and uniqueness of solutions to differential equations (with appropriate boundary or initial conditions) is its own subject of research. For some equations that arise in practice one can show such theorems, usually with the help of heavy mathematical machinery. Unfortunately, for many important differential equations no existence and uniqueness results have been found (yet). Famously, this question in the special case of the *Navier-Stokes equations* (which we will encounter in section 5) is one of the Clay Institute of Mathematics' *millenium problems*. For practical purposes (and thereby for this thesis), these theoretical questions luckily pose no hurdle. After all, if a partial differential equation that was derived using nothing but simple laws of nature would not admit a (unique) solution, then mathematical modeling as a whole would be in all different kinds of trouble philosophically.

2 Vector Analysis

The appropriate mathematical framework for modeling fluid flow is the three-dimensional real space $\mathbb{R}^3$. This section will collect all of the relevant theorems and definitions surrounding the integration and differentiation of three-dimensional functions. They serve as the theoretical backdrop for the models of the following chapter. Most of this information can be found in any standard textbook on (vector) analysis. A compact introduction is given in [8] for example. It should be pointed out that we will use the typical notation from fluid dynamics in this text. This means (i) that vectors will be set in bold, e. g. $\boldsymbol{x} \in \mathbb{R}^3$, and (ii) that the components will usually be notated in accordance with the first component, e. g. $\boldsymbol{x} = (x, y, z)^{\mathrm{T}}$.

Let us begin by introducing the types of functions that this section will focus on.

Definition 2.1 *Let $\Omega \subseteq \mathbb{R}^3$ be a set. Then a vector-valued function $\boldsymbol{f} : \Omega \to \mathbb{R}^3$ is called a* vector field. *Its component functions are often notated as $\boldsymbol{f}(\boldsymbol{x}) = (f(\boldsymbol{x}), g(\boldsymbol{x}), h(\boldsymbol{x}))^{\mathrm{T}}$ where $\boldsymbol{x} = (x, y, z)^{\mathrm{T}} \in \Omega$. Similarly, a scalar-valued function $\phi : \Omega \to \mathbb{R}$ is called a* scalar field.

Typical examples of vector fields are velocity, gravitational or magnetic fields. Typical examples of scalar fields are temperature, pressure or density.

Recall that scalar fields can be integrated with the three-dimensional (Lebesgue) integral

$$\int_\Omega \phi(x, y, z)\,\mathrm{d}(x, y, z) = \int_\Omega \phi(\boldsymbol{x})\,\mathrm{d}\boldsymbol{x} \tag{2.1}$$

as long as Ω is (Lebesgue-)measurable and ϕ sufficiently well-behaved. Integrating vector fields comes down to integrating the component scalar fields like in (2.1), so

$$\int_\Omega \boldsymbol{f}(\boldsymbol{x})\,\mathrm{d}\boldsymbol{x} := \begin{pmatrix} \int_\Omega f(\boldsymbol{x})\,\mathrm{d}\boldsymbol{x} \\ \int_\Omega g(\boldsymbol{x})\,\mathrm{d}\boldsymbol{x} \\ \int_\Omega h(\boldsymbol{x})\,\mathrm{d}\boldsymbol{x} \end{pmatrix},$$

again given the (Lebesgue-)measurability of Ω and well-behavedness of f, g and h. Both types of integrals will be referred to as *volume integrals* for obvious reasons and $\mathrm{d}\boldsymbol{x} = \mathrm{d}(x, y, z)$ is called the *volume element*.

The notion of *surface integrals* will also play an important role. The first type that we require is the scalar-valued surface integral

$$\int_{\partial\Omega} \phi(x, y, z)\,\mathrm{d}s = \int_{\partial\Omega} \phi(\boldsymbol{x})\,\mathrm{d}s$$

where $\mathrm{d}s$ is the *scalar surface element*. In this context $\partial\Omega$ is the surface (the boundary, speaking in topological terms) of the volume Ω. We can also define a vectorized surface integral

$$\int_{\partial\Omega} \phi(x, y, z)\boldsymbol{n}(x, y, z)\,\mathrm{d}s = \int_{\partial\Omega} \phi(\boldsymbol{x})\boldsymbol{n}(\boldsymbol{x})\,\mathrm{d}s$$

where $\mathrm{d}\boldsymbol{s} := \boldsymbol{n}(\boldsymbol{x})\mathrm{d}s$ is the *vectorial surface element*. In this case $\boldsymbol{n}(\boldsymbol{x})$ is the unit normal

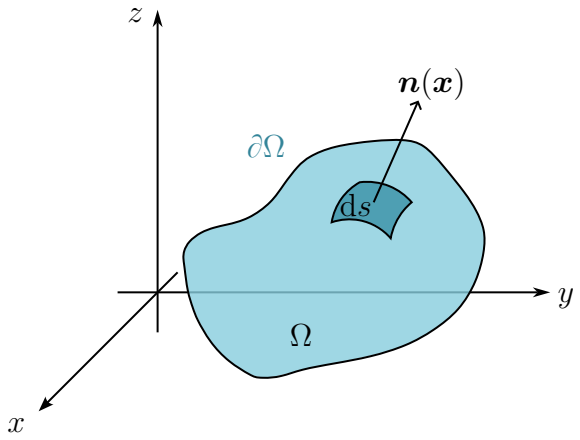

Figure 2.1: A volume Ω with boundary $\partial\Omega$, surface element $\mathrm{d}s$ and its outward normal $\boldsymbol{n}$ at $\boldsymbol{x} \in \partial\Omega$.

vector pointing out of Ω at a point $\boldsymbol{x} \in \partial\Omega$. It should be clear that this construction again requires certain conditions on both the shape of the set Ω and the function ϕ which we will not go into here.

Next, let us turn to differentiation. For a differentiable scalar field $\phi : \Omega \to \mathbb{R}$ on an open subset $\Omega \subseteq \mathbb{R}^3$ the *gradient* vector

$$\nabla\phi(\boldsymbol{x}) := \left(\frac{\partial\phi}{\partial x}(\boldsymbol{x}), \frac{\partial\phi}{\partial y}(\boldsymbol{x}), \frac{\partial\phi}{\partial z}(\boldsymbol{x})\right)^{\mathrm{T}}, \quad x \in \Omega$$

contains the partial derivatives. For vector fields $\boldsymbol{f} : \Omega \to \mathbb{R}^3$ with component functions $\boldsymbol{f} = (f, g, h)^{\mathrm{T}}$ where Ω is again open, we write

$$\operatorname{div} \boldsymbol{f}(\boldsymbol{x}) := \frac{\partial f}{\partial x}(\boldsymbol{x}) + \frac{\partial g}{\partial y}(\boldsymbol{x}) + \frac{\partial h}{\partial z}(\boldsymbol{x}), \quad x \in \Omega$$

for its *divergence*. If we notate the standard Euclidean inner product in $\mathbb{R}^3$ as $\boldsymbol{a}\cdot\boldsymbol{b} := \boldsymbol{a}^{\mathrm{T}}\boldsymbol{b} = \sum_{i=1}^{3} a_i b_i$ for two vectors $\boldsymbol{a} = (a_1, a_2, a_3)^{\mathrm{T}}$ and $\boldsymbol{b} = (b_1, b_2, b_3)^{\mathrm{T}}$, then we can think of taking the divergence as a scalar product of $\boldsymbol{f}$ with the formal vector $\nabla := (\partial/\partial x, \partial/\partial y, \partial/\partial z)^{\mathrm{T}}$,

the *nabla operator*. This suggests the notation $\nabla \cdot \boldsymbol{f} = \operatorname{div} \boldsymbol{f}$ which is commonly used in fluid dynamics.

Our first theorem converts volume into surface integrals.

Theorem 2.2 (Gauss integral theorem)
Let $D \subseteq \mathbb{R}^3$ be an open set, $\boldsymbol{f} : D \to \mathbb{R}^3$ a continuously-differentiable function and $\Omega \subseteq D$ a sufficiently well-behaved subset. If $\boldsymbol{n}(\boldsymbol{x})$ denotes the outward unit normal vector on $\boldsymbol{x} \in \partial\Omega$, then

$$\int_\Omega \nabla \cdot \boldsymbol{f}(\boldsymbol{x}) \,\mathrm{d}\boldsymbol{x} = \int_{\partial\Omega} \boldsymbol{f}(\boldsymbol{x}) \cdot \boldsymbol{n}(\boldsymbol{x}) \,\mathrm{d}s.$$

A proof can be found in [8, Satz 10.11.1].

As a direct consequence, we can show the following version of Gauss' integral theorem for the vector field induced by a scalar field's gradient.

Corollary 2.3 *Let $D \subseteq \mathbb{R}^3$ be an open set, $\phi : D \to \mathbb{R}$ a continuously-differentiable function and $\Omega \subseteq D$ a sufficiently well-behaved subset. Then*

$$\int_\Omega \nabla\phi(\boldsymbol{x}) \,\mathrm{d}\boldsymbol{x} = \int_{\partial\Omega} \phi(\boldsymbol{x})\boldsymbol{n}(\boldsymbol{x}) \,\mathrm{d}s,$$

where $\boldsymbol{n}(\boldsymbol{x})$ denotes the outward unit normal vector on $\boldsymbol{x} \in \partial\Omega$.

Proof: Let $\boldsymbol{c} := (c_1, c_2, c_3)^{\mathrm{T}} \in \mathbb{R}^3$ be a fixed constant. Notice that $\boldsymbol{x} \mapsto \phi(\boldsymbol{x})\boldsymbol{c}$ defines a vector field on D. Its divergence is given via

$$\begin{aligned}
\nabla \cdot \big(\phi(\boldsymbol{x})\boldsymbol{c}\big) &= \frac{\partial}{\partial x}\big(\phi(\boldsymbol{x})c_1\big) + \frac{\partial}{\partial y}\big(\phi(\boldsymbol{x})c_2\big) + \frac{\partial}{\partial z}\big(\phi(\boldsymbol{x})c_3\big) \\
&= c_1\frac{\partial\phi}{\partial x}(\boldsymbol{x}) + c_2\frac{\partial\phi}{\partial y}(\boldsymbol{x}) + c_3\frac{\partial\phi}{\partial z}(\boldsymbol{x}) \\
&= \boldsymbol{c} \cdot \nabla\phi(\boldsymbol{x})
\end{aligned}$$

because $\boldsymbol{c}$ is constant. Now we use the Gauss integral theorem 2.2 to find

$$\boldsymbol{c} \cdot \left[\int_\Omega \nabla\phi(\boldsymbol{x}) \,\mathrm{d}\boldsymbol{x}\right] = \int_\Omega \nabla \cdot \big(\phi(\boldsymbol{x})\boldsymbol{c}\big) \,\mathrm{d}\boldsymbol{x} = \int_{\partial\Omega} \big(\phi(\boldsymbol{x})\boldsymbol{c}\big) \cdot \boldsymbol{n}(\boldsymbol{x}) \,\mathrm{d}s = \boldsymbol{c} \cdot \left[\int_{\partial\Omega} \phi(\boldsymbol{x})\boldsymbol{n}(\boldsymbol{x}) \,\mathrm{d}s\right].$$

By setting $\boldsymbol{c}$ equal to the standard unit vectors $\boldsymbol{e}_1, \boldsymbol{e}_2$ and $\boldsymbol{e}_3$ in $\mathbb{R}^3$ we obtain the desired identity. ■

The last terminology of this section is that of an *outer product*: Given two vectors $\boldsymbol{a} = (a_1, a_2, a_3)^{\mathrm{T}}, \boldsymbol{b} = (b_1, b_2, b_3)^{\mathrm{T}} \in \mathbb{R}^3$ this object is a matrix in $\mathbb{R}^{3\times3}$ defined as

$$\boldsymbol{a} \otimes \boldsymbol{b} := \boldsymbol{a}\boldsymbol{b}^{\mathrm{T}} = (a_i b_j)_{i,j=1,2,3} = \begin{pmatrix} a_1b_1 & a_1b_2 & a_1b_3 \\ a_2b_1 & a_2b_2 & a_2b_3 \\ a_3b_1 & a_3b_2 & a_3b_3 \end{pmatrix}.$$

In this context the notation

$$\nabla \cdot \begin{pmatrix} a_{11} & a_{12} & a_{13} \\ a_{21} & a_{22} & a_{23} \\ a_{31} & a_{32} & a_{33} \end{pmatrix} := \begin{pmatrix} \nabla \cdot (a_{11}, a_{12}, a_{13})^{\mathrm{T}} \\ \nabla \cdot (a_{21}, a_{22}, a_{23})^{\mathrm{T}} \\ \nabla \cdot (a_{31}, a_{32}, a_{33})^{\mathrm{T}} \end{pmatrix} = \begin{pmatrix} \frac{\partial a_{11}}{\partial x} + \frac{\partial a_{12}}{\partial y} + \frac{\partial a_{13}}{\partial z} \\ \frac{\partial a_{21}}{\partial x} + \frac{\partial a_{22}}{\partial y} + \frac{\partial a_{23}}{\partial z} \\ \frac{\partial a_{31}}{\partial x} + \frac{\partial a_{32}}{\partial y} + \frac{\partial a_{33}}{\partial z} \end{pmatrix} \in \mathbb{R}^3,$$

will turn out to be quite practical. This can be seen as a matrix version of the divergence where $A = (a_{ij})_{i,j=1,2,3} \in \mathbb{R}^{3\times 3}$ is the matrix and each of the components a_{ij} (for $i, j = 1, 2, 3$) is a scalar-valued function of x, y and z.

Our final result allows a reformulation of the divergence of an outer product.

Lemma 2.4 *Let $\Omega \subseteq \mathbb{R}^3$ be a set, $\phi : \Omega \to \mathbb{R}$ a scalar field and $\boldsymbol{f}, \boldsymbol{g} : \Omega \to \mathbb{R}^3$ two vector fields. All functions and Ω are assumed to be sufficiently well-behaved. Then we find*

$$\int_{\partial\Omega} \boldsymbol{f}(\boldsymbol{x})\big(\boldsymbol{g}(\boldsymbol{x}) \cdot \boldsymbol{n}(\boldsymbol{x})\big)\,\mathrm{d}s = \int_{\Omega} \nabla \cdot \big(\boldsymbol{f}(\boldsymbol{x}) \otimes \boldsymbol{g}(\boldsymbol{x})\big)\,\mathrm{d}\boldsymbol{x},$$

where $\boldsymbol{n}(\boldsymbol{x})$ is the outward unit normal vector in $\boldsymbol{x} \in \partial\Omega$.

The proof is a simple application of Gauss' integral theorem 2.2 to each component of $\boldsymbol{f}$ separately.

3 Conservation Laws

On a surface level subjects like physics, chemistry and biology appear mostly unrelated. On a mathematical level, however, their models often show similarities. One very common class of differential equations that appear frequently are conservation laws. This section explains their origin (similar to [23]) and introduces their theoretical treatment (based on [20] and [27]).

When conservation laws appear in practice some sort of balance law is always involved. To this end, consider some fixed region $\Omega \subseteq \mathbb{R}^3$ and in it some quantity with a density or concentration q which is itself a scalar-valued function of time $t > 0$ and space $\boldsymbol{x} = (x, y, z)^{\mathrm{T}} \in \mathbb{R}^3$. What happens to the quantity inside of Ω as time passes? Typically one has the following relation:

$$\begin{aligned} \text{time rate of change of quantity} = {} & \text{rate at which quantity flows into } \Omega \\ & - \text{rate at which quantity flows out of } \Omega \\ & + \text{rate at which quantity is produced in } \Omega \\ & - \text{rate at which quantity is destroyed in } \Omega. \end{aligned} \tag{3.1}$$

To illustrate this, consider an example from population biology. If the quantity corresponds to the population size of some species (e. g. foxes) in a fixed area Ω (e. g. Bavaria), then (3.1) can be formulated as

$$\text{rate of population change} = \text{immigration rate} - \text{emigration rate} + \text{birth rate} - \text{death rate}.$$

The natural mathematical way to phrase (3.1) is via integrals over the region Ω and its boundary $\partial\Omega$. The total quantity inside of Ω is given via the volume integral

$$\int_{\Omega} q(\boldsymbol{x}, t)\,\mathrm{d}\boldsymbol{x}.$$

Notice that this is a function that varies only with time. Its derivative corresponds to the left side of (3.1).

The inflow and outflow can be combined into one net term, if we introduce a *flux function* $(\boldsymbol{x}, t) \mapsto \boldsymbol{f}(\boldsymbol{x}, t)$. Its components correspond to the amount of the quantity q flowing through the surface $\partial\Omega$ at the point the point $\boldsymbol{x}$ on the surface and time t per unit area and per unit time in the component's direction. By convention, we will say that a component of the flux function is positive, if the flow is out of the surface, and negative, if it is into the surface. This way the integral

$$-\int_{\partial\Omega} \boldsymbol{f}(\boldsymbol{x}, t) \cdot \boldsymbol{n}(\boldsymbol{x}) \,\mathrm{d}s \tag{3.2}$$

subsumes the first two terms on the right side of (3.1). Here $\boldsymbol{n}(\boldsymbol{x})$ is the unit normal vector on $\boldsymbol{x} \in \partial\Omega$ pointing out of Ω. The minus sign is due to the outward-facing direction of $\boldsymbol{n}$.

The production and destruction can be handled in somewhat the same way with a scalar-valued *source function* $(q, \boldsymbol{x}, t) \mapsto \psi(q, \boldsymbol{x}, t)$. Notice that ψ can generally vary with the quantity q. If the source function is positive, we speak of a *source*, and if it is negative, we speak of a *sink*. The last two terms on the right side of (3.1) can then be represented as

$$\int_\Omega \psi(q(\boldsymbol{x}, t), \boldsymbol{x}, t) \,\mathrm{d}\boldsymbol{x}.$$

If we use Gauss' integral theorem 2.2 to transform the surface integral (3.2) into a volume integral, we can state (3.1) as

$$\frac{\mathrm{d}}{\mathrm{d}t}\left(\int_\Omega q(\boldsymbol{x}, t) \,\mathrm{d}\boldsymbol{x}\right) = -\int_\Omega \nabla \cdot \boldsymbol{f}(\boldsymbol{x}, t) \,\mathrm{d}\boldsymbol{x} + \int_\Omega \psi(q(\boldsymbol{x}, t), \boldsymbol{x}, t) \,\mathrm{d}\boldsymbol{x}. \tag{3.3}$$

In the case where q is a sufficiently smooth function, the derivative on the left may be pulled into the integral. And since Ω is an arbitrary region, the smoothness of the involved functions would imply the differential equation

$$q_t + \nabla \cdot \boldsymbol{f}(\boldsymbol{x}, t) = \psi(q, \boldsymbol{x}, t).$$

Its unknowns are q and $\boldsymbol{f}$ while ψ is given. However, in many applications it is possible to write $\boldsymbol{f}$ as a function of q directly. Notice that this is a special case of the form above since q itself depends on $(\boldsymbol{x}, t)$. In said case the differential equation becomes

$$q_t + \nabla \cdot \boldsymbol{f}(q) = \psi(q, \boldsymbol{x}, t) \tag{3.4}$$

or

$$q_t + f(q)_x + g(q)_y + h(q)_z = \psi(q, \boldsymbol{x}, t) \tag{3.5}$$

by writing out the divergence operator $\nabla\cdot$ and using the notation $\boldsymbol{f} = (f, g, h)^{\mathrm{T}}$ for the components. The corresponding formulation of (3.3) takes the form

$$\int_\Omega q_t(\boldsymbol{x}, t) + \nabla \cdot \boldsymbol{f}\big(q(\boldsymbol{x}, t)\big) \,\mathrm{d}\boldsymbol{x} = \int_\Omega \psi(q(\boldsymbol{x}, t), \boldsymbol{x}, t) \,\mathrm{d}\boldsymbol{x}. \tag{3.6}$$

Equations (3.6) and (3.4) are the *integral* and *differential* form of a *conservation law*. The unknown function here is q while $\boldsymbol{f}$ and ψ are known. We note that if one is given several conservation laws at the same time, then they can be combined into a vectorized version of (3.5) via

$$\boldsymbol{q}_t + \boldsymbol{f}(\boldsymbol{q})_x + \boldsymbol{g}(\boldsymbol{q})_y + \boldsymbol{h}(\boldsymbol{q})_z = \boldsymbol{\psi}(\boldsymbol{q}, \boldsymbol{x}, t). \tag{3.7}$$

Here $\boldsymbol{q}$ is a vector of conserved quantities; $\boldsymbol{f}$, $\boldsymbol{g}$ and $\boldsymbol{\psi}$ are defined accordingly, so that each component of (3.7) corresponds to one of the given conservation laws.

Notice that only the case where the source term vanishes is a proper conservation in the colloquial sense. Consequently, equations with a non-trivial $\boldsymbol{\psi}$ are sometimes referred to as *balance laws* instead. Section 5 will show two concrete examples of conservation laws in the context of fluid flow. The first one being conservation of mass, which will not yield a source term, and the second one being conservation of momentum, which will yield a source term.

Next up, we want to introduce what it means for the one-dimensional conservation law

$$\boldsymbol{q}_t(x,t) + \boldsymbol{f}\big(\boldsymbol{q}(x,t)\big)_x = \boldsymbol{\psi}(\boldsymbol{q}(x,t),x) \quad \text{for all } (x,t) \in \mathbb{R} \times]0,\infty[\,, \tag{3.8}$$

to be hyperbolic. We will only study the one-dimensional case in this thesis. A suitable generalization for several dimensions exists and can, for example, be found in [20, Section 18.5]. Recall that we already defined the term hyperbolic for second-order scalar linear partial differential equations in section 1. We must now expand this terminology somewhat, beginning with a *linear system* of conservation laws

$$\boldsymbol{q}_t + A\boldsymbol{q}_x = \boldsymbol{\psi}(\boldsymbol{q},x) \tag{3.9}$$

for some function $\boldsymbol{q} : \mathbb{R} \times]0,\infty[\to \mathbb{R}^m$ and a constant matrix $A \in \mathbb{R}^{m\times m}$. In this case, we say that (3.9) is hyperbolic, if A is diagonalizable with real eigenvalues. If we were instead given a *quasilinear system* of conservation laws

$$\boldsymbol{q}_t + A(\boldsymbol{q},x,t)\boldsymbol{q}_x = \boldsymbol{\psi}(\boldsymbol{q},x), \tag{3.10}$$

then we say that (3.10) is hyperbolic, if the variable matrix $A(\boldsymbol{q},x,t) \in \mathbb{R}^{m\times m}$ is diagonalizable with real eigenvalues at every point $(\boldsymbol{q},x,t)$. To define hyperbolicity for (3.8), we carry out the derivative in terms of x with the chain rule to find

$$\boldsymbol{q}_t + \boldsymbol{f}'(\boldsymbol{q})\boldsymbol{q}_x = \boldsymbol{\psi}(\boldsymbol{q},x), \tag{3.11}$$

which is valid, if $\boldsymbol{q}$ is smooth. Here

$$\boldsymbol{f}' = \begin{pmatrix} \dfrac{\partial f_1}{\partial q_1} & \dfrac{\partial f_1}{\partial q_2} & \cdots & \dfrac{\partial f_1}{\partial q_m} \\ \vdots & \vdots & \ddots & \vdots \\ \dfrac{\partial f_m}{\partial q_1} & \dfrac{\partial f_m}{\partial q_2} & \cdots & \dfrac{\partial f_m}{\partial q_m} \end{pmatrix} \in \mathbb{R}^{m\times m}$$

is the Jacobian matrix of $\boldsymbol{f} = (f_1, f_2, \ldots, f_m)^{\mathrm{T}}$ for $\boldsymbol{q} = (q_1, q_2, \ldots, q_m)^{\mathrm{T}}$. Hence (3.11) is a quasilinear system. We will say that (3.8) is hyperbolic, if (3.11) is hyperbolic for each (physically-relevant) value of $\boldsymbol{q}$.

Let us now turn to the theoretical investigation of conservation laws, focusing first on an appropriate notion of solution. The traditional solution concept turns out to be too restrictive because (i) certain applications require discontinuous initial conditions (cf. dam break in section 4) and (ii) solutions can start out smooth but develop discontinuities as time goes on (e. g. the breaking of a wave). This forces us to define a new kind of solution which admits discontinuities. The derivation above already suggests one way to do this: Notice that the differential form of the conservation law was derived from the

integral form (3.3). So in a way the integral equation is the more fundamental object. And indeed, the integral equation can still hold even when discontinuities are present. As it turns out, this particular integral form just so happens to be difficult to work with mathematically. For this reason, a different (but equivalent) integral form is preferred for theoretical investigations. We will illustrate its derivation for the simple scalar conservation law

$$q_t + f(q)_x = 0 \quad \text{for } (x,t) \in \mathbb{R} \times]0,\infty[\,, \tag{3.12}$$

but this approach generalizes to more complicated settings. The idea is to shift the differentiability away from q to some helper function $\phi : \mathbb{R} \times]0,\infty[\to \mathbb{R}$. A viable set of helper functions happens to be the set of *test functions* C_c^1. A function ϕ is called a test function, if it is continuously differentiable and has *compact support*. The support of a function is the closure of the set of points where it is nonzero, so in this case $\operatorname{supp}\phi := \overline{\{x \in \mathbb{R} \times]0,\infty[\mid \phi(x) \neq 0\}}$ needs to be a compact subset of $\mathbb{R}^2$. After multiplying (3.12) with such a function, we can be sure that integration over the entire domain

$$\int_0^\infty \int_{-\infty}^\infty \big(q_t + f(q)_x\big)\phi(x,t)\,\mathrm{d}x\mathrm{d}t = 0$$

is permitted. Now we utilize integration by parts to shift the differentiation to the test function:

$$\int_0^\infty \int_{-\infty}^\infty q\phi_t + f(q)\phi_x\,\mathrm{d}x\mathrm{d}t = -\int_{-\infty}^\infty q(x,0)\phi(x,0)\,\mathrm{d}x. \tag{3.13}$$

This also relies on the convenient cancellation of nearly all the boundary terms thanks to the compact support of ϕ. We call (3.13) the *weak form* of (3.12) and a function $(x,t) \mapsto q(x,t)$ is called a *weak solution* of (3.12) combined with some initial data $q(x,0) = q_0(x)$ for all $x \in \mathbb{R}$, if (3.13) holds for all functions $\phi \in C_c^1$.

A natural next question to ask at this point is whether or not a weak solution exists and is unique. We cannot comment on this in detail, although in general one finds that a solution exists but is not unique. This motivates the derivation of so-called *entropy conditions* which provide a way of identifying the physically-relevant solution among the torrent of possible solutions, see [21] for details. It is also worth noting that few theoretical results exist for the general conservation law (3.7). Given its practical relevance, that should come as somewhat of a surprise. As of now, only the case with one spatial dimension can be treated [9, chapter 11].

For the purposes of this text we will also require a very special type of initial value problem which arises when studying a homogeneous conservation law in one spatial dimension

$$\boldsymbol{q}_x + \boldsymbol{f}(\boldsymbol{q})_x = \boldsymbol{0} \quad \text{for all } (x,t) \in \mathbb{R} \times \big]\bar{t},\infty\big[\tag{3.14}$$

with piecewise constant initial data

$$\boldsymbol{q}(x,\bar{t}) = \left\{ \begin{array}{ll} \boldsymbol{q}_\ell, & \text{if } x < \overline{x}, \\ \boldsymbol{q}_\mathrm{r}, & \text{if } x > \overline{x} \end{array} \right\} \quad \text{for all } x \in \mathbb{R}.$$

Since the value at the jump is not of importance, it is usually not assigned a corresponding output. Here $\bar{t} > 0$ is a given time and $\overline{x} \in \mathbb{R}$ a given point. The vectors $\boldsymbol{q}_\ell \in \mathbb{R}^m$ and $\boldsymbol{q}_\mathrm{r} \in \mathbb{R}^m$ are also known. More generally, hyperbolic partial differential equations in combination with such a piecewise jump are referred to as *Riemann problems*. There are several reasons which motivate their investigation:

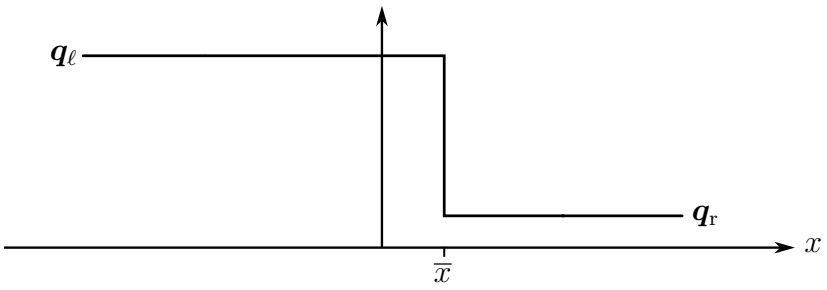

Figure 3.1: Initial data in a Riemann problem.

- Riemann problems yield interesting test problems for numerical algorithms. For example, the Riemann problem for the shallow-water equations is simply the dam-break problem, cf. section 4.
- Nonlinear equations can develop singularities even for smooth initial conditions. And the simplest kind of non-smooth initial data is a Riemann problem. Yet, all typical phenomena surrounding hyperbolic equations (e. g. shocks, rarefaction waves, supercritical flow) arise during their solution.
- Thanks to the simplicity of the initial conditions, exact solutions can be found even for complicated (nonlinear) conservation laws. (The same is not generally true for balance laws, however.)
- Riemann problems form the basis of the numerical methods which will be described in detail in chapter III.

For the rest of this text, we will assume that the reader is somewhat familiar with the theoretical underpinnings of weak solutions to hyperbolic problems (in particular Riemann problems). A gentle introduction to these topics can be found in chapter 3 of [23] or chapter 2 of [27]. A short summary, formulated in the shallow-water context for tsunami modeling, is given in [5]. We will give only a broad review here for the results of a nonlinear conservation law in one spatial dimension (3.14). With m equations one receives a solution consisting of $m+1$ constant states which are separated by m waves, one for each eigenvalue of the Jacobian matrix $\boldsymbol{f}'(\boldsymbol{q})$. These waves may be shocks, contact waves or smooth transition waves such as rarefactions. Most importantly, the solution is actually a *similarity solution* which means that it can be written in terms of a characteristic variable

$$\xi = \frac{x - \overline{x}}{t - \overline{t}}.$$

The solution function is then of the form $\xi \mapsto \boldsymbol{q}(\xi; \boldsymbol{q}_\ell, \boldsymbol{q}_\mathrm{r})$. Notice that this also implies that the solution is constant along rays of the form $\xi = c$ where $c \in \mathbb{R}$ is a given constant. The Riemann solutions for the shallow-water system will be expanded on in section 8.

Chapter II

The Shallow-Water Equations

This chapter derives the partial differential equations that govern shallow-water flow. One application of this theory that we will focus on in particular are tsunami waves. The essential assumption of this model is that the horizontal scales are much larger than the vertical one. This allows us to neglect vertical components of the participating functions and, hence, to end up with a two-dimensional description instead of a three-dimensional one.

We now outline the structure of this chapter, beginning with section 4 in which we describe typical applications of the shallow-water equations. This provides the motivation for studying the shallow-water model in the first place. Next, we introduce some fundamental concepts from fluid dynamics in section 5. In particular, we will derive two partial differential equations that govern fluid flow more generally. We then spend section 6 on applying these equations to the special setting of the shallow-water model. On this basis we will be able to derive the full set of two-dimensional shallow-water equations in section 7. We end our discussion in section 8 with an outlook on how the shallow-water model can be extended to fit different types of phenomena. In addition, we will encounter a one-dimensional version of the shallow-water equations which will become the basis for the numerical investigations of chapter III.

4 Real-World Applications of Shallow-Water Modeling

Before we begin with the mathematical description of the shallow-water equations in the following sections, we first discuss where they may be applied and under which conditions. We do this to convince ourselves that they are worth studying and to illustrate the wide variety of phenomena that a singular mathematical model may apply to. As a welcome side-effect, these applications provide an appropriate setting for the numerical experiments of section 13, allowing practitioners to compare real-world data against computational predictions.

The shallow-water equations are a set of three (or sometimes two) nonlinear partial differential equations which govern the motion of specific types of waves in fluids. A fluid is a substance that flows and has no fixed shape. Among the most important fluids are liquids and gases — water and air are fluids, but honey and lava are as well. A wave then refers to any kind of disturbance that travels through such a fluid. Contrary to what the name would have you believe, the shallow-water equations' area of application is neither restricted to water nor to shallow fluids. In fact, the only limiting assumption that we require is that the length scale of the wave is much bigger than the depth scale. We will see what this means precisely later on.

Shallow-water theory has many different applications. It was used by John von Neu-

MANN in weather forecasts that were computed on the ENIAC (the first electronic computer) in the 1950s, marking the onset of numerical weather prediction. In another case shallow-water models were used to study the Great Red Spot on Jupiter. These and many more applications are discussed in [31, Chapter 1]. We will dive deeper into two geophysical applications in each of which the fluid will turn out to be water.

Dam Break

A dam separates two layers of water with constant height from each other. The reservoirs contain large volumes of water and are often surrounded by either man-made walls or natural terrain, e. g. narrow canyons or valleys. Dams have become an important part of modern infrastructure. They supply water for the sake of irrigation and hydroelectric power via the usage of pumps. In addition, they serve an important purpose in the deliberate control and prevention of flooding.

Besides their benefits, dams have a number of risks associated with them. The failure of a dam wall can have catastrophic consequences. The French town of Fréjus experienced such an event in 1959 where over 400 people were killed when the walls of the Malpasset dam gave way after heavy rainfall. For the sake of prevention it is important to conduct numerical simulations of these events before they happen. On their basis inundation maps can be produced which in turn lead to evacuation plans.

For theoretical purposes one often considers the flow that is observed when the dam wall is removed instantaneously. We note, however, that this type of flow can also arise

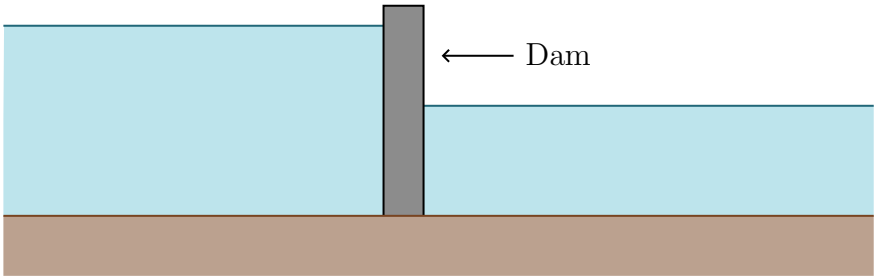

in different contexts, one example being tidal bores in rivers. The resulting waves are comparable to shock waves in aerodynamics. In mathematics, dam breaks show the need for numerical methods which can handle (almost) discontinuous functions well. They provide the simplest real-world example of such a wave.

Besides the failure of the dam wall, a different danger that is associated with dams are landslides from neighboring hills into the upper reservoir. These incidents are known to cause flood waves of sufficient height to overtop the dam and thus cause destructive flow downstream. In 1963 such an incident occurred in Italy, killing over 2000 people in its wake, when a large piece of rock broke off a mountain near a dam constructed around the river Vajont. The resulting type of wave actually belongs to a different class of applications of the shallow-water equations which will be introduced next.

Tsunamis

In Japanese the words *tsu* and *nami* translate to harbor and wave. Tsunamis are certain types of gravity waves that are caused by sudden displacement of water. They are most commonly triggered by underwater earthquakes: The earth's mantle is made up of many

tectonic plates that are in constant motion. At the boundary between two plates one plate moves, or *subducts*, beneath the other (in almost all cases). This motion does not happen in a smooth fashion. Rather, the two neighboring plates build up stress, causing the overriding plate to bulge up. This process comes to a violent end in a sudden snap during which the higher plate jumps up several meters, allowing the lower plate to slide by. The motion of the seafloor then sets off a tsunami wave that is typically several 100 kilometers long. This generation process is illustrated in figure 4.1. The displacement of

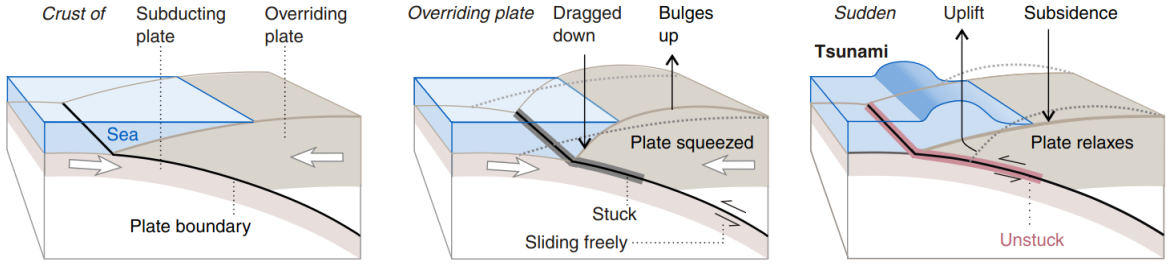

Figure 4.1: Origin of earthquake-generated tsunamis. Taken from [2].

the water immediately releases a huge amount of potential energy into the ocean (as much as 10 megatons of TNT). An exact value can be obtained by integrating over the affected region

$$\iiint_{\eta_s}^{\eta(x,y)} \varrho g z \,\mathrm{d}z\mathrm{d}x\mathrm{d}y = \iint \frac{1}{2}\varrho g[\eta(x,y) - \eta_s]^2 \,\mathrm{d}x\mathrm{d}y,$$

using the height of the water $\eta(x, y)$ after the displacement, the average sea level η_s as well as the density of ocean water ϱ and the acceleration due to gravity g. The length of such a rupture can be on the order of 1000s of kilometers, displacing water over an area of about 100 km width. Meanwhile, the ocean floor is displaced on the order of several meters. The released energy is dissipated mainly through friction at the bottom of the ocean.

Besides earthquakes, other sources of tsunamis are underwater volcanic eruptions as well as asteroid impacts. In addition, landslides (both from land into water and underwater) have been observed to cause tsunami waves. This thesis will mainly focus on tsunamis that were caused by earthquakes, though. These are the most common and typically the most destructive type. The fundamental property that we will take advantage of is that the earthquake that caused the tsunami displaces the entire water column over a rather large area. This allows us to use two-dimensional models which require much less computation than three-dimensional ones.

The speed of a tsunami wave depends heavily on the depth of the underlying ocean floor. On average, the ocean is roughly 4 kilometers deep. Over this kind of depth a tsunami wave travels at a speed of about 700 kilometers per hour. As the wave approaches the shore, however, it drastically slows down. In a depth of 100 meters the speed is only on the order of 100 kilometers per hour, for example. In the open ocean, tsunami waves have a barely noticeable height in the centimeter region, but as they approach shore they can become up to 20 meters tall. Figure 4.2 shows the elevation of the earth. For our purposes we are particularly interested in the earth's bathymetry, i. e. the topography below sea level. It is clearly visible that the ocean floor near continents tends to be relatively shallow (continental shelf, red). From this region a steep cliff leads to a deeper oceanic layer (abyssal plains, blue and purple). Landslides at these cliffs can cause strong tsunamis, as

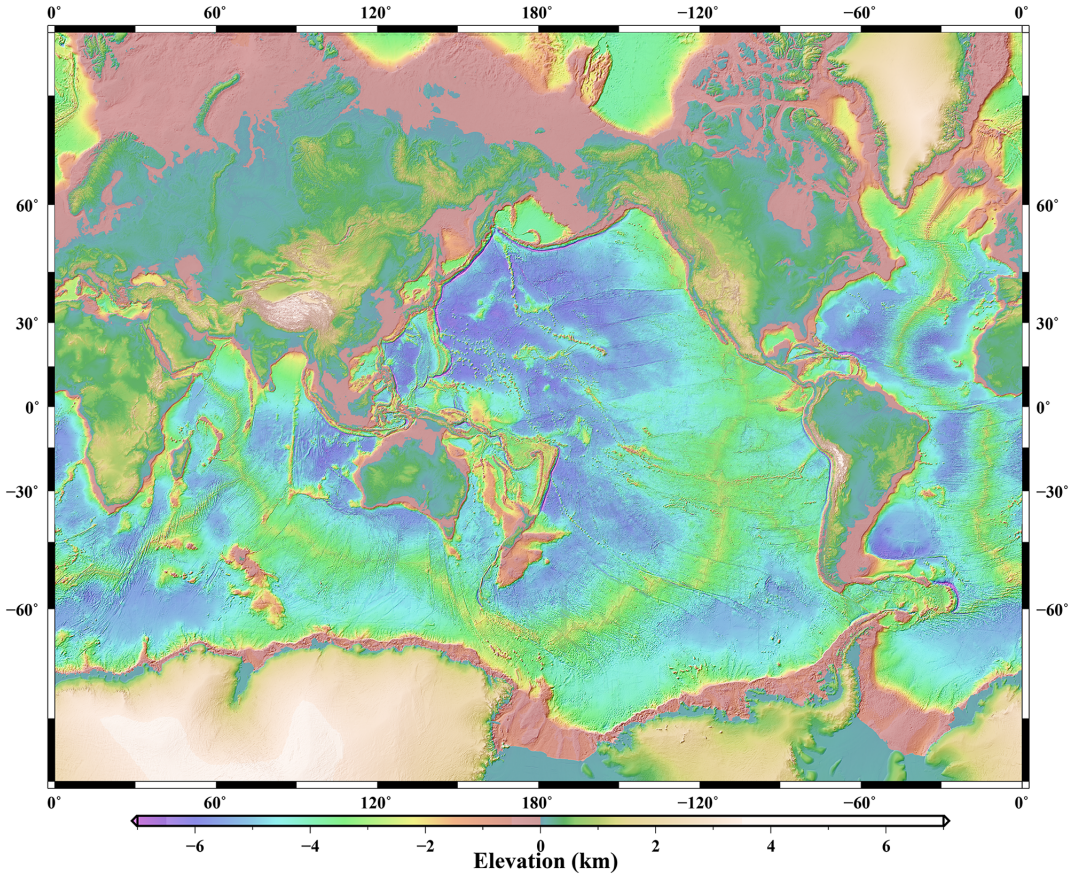

Figure 4.2: Topography of the earth. Taken from [29].

mentioned above. The deep layer contains trenches which extend much further down, the famous Mariana trench being the most extreme example. It harbors the deepest point on earth about 11 kilometers below the sea's surface. Between the shallow and the deep layer there exist areas of mid-level elevation (mid-ocean ridges, green and yellow) that can be found at boundaries of tectonic plates where lava rises up to form underwater mountain ranges.

5 Background from Fluid Dynamics

This section recalls some of the mathematics that is commonly used to model fluids such as water or air. The underlying framework is that of continuum mechanics and our description of these topics is inspired by [11] and [17]. We use the Eulerian viewpoint of fluids in which a reference system that is fixed in space is studied (instead of moving the frame to follow a fluid parcel around wherever it is advected) [30]. To this end, let $\Omega \subseteq \mathbb{R}^3$ be a fixed set inside of a fluid which flows through it during a time $t \in [0, T]$ where $T > 0$ denotes the end of this time period. We assume Ω to be a "well-behaved" subset by which we mean that it fulfills all the requirements of the theorems that we wish to apply to it (namely those from section 2). We call such sets *control volumes*. The flow through Ω is then characterized by

three functions:

$$\begin{aligned} \boldsymbol{u} &: \Omega \times [0,T] \longrightarrow \mathbb{R}^3 \qquad \text{(velocity)}, \\ p &: \Omega \times [0,T] \longrightarrow \mathbb{R} \qquad \text{(pressure)}, \\ \varrho &: \Omega \times [0,T] \longrightarrow \mathbb{R} \qquad \text{(density)}. \end{aligned}$$

If $\boldsymbol{x} = (x,y,z)^{\mathrm{T}} \in \Omega$ denotes an arbitrary point in space and $t \in [0,T]$ denotes an arbitrary time, then the components of velocity will be denoted $\boldsymbol{u}(\boldsymbol{x},t) = (u(\boldsymbol{x},t), v(\boldsymbol{x},t), w(\boldsymbol{x},t))^{\mathrm{T}}$. These are the standard labeling conventions in fluid dynamics, so we will stick with them, even though they might give rise to some confusion: Notice that $\boldsymbol{x}$ is the position vector while x is its first component and hence a scalar. The same goes for $\boldsymbol{u}(\boldsymbol{x},t)$ and $u(\boldsymbol{x},t)$. Recall that vectors will always be set in bold in this thesis.

The basic assumption of continuum mechanics is that the modeled substance is continuous, i. e., not made of atoms but infinitely divisible. Given that a cubic centimeter of a typical fluid like air or water is filled with roughly 10^{23} molecules (Avogadro's number), this assumption does not seem too far-fetched. In addition, we will require the functions $\boldsymbol{u}, p$ and ϱ to be sufficiently smooth. This is necessary to obtain differential equations, but not their weak forms as discussed in section 3.

Our goal for the remainder of this section will be the derivation of two basic partial differential equations that govern the motion of fluids. Both equations will be based on conservation laws: the first on conservation of mass and the second on conservation of momentum.

The continuity equation

Notice that the mass inside of Ω changes with time as the fluid flows in and out of it. In fact, mass is a function of time that is given via the volume integral

$$\int_\Omega \varrho(\boldsymbol{x},t)\,\mathrm{d}\boldsymbol{x}.$$

If $\boldsymbol{n}(\boldsymbol{x})$ denotes the outward unit normal vector at the point $\boldsymbol{x}$ on the surface of Ω (i. e. $\boldsymbol{x} \in \partial\Omega$), then the flow of fluid out(!) of $\partial\Omega$ as a function of time is given via the scalar-valued surface integral

$$\int_{\partial\Omega} \varrho(\boldsymbol{x},t)\boldsymbol{u}(\boldsymbol{x},t) \cdot \boldsymbol{n}(\boldsymbol{x})\,\mathrm{d}s$$

where $\cdot : \mathbb{R}^3 \times \mathbb{R}^3 \to \mathbb{R}$ denotes the standard Euclidean inner product. Let us now assume *conservation of mass*, i. e., matter is neither created nor destroyed inside of the fluid. This means that the change of mass in Ω has to be due to the flow of fluid into(!) Ω across $\partial\Omega$. Dropping the variables for the sake of space, this means

$$\frac{\mathrm{d}}{\mathrm{d}t}\left(\int_\Omega \varrho\,\mathrm{d}\boldsymbol{x}\right) = -\int_{\partial\Omega} \varrho\boldsymbol{u}\cdot\boldsymbol{n}\,\mathrm{d}s. \tag{5.1}$$

We can use Gauss' integral theorem 2.2 on the right side of (5.1) to get

$$\int_{\partial\Omega} \varrho\boldsymbol{u}\cdot\boldsymbol{n}\,\mathrm{d}s = \int_\Omega \nabla\cdot(\varrho\boldsymbol{u})\,\mathrm{d}\boldsymbol{x}, \tag{5.2}$$

where $\nabla \cdot (\varrho \boldsymbol{u}) = \operatorname{div}(\varrho \boldsymbol{u})$ denotes the divergence as discussed in section 2. When we plug (5.2) into (5.1), we receive

$$\frac{\mathrm{d}}{\mathrm{d}t}\left(\int_\Omega \varrho \,\mathrm{d}\boldsymbol{x}\right) = -\int_\Omega \nabla \cdot (\varrho \boldsymbol{u}) \,\mathrm{d}\boldsymbol{x}$$

and since we assumed ϱ to be sufficiently smooth, the derivative may be carried out inside of the integral to give

$$\int_\Omega \left(\frac{\partial \varrho}{\partial t} + \nabla \cdot (\varrho \boldsymbol{u})\right) \mathrm{d}\boldsymbol{x} = 0. \tag{5.3}$$

Since $\Omega \subseteq \mathbb{R}^3$ was arbitrary and the integrand is continuous (ϱ and $\boldsymbol{u}$ are sufficiently smooth by assumption), it is easy to see that (5.3) implies

$$\frac{\partial \varrho}{\partial t} + \nabla \cdot (\varrho \boldsymbol{u}) = 0. \tag{5.4}$$

Equations (5.3) and (5.4) are the integral and differential form of the so-called *continuity equation*.

The Euler equations

Recall that according to Newton's second law we have *conservation of momentum*, i. e.

$$\begin{aligned} &\text{change of momentum of fluid in } \Omega \\ &\quad = \text{ sum of all acting forces on fluid in } \Omega \\ &\qquad + \text{ rate of flow of momentum across } \partial\Omega \text{ into } \Omega \end{aligned} \tag{5.5}$$

(the second summand arises from the fact that we fixed our volume Ω). The momentum vector of the fluid in Ω as a function of time is given via the volume integral

$$\int_\Omega \varrho(\boldsymbol{x}, t)\boldsymbol{u}(\boldsymbol{x}, t) \,\mathrm{d}\boldsymbol{x}$$

and the rate of momentum flow over the boundary is given via the vector-valued surface integral

$$-\int_{\partial\Omega} \varrho(\boldsymbol{x}, t)\boldsymbol{u}(\boldsymbol{x}, t)\big(\boldsymbol{u}(\boldsymbol{x}, t) \cdot \boldsymbol{n}(\boldsymbol{x})\big) \,\mathrm{d}s$$

where $\boldsymbol{n}(\boldsymbol{x})$ is again the outward-facing unit normal vector on $\boldsymbol{x} \in \partial\Omega$.

As for the forces, we distinguish two different types: So-called *body forces* have an external source and are roughly the same for all particles. They can be expressed in terms of a volume integral

$$\int_\Omega \varrho(\boldsymbol{x}, t)\boldsymbol{f}(\boldsymbol{x}) \,\mathrm{d}\boldsymbol{x}$$

where $\boldsymbol{f} : \Omega \to \mathbb{R}^3$ is the body force acceleration (=force per unit mass). Common examples of body forces are gravity, the coriolis force aswell as electric or magnetic forces. The second type of forces are those that act at the surface of the volume, so-called *contact forces*, that are due to the internal interaction between nearby fluid molecules. In general, one would consider both pressure and viscosity (=internal friction). Here we will focus on the inviscid case only. This means our derivation no longer applies to substances like honey or lava,

but the fluid at the center of this thesis, namely water, is still being portrayed accurately. The contact force vector due to pressure can be expressed via the surface integral

$$\int_{\partial\Omega} p(\boldsymbol{x},t)\boldsymbol{n}(\boldsymbol{x})\,\mathrm{d}s.$$

We emphasize again that, by definition, $\boldsymbol{n}$ points outward of Ω.

We can now formulate (5.5) mathematically. Once more dropping the variables for the sake of clarity, we get

$$\frac{\mathrm{d}}{\mathrm{d}t}\left(\int_\Omega \varrho\boldsymbol{u}\,\mathrm{d}\boldsymbol{x}\right) = \left[\int_\Omega \varrho\boldsymbol{f}\,\mathrm{d}\boldsymbol{x} - \int_{\partial\Omega} p\boldsymbol{n}\,\mathrm{d}s\right] - \int_{\partial\Omega} \varrho\boldsymbol{u}(\boldsymbol{u}\cdot\boldsymbol{n})\,\mathrm{d}s. \tag{5.6}$$

Let us transform the surface integrals into volume integrals to simplify this further: For the contact force Gauss' integral theorem 2.3 yields a reformulation in terms of the pressure gradient ∇p to give

$$\int_{\partial\Omega} p(\boldsymbol{x},t)\boldsymbol{n}(\boldsymbol{x})\,\mathrm{d}s = \int_\Omega \nabla p(\boldsymbol{x},t)\,\mathrm{d}\boldsymbol{x}$$

and for the flow of momentum lemma 2.4 shows

$$\int_{\partial\Omega} \varrho(\boldsymbol{x},t)\boldsymbol{u}(\boldsymbol{x},t)\big(\boldsymbol{u}(\boldsymbol{x},t)\cdot\boldsymbol{n}(\boldsymbol{x})\big)\,\mathrm{d}s = \int_\Omega \nabla\cdot\big([\varrho(\boldsymbol{x},t)\boldsymbol{u}(\boldsymbol{x},t)]\otimes\boldsymbol{u}(\boldsymbol{x},t)\big)\,\mathrm{d}\boldsymbol{x}$$

where $\otimes$ is the dyadic product which outputs a matrix and $\nabla\cdot$ = div its divergence (as defined in section 2). So (5.6) turns into

$$\int_\Omega \left(\frac{\partial}{\partial t}(\varrho\boldsymbol{u}) + \nabla\cdot(\varrho\boldsymbol{u}\otimes\boldsymbol{u}) + \nabla p\right)\,\mathrm{d}\boldsymbol{x} = \int_\Omega \varrho\boldsymbol{f}\,\mathrm{d}\boldsymbol{x}, \tag{5.7}$$

if we use the smoothness of $\varrho\boldsymbol{u}$ and rearrange, again dropping the variables for the sake of readability. Just like before this integral form implies the differential form

$$\frac{\partial}{\partial t}(\varrho\boldsymbol{u}) + \nabla\cdot(\varrho\boldsymbol{u}\otimes\boldsymbol{u}) + \nabla p = \varrho\boldsymbol{f} \tag{5.8}$$

under the sufficiently-strong smoothness assumptions for all involved functions. Equations (5.7) and (5.8) are the integral and differential form of the so-called *Euler equations*. Written out in their components, they include three scalar partial differential equations (one for each component of the momentum vector).

The attentive reader will surely have noticed that our derivation of the integral forms has actually already relied on smoothness assumptions (we used Gauss' integral theorem). We note that it is possible to derive the integral forms directly without prior smoothness assumptions, too. However, this requires a certain amount of care and is hence a more involved process. The interested reader may find a detailed discussion in the book [6] by Chorin and Marsden.

We end this section with a remark about the viscous case of the Euler equation.

Remark 5.1 (Navier-Stokes equations)
In our derivation of the Euler equations (5.8) above, we omitted the contact forces due to internal friction. The more general model that considers both pressure and viscosity leads

to the so-called *Navier-Stokes equations*. These are often considered the most fundamental equations of fluid dynamics, modeling everything from gases, water and oil to phenomena like the flow of air around the wing of an airplane, ocean waves colliding at shore or the movement of glaciers. Unfortunately, solving the Navier-Stokes equations is notoriously difficult. For this reason certain simplifications (like the Euler equations) have received much attention. For the purposes of this thesis, the Euler equation will suffice to derive the shallow-water equations in the following sections. ◆

6 The Setting of Shallow-Water Theory

This section introduces the modeling framework from which we will be able to derive the shallow-water equations later on. To have a concrete visual in front of us, we will phrase everything in the context of tsunami modeling. The adaptation to different applications (cf. section 4) should be straight forward. Our notation will closely follow that of Randall LeVeque, David George and Marsha Berger who have famously investigated the numerical simulation of tsunamis with finite-volume methods [22].

The derivation of the full set of two-dimensional shallow water equations will take the following steps:

1. Introducing the model
2. Simplifying the governing equations for incompressible flow
3. Analyzing the scales of the governing equations and neglecting small terms
4. Formulating boundary conditions
5. Removing the vertical components by depth-averaging

Since this entire process is somewhat lengthy, it is split into this and the next section. Here we deal with steps 1., 2. and 3. in which our goal will be to remove the vertical velocity component w from the governing equations. The following section will then finish these arguments. Our presentation is a combination of that in [31] and [28].

To set the scene, we consider a right-handed coordinate system where x and y denote the horizontal and z the vertical axis. As usual, we combine them into a vector $\boldsymbol{x} = (x, y, z)^{\mathrm{T}} \in \mathbb{R}^3$. The geometry that we have in mind is shown in figure 6.1. A function $(x, y, t) \mapsto b(x, y, t) \geqslant 0$ models the height of a bottom layer, measured over an underlying reference level $z = 0$, that depends both on the horizontal location (x, y) and on time $t > 0$. Above this ground layer we have some water of height $h(x, y, t)$. The sum of the bottom elevation and the wave height

$$\eta(x, y, t) := b(x, y, t) + h(x, y, t)$$

gives us the z-coordinate of the water surface in our reference frame. We will refere to η_s as the average depth of the ocean. Places where $b(x, y, t) - \eta_s < 0$ correspond to bathymetry and places where $b(x, y, t) - \eta_s > 0$ to topography. Notice that our tsunami framing leaves us no other choice but to view b as a function of time, if we want to model earthquakes. However, we can get around this by including the wave-inducing earthquake disturbance

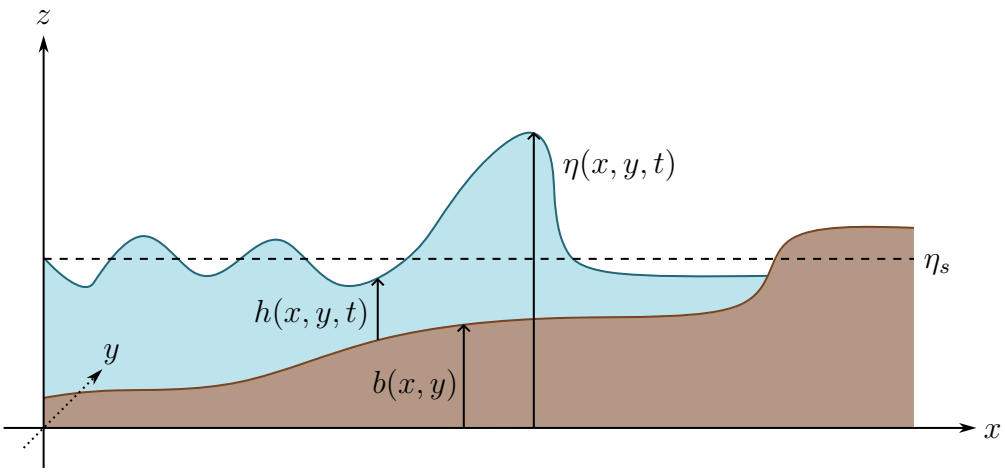

Figure 6.1: Geometry of the shallow-water model for tsunamis.

in the initial wave height. Therefore we may in fact assume b to be time-independent, i. e. $b(x, y, t) = b(x, y)$ for all $t > 0$, without loss of generality. At each point $\boldsymbol{x}$ inside of the water we have a water velocity $\boldsymbol{u} = (u(\boldsymbol{x}, t), v(\boldsymbol{x}, t), w(\boldsymbol{x}, t))^{\mathrm{T}}$ and our derivation's final result will be a set of differential equations from which the horizontal velocities u, v and the wave height h can be deduced.

In all of our discussions we shall consider ocean water to be *incompressible*, i. e., its density ϱ is not a function of pressure. In fact, we will go even further and just assume it to be constant. In reality it could still vary with other factors like the temperature or the salinity of the water, but these may safely be ignored in most cases [19, Subsection 1.2.3]. This concludes step 1. of our derivation.

The water in our scenario must obey the equations from section 5. The continuity equation (5.4) takes the form

$$\nabla \cdot \boldsymbol{u}(\boldsymbol{x}, t) = 0 \tag{6.1}$$

because density was assumed to be constant. To see what shape the Euler equations (5.8) assume, we must first examine the body forces in our scenario. We will only consider gravity $\boldsymbol{f} := \boldsymbol{g} = (0, 0, -g)^{\mathrm{T}}$ here, but discuss this further in section 8. The letter g refers to the acceleration due to gravity at the surface of the earth. This value is a constant that can be measured. By dividing by the density (which is constant by assumption) and rearranging, the Euler equations then take the form

$$\frac{\partial \boldsymbol{u}}{\partial t} + \nabla \cdot (\boldsymbol{u} \otimes \boldsymbol{u}) = -\frac{1}{\varrho} \nabla p + \boldsymbol{g}. \tag{6.2}$$

Both equations hold for all $t > 0$ where $x, y \in \mathbb{R}$ with $b(x, y) \leqslant z \leqslant \eta(x, y, t)$, which is to say inside of the ocean. In their full form (6.1) and (6.2) yield the system

$$\frac{\partial u}{\partial x} + \frac{\partial v}{\partial y} + \frac{\partial w}{\partial z} = 0, \tag{6.3}$$

$$\frac{\partial u}{\partial t} + u\frac{\partial u}{\partial x} + v\frac{\partial u}{\partial y} + w\frac{\partial u}{\partial z} = -\frac{1}{\varrho}\frac{\partial p}{\partial x}, \tag{6.4}$$

$$\frac{\partial v}{\partial t} + u\frac{\partial v}{\partial x} + v\frac{\partial v}{\partial y} + w\frac{\partial v}{\partial z} = -\frac{1}{\varrho}\frac{\partial p}{\partial y}, \tag{6.5}$$

$$\frac{\partial w}{\partial t} + u\frac{\partial w}{\partial x} + v\frac{\partial w}{\partial y} + w\frac{\partial w}{\partial z} = -\frac{1}{\varrho}\frac{\partial p}{\partial z} - g, \tag{6.6}$$

thus bringing step 2. to an end.

We next turn our attention to the scales of the governing equations. The idea is to gain a rough order-of-magnitude estimate for most of the terms in the equations above. If some of them turn out to be very small, we can save ourselves much computational work by neglecting them. The scales that we can infer from our real-world tsunami scenario are

$$\begin{aligned} \text{horizontal extend:} \quad & L = 100 \text{ km}, \\ \text{vertical extend:} \quad & H = 1 \text{ km}, \\ \text{horizontal velocity:} \quad & U = V = 100 \ \tfrac{\text{km}}{\text{h}}, \\ \text{time-scale:} \quad & T = L/U = 1 \text{ h}. \end{aligned}$$

It is important to note that these are not to be understood as the precise values of x, y, z, u, v and t. It is okay for a wave to travel for over 10 hours, for example. But we would not expect it to disappear after mere seconds or microseconds. In addition, we use the following values

$$g = 9.81 \ \tfrac{\text{m}}{\text{s}^2} = 127000 \ \tfrac{\text{km}}{\text{h}^2}, \qquad \varrho = 1.03 \ \tfrac{\text{g}}{\text{cm}^3} = 1.03 \times 10^{12} \ \tfrac{\text{kg}}{\text{km}^3},$$

for the gravitational acceleration and the density of ocean water (we will see later on that we actually do not need a concrete value for ϱ). The fundamental assumption of shallow-water theory is that H is much smaller than L, so that $H/L \ll 1$. What does small mean in this case? According to [31] a suitable upper limit is given via $H/L < 0.05$, so we may safely assume our tsunami scenario to be covered by shallow-water theory.

So far we cannot conduct a full scale analysis of the governing equations (6.3)–(6.6) because we are still missing the scale of W among others. Luckily, its magnitude can be deduced from what we already know. To this end, notice that

$$[x] = [y] = L = 100 \text{ km}, \qquad [z] = H = 1 \text{ km}, \qquad [u] = [v] = U = V = 100 \ \tfrac{\text{km}}{\text{h}}.$$

So we expect a rough dimensional estimate of the first two accelerations in the continuity equation (6.3) to be

$$\left[\frac{\partial u}{\partial x}\right] \propto \frac{U}{L} \qquad \text{and} \qquad \left[\frac{\partial v}{\partial y}\right] \propto \frac{U}{L}.$$

There is no ground for thinking that these two summands would cancel each other, so it is reasonable to assume that their sum is indeed of size U/L itself. In order for (6.3) to hold then, we would require $\partial w/\partial z$ to be of magnitude U/L, too. This implies

$$[w] = W \propto \frac{U}{L} H = 1 \ \tfrac{\text{km}}{\text{h}}.$$

So $[w]$ turns out to be rather small compared to $[u] = [v] = 100$ km/h which means there is hope for simplifications on the horizon. To this end, let us view the vertical momentum equation (6.6) since it involves w the most: The terms on the left all turn out to be of the same (small) size:

$$\left[\frac{\partial w}{\partial t}\right] \propto \frac{1 \ \frac{\text{km}}{\text{h}}}{1 \text{ h}} = 1 \ \tfrac{\text{km}}{\text{h}^2}, \qquad \left[u\frac{\partial w}{\partial x}\right] \propto 100 \ \tfrac{\text{km}}{\text{h}} \frac{1 \frac{\text{km}}{\text{h}}}{100 \text{ km}} = 1 \ \tfrac{\text{km}}{\text{h}^2},$$

$$\left[v\frac{\partial w}{\partial y}\right] \propto 100 \ \tfrac{\text{km}}{\text{h}} \frac{1 \frac{\text{km}}{\text{h}}}{100 \text{ km}} = 1 \ \tfrac{\text{km}}{\text{h}^2}, \qquad \left[w\frac{\partial w}{\partial z}\right] \propto 1 \ \tfrac{\text{km}}{\text{h}} \frac{1 \frac{\text{km}}{\text{h}}}{1 \text{ km}} = 1 \ \tfrac{\text{km}}{\text{h}^2}.$$

At the same time we know that g is on the order of 10^5 km/h^2 compared to which the terms on the left are negligibly small. This allows us to simplify equation (6.6) to so-called *hydrostatic balance*

$$\frac{\partial p}{\partial z} = -\varrho g.$$

In physics hydrostasis describes a scenario where the upward pressure forces exactly balance out the downward gravitational and pressure forces. This concludes step 3. in our derivation of the shallow-water equations. After we have now eliminated the vertical velocity component by method of scale analysis, the next section will show how we can rid ourselves of the vertical dependencies of u, v and h, too.

7 Derivation of the Shallow-Water Equations

We spent the last section simplifying the continuity equation and the Euler equations from section 5 in the special scenario that is pictured in figure 6.1. To this end, we used the incompressibility of water and the shallow-water assumption that the vertical scale is small against the horizontal one. The final set of partial differential equations that we ended up with was

$$\frac{\partial u}{\partial x} + \frac{\partial v}{\partial y} + \frac{\partial w}{\partial z} = 0, \tag{7.1}$$

$$\frac{\partial u}{\partial t} + u\frac{\partial u}{\partial x} + v\frac{\partial u}{\partial y} + w\frac{\partial u}{\partial z} = -\frac{1}{\varrho}\frac{\partial p}{\partial x}, \tag{7.2}$$

$$\frac{\partial v}{\partial t} + u\frac{\partial v}{\partial x} + v\frac{\partial v}{\partial y} + w\frac{\partial v}{\partial z} = -\frac{1}{\varrho}\frac{\partial p}{\partial y}, \tag{7.3}$$

$$\frac{\partial p}{\partial z} = -\varrho g, \tag{7.4}$$

using the notation from the previous section which will not be repeated here. The first equation corresponds to conservation of mass and the other three to conservation of momentum. This section's goal is to use these equations as a starting point for the derivation of the titular shallow-water equations. While the last section eliminated the vertical component of velocity, this one is dedicated to removing the vertical component of position (the z-component) from the horizontal velocities u and v. Our description will loosely follow section 8.2 of [24].

In terms of the recipe from the previous section, we now enter step 4. by considering the bottom and surface boundary conditions. At the bottom $z = b(x, y)$ we encounter an impenetrable boundary, i. e., no fluid can pass through the floor into the ground. This implies that the velocity component of $\boldsymbol{u}$ in the direction normal to the ground must vanish. It is well-known that a normal vector to such an implicitly-defined surface is given by $\boldsymbol{n}(x, y) := (\partial b/\partial x, \partial b/\partial y, -1)^{\mathrm{T}}$ [8, Section 10.8]. Therefore the gradient of the bottom topography (i. e., how steep the ocean floor is) plays a role here. The component of $\boldsymbol{u}$ that points in the direction of $\boldsymbol{n}$ can then be found via their dot product $\boldsymbol{u} \cdot \boldsymbol{n}$ which must vanish by the impenetrability assumption:

$$0 \overset{!}{=} \boldsymbol{u} \cdot \boldsymbol{n} = u|_{z=b}\frac{\partial b}{\partial x} + v|_{z=b}\frac{\partial b}{\partial y} - w|_{z=b} \tag{7.5}$$

where the notation $|_{z=}$ denotes an evaluation of the function at a given z-value, e. g. $w|_{z=b} = w(x, y, b(x, y))$. This is our bottom boundary condition [31].

At the surface $z = \eta(x, y, t) = b(x, y) + h(x, y, t)$ we encounter a free boundary between two fluids: water on the bottom and air on the top. Our first condition will be that the pressure function is continuous here, so that

$$p(x, y, \eta(x, y, t), t) = p_a \tag{7.6}$$

where p_a is the atmospheric pressure. (In reality this neglects surface tension and wind [17, Section 1.2].) For the sake of simplicity, we will assume this value to be constant; many texts on oceanography actually choose to omit it completely. (In reality atmospheric pressure varies both with space and time. To name just one example: The passage of pressure regions can be used to model the movements of storms [17, Section 1.2].) Our second condition will be that fluid particles cannot flow through the sea surface from the water into the air. (In reality these effects do exist and are comprised of precipitation, evaporation and runoff as well as effects related to ice [19, Subsection 1.3.2].) This implies that water particles on the surface stay there for eternity. The surface thus forms an impenetrable boundary layer between the ocean and the atmosphere. The difference to the bottom boundary condition from before is that the position of this layer may now vary with time. To model this, let us view a path $\boldsymbol{r}(t) := (\hat{x}(t), \hat{y}(t), \hat{z}(t))^{\mathrm{T}}$ of a fluid particle which remains in the surface layer for all times $t > 0$, i. e., the components of $\boldsymbol{r}$ obey the relationship

$$\hat{z}(t) = \eta\big(\hat{x}(t), \hat{y}(t), t\big).$$

We can differentiate this identity using the chain rule to find

$$\begin{aligned}\hat{z}'(t) &= \nabla\eta\big(\hat{x}(t), \hat{y}(t), t\big) \cdot \frac{\partial}{\partial t}\big(\hat{x}(t), \hat{y}(t), t\big)^{\mathrm{T}} \\ &= \frac{\partial\eta}{\partial x}\big(\hat{x}(t), \hat{y}(t), t\big)\hat{x}'(t) + \frac{\partial\eta}{\partial y}\big(\hat{x}(t), \hat{y}(t), t\big)\hat{y}'(t) + \frac{\partial\eta}{\partial t}\big(\hat{x}(t), \hat{y}(t), t\big).\end{aligned}$$

Now since $\hat{x}' = u, \hat{y}' = v$, and $\hat{z}' = w$ this implies

$$w|_{z=\eta} = \frac{\partial\eta}{\partial t} + u|_{z=\eta}\frac{\partial\eta}{\partial x} + v|_{z=\eta}\frac{\partial\eta}{\partial y} \tag{7.7}$$

which is our boundary condition at the surface. This ends step 4.

Now we turn to the last step in which we finally derive the actual shallow-water equations. The quintessential idea will be to remove the z-dependence from the velocity components by averaging the respective functions from the bottom $z = b(x, y)$ to the surface $z = \eta(x, y, t)$. To this end, let us introduce the averages

$$\begin{aligned}\overline{u}(x, y, t) &:= \frac{1}{h(x, y, t)}\int_{b(x,y,t)}^{\eta(x,y,t)} u(x, y, z, t)\,\mathrm{d}z, \\ \overline{v}(x, y, t) &:= \frac{1}{h(x, y, t)}\int_{b(x,y,t)}^{\eta(x,y,t)} v(x, y, z, t)\,\mathrm{d}z.\end{aligned} \tag{7.8}$$

Notice that neither $\overline{u}$ nor $\overline{v}$ depend on z while both u and v do. The final ingredient for our derivation is Leibniz' parameter integral rule which explains how to differentiate under the

integral sign in the case where the integration limits are themselves functions that vary. One finds that

$$\frac{\mathrm{d}}{\mathrm{d}x}\left(\int_{a(x)}^{b(x)} f(x,t)\,\mathrm{d}t\right) = f\big(x,b(x)\big)b'(x) - f\big(x,a(x)\big)a'(x) + \int_{a(x)}^{b(x)} \frac{\partial f}{\partial x}(x,t)\,\mathrm{d}t$$

Here $f : [\alpha,\beta] \times [\gamma,\delta] \to \mathbb{R}$ and $a, b : [\alpha,\beta] \to [\gamma,\delta]$ are continuously-differentiable functions and the identity holds for all $x \in]\alpha,\beta[$. With it, we can now attack the continuity equation (7.1) by integrating over z:

$$\begin{aligned}
0 &= \int_b^\eta \frac{\partial u}{\partial x} + \frac{\partial v}{\partial y} + \frac{\partial w}{\partial z}\,\mathrm{d}z \\
&= \int_b^\eta \frac{\partial u}{\partial x}\,\mathrm{d}z + \int_b^\eta \frac{\partial v}{\partial y}\,\mathrm{d}z + w|_{z=\eta} - w|_{z=b} \\
&= \frac{\partial}{\partial x}\left(\int_b^\eta u\,\mathrm{d}z\right) - u|_{z=\eta}\frac{\partial \eta}{\partial x} + u|_{z=b}\frac{\partial b}{\partial x} + \frac{\partial}{\partial y}\left(\int_b^\eta u\,\mathrm{d}z\right) - u|_{z=\eta}\frac{\partial \eta}{\partial y} + u|_{z=b}\frac{\partial b}{\partial y} \\
&\quad + w|_{z=\eta} - w|_{z=b} \\
&= \frac{\partial \eta}{\partial t} + \frac{\partial}{\partial x}(h\overline{u}) + \frac{\partial}{\partial y}(h\overline{v})
\end{aligned}$$

where the last equality follows by the boundary conditions (7.5) and (7.7) as well as the definition of $\overline{u}$ and $\overline{v}$. Since b is time-independent and $\eta = b + h$, we can rewrite this as

$$\frac{\partial}{\partial t}h + \frac{\partial}{\partial x}(h\overline{u}) + \frac{\partial}{\partial y}(h\overline{v}) = 0. \tag{7.9}$$

Equation (7.9) is the conservation of mass part of the shallow-water equations. Notice that it contains $\overline{u}$, $\overline{v}$ and h, but not w and none of these functions depend on the vertical component z.

Our next step is to integrate the hydrostatic balance equation (7.4) using the boundary condition (7.6):

$$\begin{aligned}
p(x,y,z,t) &= p_a - \int_z^{\eta(x,y,t)} \frac{\partial p}{\partial \tilde{z}}(x,y,\tilde{z},t)\,\mathrm{d}\tilde{z} \\
&= p_a + \int_z^{\eta(x,y,t)} \varrho g\,\mathrm{d}\tilde{z} \\
&= p_a + \varrho g\big(\eta(x,y,z) - z\big).
\end{aligned}$$

This representation allows the determination of the partial derivatives in equations (7.2) and (7.3), namely

$$\frac{\partial p}{\partial x}(x,y,z,t) = \varrho g\frac{\partial \eta}{\partial x}(x,y,t) \qquad \text{and} \qquad \frac{\partial p}{\partial y}(x,y,z,t) = \varrho g\frac{\partial \eta}{\partial y}(x,y,t).$$

Notice that neither term actually depends on z. The corresponding differential equations then reads

$$\frac{\partial u}{\partial t} + u\frac{\partial u}{\partial x} + v\frac{\partial u}{\partial y} + w\frac{\partial u}{\partial z} = -g\frac{\partial \eta}{\partial x}, \tag{7.10}$$

$$\frac{\partial v}{\partial t} + u\frac{\partial v}{\partial x} + v\frac{\partial v}{\partial y} + w\frac{\partial v}{\partial z} = -g\frac{\partial \eta}{\partial y}. \tag{7.11}$$

As a welcome side-effect, the density drops out everywhere and therefore does not need to be measured.

The strategy is now the same as before: We integrate both equations (7.10) and (7.11) from the bottom $z = b(x, y)$ to the surface $z = \eta(x, y, t) = b(x, y) + h(x, y, t)$. We go over the details only for the x-direction. The y-direction can be treated similarly. The procedure is then to address what happens to each term of the momentum equation in vertical integration individually [1]. But first we reformulate the left side of the integration by adding an intelligent zero with the help of (7.1) and the product rule:

$$\begin{aligned}
&\int_b^\eta \frac{\partial u}{\partial t} + u\frac{\partial u}{\partial x} + v\frac{\partial u}{\partial y} + w\frac{\partial u}{\partial z}\,\mathrm{d}z \\
&\quad= \int_b^\eta \frac{\partial u}{\partial t} + u\frac{\partial u}{\partial x} + v\frac{\partial u}{\partial y} + w\frac{\partial u}{\partial z} + u\left(\frac{\partial u}{\partial x} + \frac{\partial v}{\partial y} + \frac{\partial w}{\partial z}\right)\,\mathrm{d}z \\
&\quad= \int_b^\eta \frac{\partial u}{\partial t} + \left[2u\frac{\partial u}{\partial x}\right] + \left[u\frac{\partial v}{\partial y} + v\frac{\partial u}{\partial y}\right] + \left[u\frac{\partial w}{\partial z} + w\frac{\partial u}{\partial z}\right]\,\mathrm{d}z \\
&\quad= \underbrace{\int_b^\eta \frac{\partial}{\partial t}u\,\mathrm{d}z}_{=:\mathrm{A}} + \underbrace{\int_b^\eta \frac{\partial}{\partial x}u^2\,\mathrm{d}z}_{=:\mathrm{B}} + \underbrace{\int_b^\eta \frac{\partial}{\partial y}(uv)\,\mathrm{d}z}_{=:\mathrm{C}} + \underbrace{\int_b^\eta \frac{\partial}{\partial z}(uw)\,\mathrm{d}z}_{=:\mathrm{D}}
\end{aligned}$$

where A, B, C and D are the terms to be examined on the left side and

$$\mathrm{E} := -g\int_b^\eta \frac{\partial \eta}{\partial x}\,\mathrm{d}z$$

is the term on the right. Most of these terms can be broken up using the Leibniz rule as before. The results of the integrations are

$$\mathrm{A} = \int_b^\eta \frac{\partial}{\partial t}u\,\mathrm{d}z = \frac{\partial}{\partial t}\left(\int_b^\eta u\,\mathrm{d}z\right) - u|_{z=\eta}\frac{\partial \eta}{\partial t}, \tag{7.12}$$

$$\mathrm{B} = \int_b^\eta \frac{\partial}{\partial x}u^2\,\mathrm{d}z = \frac{\partial}{\partial x}\left(\int_b^\eta u^2\,\mathrm{d}z\right) + u^2|_{z=b}\frac{\partial b}{\partial x} - u^2|_{z=\eta}\frac{\partial \eta}{\partial x}, \tag{7.13}$$

$$\mathrm{C} = \int_b^\eta \frac{\partial}{\partial y}(uv)\,\mathrm{d}z = \frac{\partial}{\partial y}\left(\int_b^\eta (uv)\,\mathrm{d}z\right) + (uv)|_{z=b}\frac{\partial b}{\partial y} - (uv)|_{z=\eta}\frac{\partial \eta}{\partial y}, \tag{7.14}$$

$$\mathrm{D} = \int_b^\eta \frac{\partial}{\partial z}(uw)\,\mathrm{d}z = (uw)|_{z=\eta} - (uw)|_{z=b}, \tag{7.15}$$

$$\mathrm{E} = -g\int_b^\eta \frac{\partial \eta}{\partial x}\,\mathrm{d}z = -g\frac{\partial \eta}{\partial x}(\eta - b) = -gh\frac{\partial \eta}{\partial x}, \tag{7.16}$$

where for (7.12) we used that b does not depend on time, for (7.15) we used the fundamental theorem of analysis and for (7.16) we used that η does not depend on z as well as $\eta = b + h$. So in total everything rearranges to

$$\begin{aligned}
&\frac{\partial}{\partial t}\left(\int_b^\eta u\,\mathrm{d}z\right) + \frac{\partial}{\partial x}\left(\int_b^\eta u^2\,\mathrm{d}z\right) + \frac{\partial}{\partial y}\left(\int_b^\eta uv\,\mathrm{d}z\right) \\
&\qquad - u|_{z=\eta}\left[\frac{\partial \eta}{\partial t} + u|_{z=\eta}\frac{\partial \eta}{\partial x} + v|_{z=\eta}\frac{\partial \eta}{\partial y} - w|_{z=\eta}\right] \\
&\qquad + u|_{z=b}\left[u|_{z=\eta}\frac{\partial b}{\partial x} + v|_{z=b}\frac{\partial b}{\partial y} - w|_{z=b}\right]
\end{aligned}$$

$$
\begin{aligned}
&= \int_b^\eta \frac{\partial u}{\partial t} + u\frac{\partial u}{\partial x} + v\frac{\partial u}{\partial y} + w\frac{\partial u}{\partial z}\,\mathrm{d}z \\
&= -g\int_b^\eta \frac{\partial \eta}{\partial x}\,\mathrm{d}z \\
&= -gh\frac{\partial \eta}{\partial x}.
\end{aligned}
$$

The first square bracket vanishes by the surface boundary condition (7.7) and the second one by the bottom one (7.5). If we use

$$
\overline{uv}(x,y,t) := \frac{1}{h(x,y,t)}\int_{b(x,y,t)}^{\eta(x,y,t)} u(x,y,z,t)v(x,y,z,t)\,\mathrm{d}z
$$

and

$$
\overline{u^2}(x,y,t) := \frac{1}{h(x,y,t)}\int_{b(x,y,t)}^{\eta(x,y,t)} u(x,y,z,t)^2\,\mathrm{d}z
$$

as depth-averaged products in addition to $\overline{u}$ and $\overline{v}$ from (7.8), we find the partial differential equation

$$
\frac{\partial}{\partial t}(h\overline{u}) + \frac{\partial}{\partial x}(h\overline{u^2}) + \frac{\partial}{\partial y}(h\overline{uv}) = -gh\frac{\partial}{\partial x}\eta.
$$

Since $\eta = b + h$ and $h\frac{\partial h}{\partial x} = \frac{\partial}{\partial x}(\frac{1}{2}h^2)$ by the product rule, we can reformulate the right side in terms of h to give

$$
\frac{\partial}{\partial t}(h\overline{u}) + \frac{\partial}{\partial x}(h\overline{u^2} + \frac{1}{2}gh^2) + \frac{\partial}{\partial y}(h\overline{uv}) = -gh\frac{\partial}{\partial x}b. \tag{7.17}
$$

The corresponding equation for the y-direction of momentum is derived the same way and has the form

$$
\frac{\partial}{\partial t}(h\overline{v}) + \frac{\partial}{\partial x}(h\overline{uv}) + \frac{\partial}{\partial y}(h\overline{v^2} + \frac{1}{2}gh^2) = -gh\frac{\partial}{\partial y}b, \tag{7.18}
$$

where $\overline{v^2}$ is defined analogously to $\overline{u^2}$. This concludes the depth integration.

You would be forgiven to think that (7.9), (7.17) and (7.18) are the shallow-water equations. They sure look like what we set out for. But we must be precise and looks can be deceiving: Said system is not a differential equation for $\overline{u}, \overline{v}$ and h at all! Notice that in general the mixed averages are not the same as the product of the averages, i. e. $\overline{u^2} \neq \overline{u}^2$, $\overline{v^2} \neq \overline{v}^2$ and $\overline{uv} \neq \overline{u}\,\overline{v}$. They need to be expanded to give

$$
\frac{\partial}{\partial x}(h\overline{u^2}) = \frac{\partial}{\partial x}(h\overline{u}^2) + \frac{\partial}{\partial x}\left(\int_b^\eta \left(\overline{u} - u\right)^2 \mathrm{d}z\right),
$$

$$
\frac{\partial}{\partial x}(h\overline{v^2}) = \frac{\partial}{\partial x}(h\overline{v}^2) + \frac{\partial}{\partial x}\left(\int_b^\eta \left(\overline{v} - v\right)^2 \mathrm{d}z\right)
$$

and

$$
\frac{\partial}{\partial x}(h\overline{uv}) = \frac{\partial}{\partial x}(h\overline{u}\,\overline{v}) + \frac{\partial}{\partial x}\left(\int_b^\eta \left(\overline{u} - u\right)\left(\overline{v} - v\right)\mathrm{d}z\right).
$$

Only after neglecting the integral terms are we able to formulate the actual shallow-water system which we state here in full for the sake of completeness:

$$\frac{\partial}{\partial t}h + \frac{\partial}{\partial x}(h\overline{u}) + \frac{\partial}{\partial y}(h\overline{v}) = 0, \tag{7.19}$$

$$\frac{\partial}{\partial t}(h\overline{u}) + \frac{\partial}{\partial x}(h\overline{u}^2 + \frac{1}{2}gh^2) + \frac{\partial}{\partial y}(h\overline{u}\,\overline{v}) = -gh\frac{\partial}{\partial x}b, \tag{7.20}$$

$$\frac{\partial}{\partial t}(h\overline{v}) + \frac{\partial}{\partial x}(h\overline{u}\,\overline{v}) + \frac{\partial}{\partial y}(h\overline{v}^2 + \frac{1}{2}gh^2) = -gh\frac{\partial}{\partial y}b. \tag{7.21}$$

Alternatively one can include the integral terms inside of a friction term. (Friction was already neglected in the derivation of the Euler equation, though.) See [3] for more details and a discussion of how reasonable this assumption is. In terms of the recipe from the previous section step 5. is hereby finished which concludes the derivation.

8 Discussion of the Shallow-Water Model

In the previous section we obtained the *two-dimensional shallow-water system* (recall that we defined indices to symbol differentiation, e. g. $()_t := \partial/\partial t$)

$$h_t + (hu)_x + (hv)_y = 0, \tag{8.1}$$

$$(hu)_t + (hu^2 + \tfrac{1}{2}gh^2)_x + (huv)_y = -ghb_x, \tag{8.2}$$

$$(hv)_t + (huv)_x + (hv^2 + \tfrac{1}{2}gh^2)_y = -ghb_y, \tag{8.3}$$

for waves of height $(x, y, t) \mapsto h(x, y, t)$ and horizontal speeds $(x, y, t) \mapsto u(x, y, t)$, $(x, y, t) \mapsto v(x, y, t)$ where $(x, y) \mapsto b(x, y)$ describes the bottom profile and $g \approx 9.81\ \frac{\mathrm{m}}{\mathrm{s}^2}$ is the acceleration due to gravity (cf. figure 6.1). The underlying shallow-water assumption was that the horizontal scales are much larger than the vertical one. Here it is still assumed that u and v are depth-averaged, even though this is typically omitted from the notation. Recall that the first equation represents conservation of mass while the other two were derived from conservation of momentum. This section will investigate the shallow-water system further and comment on typical extensions to the model. It also serves as an outlook to several topics that this thesis could not cover. We refer to the respective literature in each case. As a general reference one can take [22] and chapter 1 of [15].

We first look at how the shallow-water equations tie into the framework of hyperbolic conservation laws from section 3. To this end, let us introduce the notation $\boldsymbol{q} := (q_1, q_2, q_3)^{\mathrm{T}} := (h, hu, hv)^{\mathrm{T}}$ for the conserved quantities. To obtain a balance law form

$$\boldsymbol{q}_t + \boldsymbol{f}(\boldsymbol{q})_x + \boldsymbol{g}(\boldsymbol{q})_y = \boldsymbol{\psi}(\boldsymbol{q}, x, y) \tag{8.4}$$

of the system (8.1), (8.2), (8.3) we also set

$$\boldsymbol{f}(\boldsymbol{q}) := \begin{pmatrix} q_2 \\ q_2^2/q_1 + \frac{1}{2}gq_1^2 \\ q_2q_3/q_1 \end{pmatrix} = \begin{pmatrix} hu \\ hu^2 + \frac{1}{2}gh^2 \\ huv \end{pmatrix}$$

and

$$\boldsymbol{g}(\boldsymbol{q}) := \begin{pmatrix} q_3 \\ q_2 q_3/q_1 \\ q_3^2/q_1 + \frac{1}{2} g q_1^2 \end{pmatrix} = \begin{pmatrix} hv \\ huv \\ hv^2 + \frac{1}{2} g h^2 \end{pmatrix}$$

for the fluxes as well as

$$\boldsymbol{\psi}(\boldsymbol{q}, x, y) := (0, -g q_1 b_x, -g q_1 b_y)^{\mathrm{T}} = (0, -ghb_x, -ghb_y)^{\mathrm{T}}$$

for the source term. If the bathymetry is approximately flat, the source vector $\boldsymbol{\psi}$ disappears and (8.4) becomes a homogeneous system.

For numerical considerations we will also frequently study the *one-dimensional shallow-water equations*

$$h_t + (hu)_x = 0, \tag{8.5}$$

$$(hu)_t + (hu^2 + \tfrac{1}{2} g h^2)_x = -ghb_x. \tag{8.6}$$

In this case the y-direction is dropped, so that the functions are $(x,t) \mapsto h(x,t), (x,t) \mapsto u(x,t)$ and $x \mapsto b(x)$. This system was first derived by Adhémar Jean Claude Barré de Saint-Venant and is thus sometimes referred to as the *Saint-Venant equations*. (Some authors use this name for the two-dimensional version, too, even though Saint-Venant did not study it.) Its original purpose was to model open-channel flow, particularly that in rivers [13]. The one-dimensional version can also be written in conservation form

$$\boldsymbol{q}_t + \boldsymbol{f}(\boldsymbol{q})_x = \boldsymbol{\psi}(\boldsymbol{q}, x)$$

by defining the vector $\boldsymbol{q} := (q_1, q_2)^{\mathrm{T}} := (h, hu)^{\mathrm{T}}$ for the conserved variables and

$$\boldsymbol{f}(\boldsymbol{q}) := \begin{pmatrix} q_2 \\ q_2^2/q_1 + \frac{1}{2} g q_1^2 \end{pmatrix} = \begin{pmatrix} hu \\ hu^2 + \frac{1}{2} g h^2 \end{pmatrix}, \quad \boldsymbol{\psi}(\boldsymbol{q}, x) := \begin{pmatrix} 0 \\ -g q_1 b_x \end{pmatrix} = \begin{pmatrix} 0 \\ -ghb_x \end{pmatrix}$$

for the flux and the source term.

Throughout the rest of this thesis we will mainly work with the one-dimensional system

$$\boldsymbol{q}_t + \boldsymbol{f}(\boldsymbol{q})_x = \boldsymbol{0} \quad \text{for all } (x,t) \in \mathbb{R} \times \left]\bar{t}, \infty\right[\tag{8.7}$$

for a given time $\bar{t} \geqslant 0$. It is therefore worth examining its theoretical properties. First, we note that, given a smooth solution, the conservation law (8.7) can be rewritten in quasilinear form

$$\boldsymbol{q}_t + \boldsymbol{f}'(\boldsymbol{q}) \boldsymbol{q}_x = \boldsymbol{0}$$

where the Jacobian matrix is given by

$$\boldsymbol{f}'(\boldsymbol{q}) = \begin{pmatrix} 0 & 1 \\ -(q_2/q_1)^2 + g q_1 & 2 q_2/q_1 \end{pmatrix} = \begin{pmatrix} 0 & 1 \\ -u^2 + gh & 2u \end{pmatrix}.$$

Simple linear algebra shows that its eigenvalues are

$$\lambda_1 = u - \sqrt{gh} \quad \text{and} \quad \lambda_2 = u + \sqrt{gh}$$

with corresponding eigenvectors

$$\boldsymbol{r}_1 = \begin{pmatrix} 1 \\ u - \sqrt{gh} \end{pmatrix} \quad \text{and} \quad \boldsymbol{r}_2 = \begin{pmatrix} 1 \\ u + \sqrt{gh} \end{pmatrix}.$$

For physically-relevant depths $h \geqslant 0$ the eigenvalues remain real-valued and as long as $h > 0$ they are actually distinct. In particular, this shows that (8.7) is a hyperbolic equation.

In the following chapters we will need the results of the Riemann problem for the one-dimensional shallow-water equations which is obtained when combining (8.7) with piecewise constant initial conditions

$$\boldsymbol{q}(x,\overline{t}) = \left\{ \begin{array}{ll} \boldsymbol{q}_\ell, & \text{if } x < \overline{x}, \\ \boldsymbol{q}_\mathrm{r}, & \text{if } x > \overline{x} \end{array} \right\} \quad \text{for all } x \in \mathbb{R}$$

with two given vectors $\boldsymbol{q}_\ell, \boldsymbol{q}_\mathrm{r} \in \mathbb{R}^2$ and a given point $\overline{x} \in \mathbb{R}$ and times $\overline{t} > 0$. This problem can be solved completely, see [28]. However, we cannot present these ideas here in their full form. For our purposes a rough understanding will suffice. One finds that that two waves always separate three constant states. Each wave is associated with an eigenvector of $\boldsymbol{f}'(\boldsymbol{q})$; the eigenvalues are the speeds of propagation. The wave corresponding to the first eigenvector is usually referred to as the 1-wave and the wave corresponding to the second the 2-wave. Each wave may be a shock or a rarefaction. Between the two constant states $\boldsymbol{q}_\ell$ and $\boldsymbol{q}_\mathrm{r}$ one finds a constant middle state $\boldsymbol{q}_\mathrm{m}$. Figure 8.1 shows a 1-rarefaction and a 2-shock. We note that the figure presents the case where one wave is going in either direction.

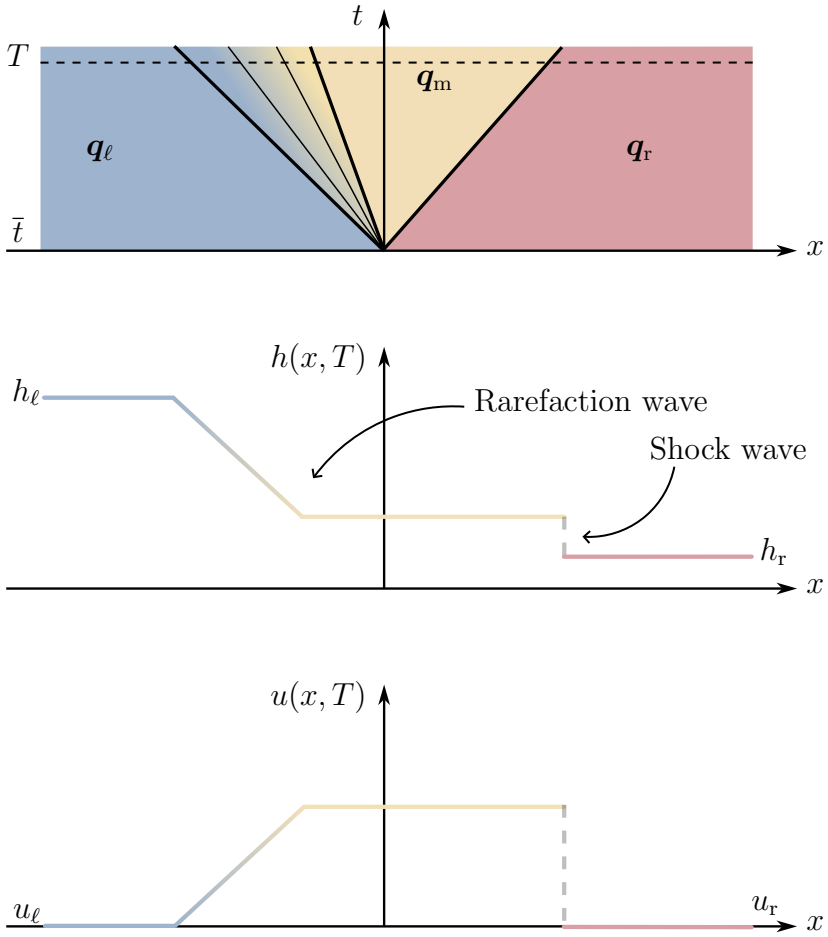

Figure 8.1: Typical solution of a Riemann problem for the one-dimensional shallow-water equations at some time $T > \overline{t}$. Adapted from [5].

This need not be the case, however. It is possible for both to go left (if $u < -\sqrt{gh}$) or

right (if $u > \sqrt{gh}$), corresponding to so-called *supercritical flow* (analogous to supersonic flow in gas dynamics). In our applications this is almost never needed – they correspond to the *subcritical* case ($\lambda_1 < 0 < \lambda_2$). For tsunamis, supercritical flow occurs only for very shallow water near the shore. The ratio $|u|/\sqrt{gh}$ is called the *Froude number* (analogous to the Mach number in gas dynamics). It is worth pointing out that these waves travel at velocities of $\pm\sqrt{gh}$ relative to the background velocity u. The speed $c := \sqrt{gh}$ is called the *gravity wave speed* (it is analogous to the speed of sound in small-amplitude acoustics). For tsunami modeling u is typically very small, so that the velocity of propagation mainly depends on $\sqrt{gh}$ and thereby on the depth. For a typical ocean depth of 4 km one finds a speed of about $200\,\frac{\mathrm{m}}{\mathrm{s}} = 720\,\frac{\mathrm{km}}{\mathrm{h}}$. In shallower waters the wave speed decreases. If we take the depth of the continental shelf (cf. section 4) to be 100 m, then the speed reduces to about $30\,\frac{\mathrm{m}}{\mathrm{s}} = 108\,\frac{\mathrm{km}}{\mathrm{h}}$.

Let us now turn to possible extensions of the shallow-water model. Recall that when we applied the Euler equations to the tsunami wave setup in section 6, we assumed that gravity was the only acting body force. This is not accurate on earth. When a particle moves on a rotating sphere, it experiences a ficticious force, the so-called *coriolis force*. This is a byproduct of viewing the particle in an accelerated frame of reference and would not appear to an outside onlooker in an inertial frame. To account for it in our momentum equations, we would add a term $-fv$ to the left side of (8.2) and a term $+fu$ to the left side of (8.3) where f is the coriolis parameter which depends on the location of the particle on earth [19]. Fortunately, this force has little effect on applications like the movement of tsunamis and can thus be neglected. Another ficticious force caused by the rotation of earth is the *centrifugal force* which is directed in the opposite direction of gravity. And while this force does have an effect on the shape of the earth, causing it to look more like an ellipsoid than a sphere, it can safely be neglected even in cases where the coriolis force is considered [7].

An idea that naturally ties into that of incorporating effects due to rotation is introducing curvilinear coordinates (e. g. spherical coordinates). A detailed derivation can be found in [31]. Interestingly, a two-dimensional problem can turn into a one-dimensional one, if it exhibits radial symmetry. Such is the case with so-called *radial dam break* which is obtained by combining the two-dimensional system (8.1), (8.2), (8.3) with initial data of the form

$$h(x,y,0) := \left\{ \begin{array}{ll} h_{\text{inside}}, & \text{if } x^2+y^2 \leqslant R^2, \\ h_{\text{outside}}, & \text{if } x^2+y^2 > R^2 \end{array} \right\}, \quad (hu)_0(x,y) := 0 \qquad \text{for all } x,y \in [-\overline{x},\overline{x}]$$

where $h_{\text{inside}} > h_{\text{outside}} > 0$ are two known constants and so is $R > 0$. The speeds are initially set to zero and bathymetry is assumed to be constant. The resulting two-dimensional system can then be rewritten in a one-dimensional form

$$\begin{aligned} h_t + (hu)_r &= -\tfrac{hu}{r}, \\ (hu)_t + (hu^2 + \tfrac{1}{2}gh^2)_r &= -\tfrac{hu^2}{r} \end{aligned} \tag{8.8}$$

using the radial direction $r := \sqrt{x^2+y^2}$. Here the involved functions are $(r,t) \mapsto h(r,t)$ and $(r,t) \mapsto u(r,t)$. In this case u represents a radial velocity. The full solution is then obtained by rotating these functions around the vertical axis. Notice how similar (8.8) looks to the one-dimensional shallow-water system (8.6). Only the source terms are different. In this case one has $\boldsymbol{\psi}(\boldsymbol{q},r) := -1/r(hu,hu^2)^{\mathrm{T}}$ instead.

During our initial derivation of the shallow-water equations, we neglected friction terms (particularly at the ocean floor). If one were to include them, they would appear in the momentum equations in the form of a drag coefficient $D(h, u, v)$ to give

$$\begin{aligned}(hu)_t + (hu^2 + \tfrac{1}{2}gh^2)_x + (huv)_y &= -ghb_x - D(h,u,v)hu,\\ (hv)_t + (huv)_x + (hv^2 + \tfrac{1}{2}gh^2)_y &= -ghb_y - D(h,u,v)hv.\end{aligned}$$

A typical profile for the drag function is

$$D(h, u, v) = n^2 g h^{-7/8}\sqrt{u^2 + v^2},$$

where the so-called *Manning coefficient* n is typically set to be around $n = 0.025$ for tsunami modeling. We did not just omitt this term to simplify the derivation. In deep water it turns out to be negligibly small compared to the other terms in the momentum equation. So it is customary to only start considering it close to shore, e. g. in depths shallower than 100 meters.

One can also consider several layers of fluid that are stacked on top of each other. The one-dimensional shallow-water equations for two layers take the form

$$\begin{aligned}(h_1)_t + (h_1u_1)_x &= 0,\\ (h_1u_1)_t + \left(h_1u_1^2 + \tfrac{1}{2}gh_1^2\right)_x &= -gh_1(h_2)_x - gh_1b_x,\\ (h_2)_t + (h_2u_2)_x &= 0,\\ (h_2u_2)_t + \left(h_2u_2^2 + \tfrac{1}{2}gh_2^2\right)_x &= -\varrho_0 gh_2(h_1)_x - gh_2b_x,\end{aligned}$$

where h_1, h_2 are the depths and u_1, u_2 the velocities of the upper and lower layer respectively. The function $x \mapsto b(x)$ is the bottom topography, ϱ_0 is the ratio of the densities ($\varrho_0 := \varrho_1/\varrho_2 < 1$) between the two fluid layers and $g \approx 9.81\ \frac{\mathrm{m}}{\mathrm{s}^2}$ is again the acceleration due to gravity [24]. Typically, the top layer could represent the flow in the upper few hundred

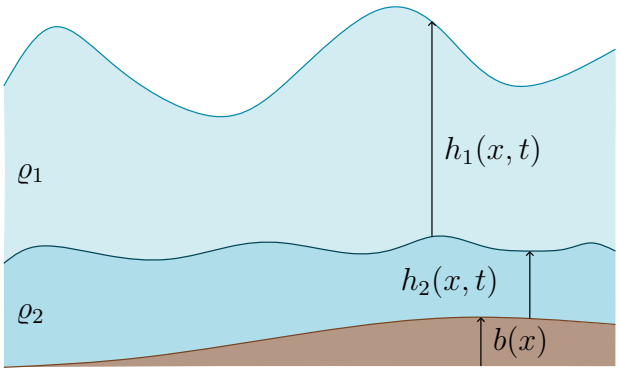

Figure 8.2: Geometry of the two-layer shallow-water equations. The lower layer is colored in to represent water. Alternatively it could represent a moving layer of ocean floor, e. g. during a landslide. Adapted from [30, Figure 3.5].

meteres of the ocean where most of the noticable movement occurs and the lower layer the deep ocean that hardly moves. One can also turn this on its head and see the two-layer shallow-water equations as an atmospheric model where the lower layer represents the active troposphere and the upper one the inactive stratosphere [30]. In addition, it serves as a model for tsunamis caused by underwater landslides.

Not only for tsunamis caused by underwater landslides do we need to augment the system (8.1), (8.2), (8.3). Different tsunami origins require different adjustments to the models. Marsha Berger has recently begun to study tsunamis caused by asteroids, for example. In this case the shallow-water equations are extended by both a stress term like above and a pressure term which is needed since the asteroid causes a shock wave infront of it as it enters the atmosphere [4]. By far the most common cause of tsunamis are suboceanic earthquakes, though, and we do expect their propagation to be modeled acurately by the standard shallow-water equations.

The shallow-water equations are not the be-all and end-all in terms of tsunami models. Many different partial differential equations have been used in an attempt to improve accuracy, see section 5.1 of [10]. It should be noted, however, that higher accuracy typically comes at the cost of computation time. And time is a valuable resource when issuing tsunami warnings and evacuating people. The shallow-water equations seem to strike a good balance between being sufficiently easy to solve to guarantee fast computation and between being sufficiently complex to model the real world accurately enough.

Chapter III

Finite-Volume Methods

This chapter gives an overview of a special class of numerical methods which were developed specifically for the solution of hyperbolic conservation laws like the shallow-water equations. As it turns out, solving the shallow-water system is a relatively difficult task which requires many advanced tools. Their detailed description would lie beyond the scope of this thesis. For this reason, we will present a very high-level view throughout this chapter, leaving the details to the respective literature. Our end goal will be to collect all the necessary tools to solve the shallow-water equations in one spatial dimension with bathymetry.

The subsequent sections are structured as follows: In section 9 we give a general introduction to the idea of finite-volume methods. As a concrete representative we then study Godunov-type methods (section 10) which use Riemann problems for their numerical updates. The Riemann problems which appear during a Godunov method are often too expensive to solve exactly. This motivates the need for approximate Riemann solvers which are the contents of section 11. And since the treatment of finite-volume methods up to this point did not include source terms, section 12 will introduce a way to handle these. All of this discussion culminates in section 13 where we test our algorithms on several examples.

9 General Derivation of Finite-Volume Methods

Countless algorithms have been developed for the numerical solution of differential equations. However, not all methods work well for all types of problems. The class of finite-volume methods were specifically developed for the solution of hyperbolic conservation laws and are hence a natural choice for the solution of the shallow-water equations. This section briefly describes the idea behind finite-volume methods. Standard references are [20] and [27].

Throughout this chapter we will consider a hyperbolic system of m conservation laws in one spatial dimension

$$\begin{aligned} \boldsymbol{q}_t + \boldsymbol{f}(\boldsymbol{q})_x &= \boldsymbol{\psi}(\boldsymbol{q}, x) \quad \text{for all } (x,t) \in \mathbb{R} \times]0, \infty[\,, \\ \boldsymbol{q}(x,0) &= \boldsymbol{q}_0(x) \qquad \text{for all } x \in \mathbb{R}, \end{aligned} \tag{9.1}$$

where $\boldsymbol{q}(x,t) \in \mathbb{R}^m$ is the vector of conserved quantities, $\boldsymbol{q}_0 : \mathbb{R} \to \mathbb{R}^m$ an initial value, $\boldsymbol{f}(\boldsymbol{q}) \in \mathbb{R}^m$ the vector of fluxes and $\boldsymbol{\psi}(\boldsymbol{q}, x) \in \mathbb{R}^m$ the vector of source terms. While $\boldsymbol{q}$ is unknown, $\boldsymbol{f}$, $\boldsymbol{q}_0$ and $\boldsymbol{\psi}$ are given. The general derivation of finite-volume methods relies on the special case where (9.1) is homogeneous, i. e. $\boldsymbol{\psi} \equiv 0$. As we have noted before, this is the original form of a conservation law, wheras the form with the source term is often called a balance law. Integrating the source terms adequately will be the focus of a subsequent section.

For numerical considerations, we introduce a discretization of the x-t-plane with a mesh width $\Delta x > 0$ and a time step $\Delta t > 0$. Both values are assumed to be fixed for the sake of simplicity, though this is by no means necessary. These step sizes allow the introduction of grid points

$$\begin{aligned} x_i &:= i\Delta x, \qquad i = \ldots, -2, -1, 0, 1, 2, \ldots, \\ t_n &:= n\Delta t, \qquad n = 0, 1, 2, \ldots \end{aligned}$$

We will also require the notation

$$x_{i\pm1/2} = x_i \pm \frac{\Delta x}{2} = \left(i \pm \frac{1}{2}\right)\Delta x, \qquad i = \ldots, -2, -1, 0, 1, 2, \ldots$$

to denote the points in the middle of the inveralls $[x_i, x_{i+1}]$ and $[x_{i-1}, x_i]$ respectively. Around each point x_i the interval $\mathcal{C}_i := [x_{i-1/2}, x_{i+1/2}]$ is called the i-th *grid cell*. Notice that from this perspective the points $x_{i\pm1/2}$ are the cell boundaries of $\mathcal{C}_i$. For the sake of simplicity we will not restate the sets of indices for each occurrence of i and n. Whenever the reader encounters them, both $i \in \mathbb{Z}$ and $n \in \mathbb{N}_0$ are usually implied.

As we have already seen in section 3 the more natural formulation of a conservation law is not the differential form (9.1), but rather its integral form

$$\frac{\mathrm{d}}{\mathrm{d}t}\left(\int_{\mathcal{C}_i} \boldsymbol{q}(x,t)\,\mathrm{d}x\right) = \boldsymbol{f}\big(\boldsymbol{q}(x_{i-1/2},t)\big) - \boldsymbol{f}\big(\boldsymbol{q}(x_{i+1/2},t)\big) \tag{9.2}$$

(cf. equation (3.3)). This is the starting point for the derivation of all finite-volume methods. To this end, let us begin by integrating (9.2) from t_n to t_{n+1}. The result is

$$\int_{\mathcal{C}_i} \boldsymbol{q}(x,t_{n+1})\,\mathrm{d}x - \int_{\mathcal{C}_i} \boldsymbol{q}(x,t_n)\,\mathrm{d}x = \int_{t_n}^{t_{n+1}} \boldsymbol{f}\big(\boldsymbol{q}(x_{i-1/2},t)\big)\,\mathrm{d}t - \int_{t_n}^{t_{n+1}} \boldsymbol{f}\big(\boldsymbol{q}(x_{i+1/2},t)\big)\,\mathrm{d}t \tag{9.3}$$

which is clearly equivalent to

$$\begin{aligned} &\frac{1}{\Delta x}\int_{\mathcal{C}_i} \boldsymbol{q}(x,t_{n+1})\,\mathrm{d}x - \frac{1}{\Delta x}\int_{\mathcal{C}_i} \boldsymbol{q}(x,t_n)\,\mathrm{d}x \\ &\qquad = -\frac{\Delta t}{\Delta x}\left(\frac{1}{\Delta t}\int_{t_n}^{t_{n+1}} \boldsymbol{f}\big(\boldsymbol{q}(x_{i+1/2},t)\big)\,\mathrm{d}t - \frac{1}{\Delta t}\int_{t_n}^{t_{n+1}} \boldsymbol{f}\big(\boldsymbol{q}(x_{i-1/2},t)\big)\,\mathrm{d}t\right). \end{aligned} \tag{9.4}$$

Instead of trying to approximate the solution function $\boldsymbol{q}$ directly, finite-volume methods instead try to approximate the integral terms in (9.4) for each cell $\mathcal{C}_i$ at any given time t_n. This approach is more suitable for discontinuous solutions since it does not rely on $\boldsymbol{q}$ being defined at every point. The reason that we prefer (9.4) over (9.3) is the following interpretation: If $f : [a,b] \to \mathbb{R}$ is any integrable function, then from elementary calculus it is well-known that $\frac{1}{b-a}\int_a^b f(x)\,\mathrm{d}x$ can be seen as its average value over the interval $[a,b]$. In this sense each term in (9.4) admits a physical interpretation as either a spatial average of the solution function at a fixed time or as a time average of the flux function at the left or right boundary point of the i-th cell. It is customary to denote approximations with upper case and exact values with lower case letters, i. e., we will write

$$\begin{aligned} \boldsymbol{Q}_i^n &\approx \frac{1}{\Delta x}\int_{\mathcal{C}_i} \boldsymbol{q}(x,t_n)\,\mathrm{d}x =: \boldsymbol{q}_i^n, \\ \boldsymbol{F}_{i\pm1/2}^n &\approx \frac{1}{\Delta t}\int_{t_n}^{t_{n+1}} \boldsymbol{f}\big(\boldsymbol{q}(x_{i\pm1/2},t)\big)\,\mathrm{d}t =: \boldsymbol{f}_{i\pm1/2}^n. \end{aligned}$$

Superscripts always indicate the time step and subscripts always the cell. In particular, the superscript does not signal exponentiation here! With this notation (9.4) can be written as

$$\boldsymbol{q}_i^{n+1} = \boldsymbol{q}_i^n - \frac{\Delta t}{\Delta x}(\boldsymbol{f}_{i+1/2}^n - \boldsymbol{f}_{i-1/2}^n)$$

which suggest that our numerical method should be of the form

$$\boldsymbol{Q}_i^{n+1} = \boldsymbol{Q}_i^n - \frac{\Delta t}{\Delta x}(\boldsymbol{F}_{i+1/2}^n - \boldsymbol{F}_{i-1/2}^n). \tag{9.5}$$

The numerical approximation to the exact solution function $\boldsymbol{q}$ is then given as the step

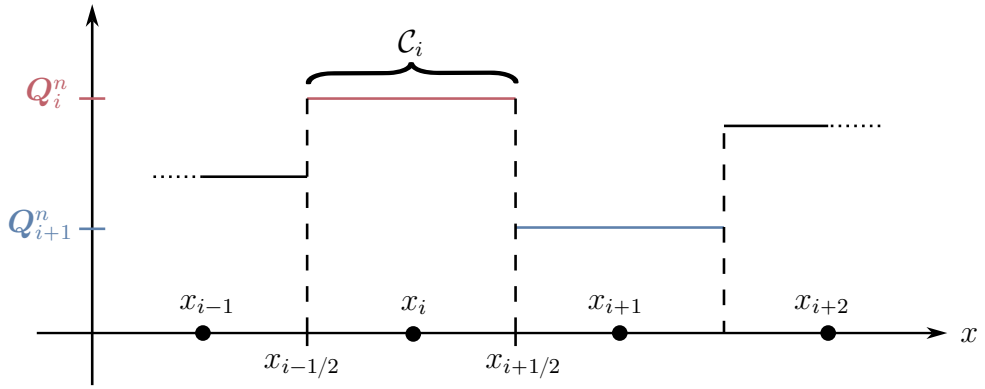

Figure 9.1: Numerical approximation to $x \mapsto \boldsymbol{q}(x, t_n)$. Adapted from [27, Figure 6.1].

function which is obtained by assigning the value $\boldsymbol{Q}_i^n$ to the entire cell $\mathcal{C}_i$ at any fixed point in time t_n, cf. figure 9.1.

While the $\boldsymbol{Q}_i^n$ term in (9.5) will be known at each point in the iteration (because in an initial value problem $\boldsymbol{q}(x, 0)$ is known), we have yet to explain how one can suitably

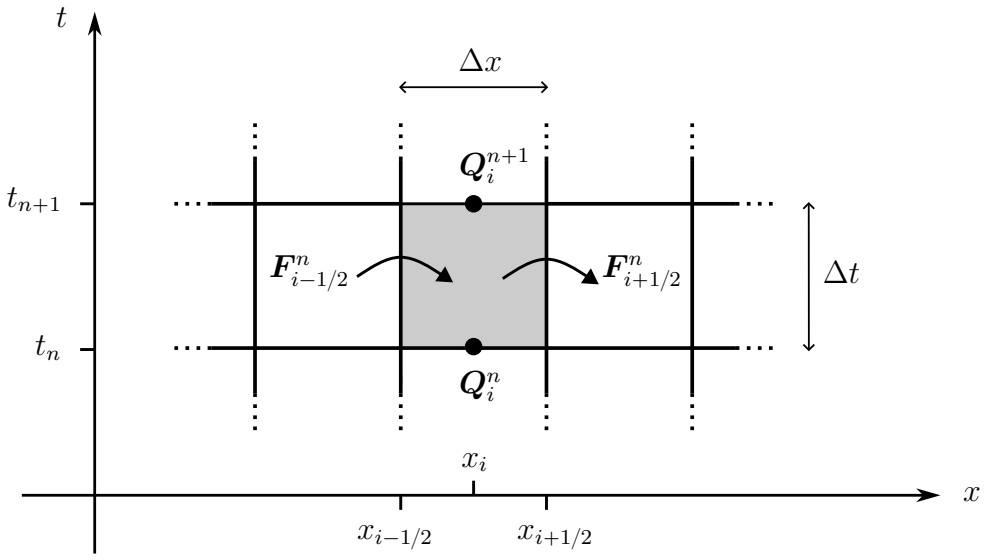

Figure 9.2: Change from time step t_n to t_{n+1} in cell $\mathcal{C}_i$ as seen from the x-t-plane. Adapted from [20, Figure 4.1].

approximate the flux averages. Indeed, the main focus of any specific finite-volume method

will be a clever procedure to do exactly this. We note, however, that generally one would hope to find a relationship of the form $\boldsymbol{F}^n_{i-1/2} = \mathcal{F}(\boldsymbol{Q}^n_{i-1}, \boldsymbol{Q}^n_i)$ where $\mathcal{F}$ is a so-called *numerical flux function*. With it the general finite-volume method (9.5) would take the form

$$\boldsymbol{Q}^{n+1}_i = \boldsymbol{Q}^n_i - \frac{\Delta t}{\Delta x}\big[\mathcal{F}(\boldsymbol{Q}^n_i, \boldsymbol{Q}^n_{i+1}) - \mathcal{F}(\boldsymbol{Q}^n_{i-1}, \boldsymbol{Q}^n_i)\big].$$

The following section will showcase concrete examples of such numerical flux functions.

Notice that algorithm (9.5) actually mirrors the conservation law in a way. A first indication of this is given by rewriting it as

$$\frac{\boldsymbol{Q}^{n+1}_i - \boldsymbol{Q}^n_i}{\Delta t} + \frac{\boldsymbol{F}^n_{i+1/2} - \boldsymbol{F}^n_{i-1/2}}{\Delta x} = \boldsymbol{0}.$$

This looks like a version of the original conservation law (9.1) where the partial derivatives were discretized with finite differences. But there is more: In these methods, the change in the cell's average value is given by the difference of the fluxes across the boundary of the cell. In fact, this even remains true, if we consider several cells at once. Between the I-th and the J-th cell ($I, J \in \mathbb{Z}$) we find by summing (9.5) that a telescoping sum emerges because $\boldsymbol{F}^n_{i+1/2} = \boldsymbol{F}^n_{(i+1)-1/2}$, namely

$$\sum_{i=I}^{J} \boldsymbol{Q}^{n+1}_i \Delta x = \sum_{i=I}^{J} \boldsymbol{Q}^n_i \Delta x - \Delta t(\boldsymbol{F}^n_{J+1/2} - \boldsymbol{F}^n_{I-1/2}).$$

This shows that, no matter how the $\boldsymbol{F}^n_{i\pm1/2}$ are chosen, all of the fluxes cancel except for the ones at the boundaries. Since the sums represent the numerical approximations to the integral of $\boldsymbol{q}$ over the entire interval $[x_{I-1/2}, x_{J+1/2}]$, this tells us that the change between cell $\mathcal{C}_I$ and cell $\mathcal{C}_J$ from any point in time t_n to the next t_{n+1} is only due to difference in flux across the boundaries of said interval. In this sense the numerical solutions actually mirror the physical features of the actual solution. Methods with this desirable property are more generally called *conservative*. Hence, any finite-volume method is conservative by construction.

We do not have the time to elaborate on the theoretical considerations which usually surround numerical methods (convergence, speed, stability, et cetera). A thorough discussion is given in chapter 8 of [20]. It is worth noting that the method which is presented here is only of first order, meaning that it takes a relatively long time to achieve high accuracy. In many practical applications fast results are a key, however. In this case, schemes of higher order must be employed.

10 Godunov-Type Methods

In the previous section we derived the general form of a finite-volume method

$$\boldsymbol{Q}^{n+1}_i = \boldsymbol{Q}^n_i - \frac{\Delta t}{\Delta x}(\boldsymbol{F}^n_{i+1/2} - \boldsymbol{F}^n_{i-1/2}) \tag{10.1}$$

for the solution of the conservation law (9.1) without source terms. Like in the last section, every occurrence of i and n is to be understood in the sense of "for all $i \in \mathbb{Z}$ and all $n \in \mathbb{N}_0$".

This section explores one common method of approximating the numerical fluxes $\boldsymbol{F}^n_{i\pm1/2}$, the so-called *Godunov method*. Its fundamental idea is to solve Riemann problems at the boundaries between the different cells. A more detailed description than ours can be found in chapter 6 of [27].

To see how Godunov's method works in detail, let us assume that all cell averages $\boldsymbol{Q}^n_i$ have already been computed at a time t_n. To begin, we use these values to define a piecewise constant function $\tilde{\boldsymbol{q}}^n_{\text{initial}} : \mathbb{R} \to \mathbb{R}^m$ via

$$\tilde{\boldsymbol{q}}^n_{\text{initial}}(x) := \boldsymbol{Q}^n_i \quad \text{for all } x \in \mathcal{C}_i = [x_{i-1/2}, x_{i+1/2}] \tag{10.2}$$

(cf. figure 9.1). This function now serves as the initial condition for the intermediate problem

$$\begin{aligned} (\tilde{\boldsymbol{q}}^n)_t + \boldsymbol{f}(\tilde{\boldsymbol{q}}^n)_x &= \boldsymbol{0} && \text{for all } (x,t) \in \mathbb{R} \times \,]t_n, \infty[\,, \\ \tilde{\boldsymbol{q}}^n(x, t_n) &= \tilde{\boldsymbol{q}}^n_{\text{initial}}(x) && \text{for all } x \in \mathbb{R}, \end{aligned} \tag{10.3}$$

which is simply the original conservation law with the now-modified initial data from (10.2). Its solution function $(x,t) \mapsto \tilde{\boldsymbol{q}}^n(x,t)$ can already be viewed as an approximate solution to the original conservation law, although we will not use it as such. Notice that the initial data is essentially a sequence of Riemann problems because $\tilde{\boldsymbol{q}}^n_{\text{initial}}$ is piecewise-constant. For example, at the boundary $x_{i-1/2}$ one has to solve the Riemann problem

$$\begin{aligned} \tilde{\boldsymbol{q}}_t + \boldsymbol{f}(\tilde{\boldsymbol{q}})_x &= 0 && \text{for all } (x,t) \in \mathbb{R} \times \,]t_n, \infty[\,, \\ \tilde{\boldsymbol{q}}(x, t_n) &= \left\{ \begin{array}{ll} \boldsymbol{Q}^n_{i-1}, & \text{if } x < x_{i-1/2}, \\ \boldsymbol{Q}^n_i, & \text{if } x > x_{i-1/2} \end{array} \right\} && \text{for all } x \in \mathbb{R}. \end{aligned} \tag{10.4}$$

Each individual Riemann problem has its own solution wave associated with it. In principle, one can obtain the exact solution to (10.3) by simply piecing together the respective solutions of all the Riemann problems at each boundary — given that the waves from neighboring Riemann problems do not start interacting, that is. We can make sure of this by choosing a sufficiently small time step Δt. If $\lambda_{\max}$ denotes the maximum wave velocity that is encountered at any of the Riemann problems, then we must require

$$\Delta t \leqslant \frac{\Delta x}{\lambda_{\max}} \tag{10.5}$$

for this to be the case, i. e., the fastest characteristic generated at an interface cannot travel farther than one cell width within one time step. The term $C_{\text{Courant}} := \lambda_{\max} \Delta t / \Delta x$ is more generally referred to as the *Courant number*. Hence, our setting requires a Courant number of at most one. We note that this condition does allow the interaction of waves from neighboring Riemann problems, as long as they are contained within a fixed mesh cell. Luckily, there is no need to calculate these interactions explicitly because we only require the cell average over $[t_n, t_{n+1}]$ at a boundary point which is still easy to compute because the solution's value there does not change within a cell.

If this is given, then Godunov's method may be derived as follows. Notice that evaluation of $\tilde{\boldsymbol{q}}^n$ at t_{n+1} produces the function $x \mapsto \tilde{\boldsymbol{q}}^n(x, t_{n+1})$. In Godunov's method the next iterate is found by averaging this function over each grid cell, i. e.

$$\boldsymbol{Q}^{n+1}_i := \frac{1}{\Delta x} \int_{\mathcal{C}_i} \tilde{\boldsymbol{q}}^n(x, t_{n+1}) \, \mathrm{d}x.$$

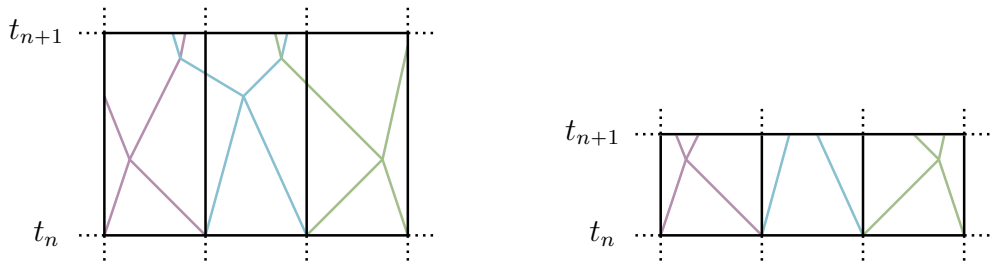

Figure 10.1: Waves from Riemann problems starting from the cell boundaries. (a) The time step is too large; the waves can cross into the neighboring cell. (b) The time step obeys the condition (10.5); the waves can interact, but without crossing into neighboring cells. Figure adapted from [20, Figure 15.1].

This process yields a particular finite-volume method (10.1) where the numerical flux function is given as

$$\boldsymbol{F}^n_{i-1/2} = \mathcal{F}(\boldsymbol{Q}^n_{i-1}, \boldsymbol{Q}^n_i) = \frac{1}{\Delta t} \int_{t_n}^{t_{n+1}} \boldsymbol{f}\big(\tilde{\boldsymbol{q}}^n(x_{i-1/2}, t)\big)\, \mathrm{d}t. \tag{10.6}$$

In fact, we can still simplify this somewhat. As we know from the discussions in section 3, the solution of the Riemann problem (10.4) is a similarity solution. As usual we will denote its solution function with $\tilde{\boldsymbol{q}}(\xi; \boldsymbol{q}_\ell, \boldsymbol{q}_\mathrm{r})$ where

$$\xi = \frac{x - x_{i-1/2}}{t - t_n}$$

is its characteristic variable, $\boldsymbol{q}_\ell$ is the value on the left side of the discontinuity and $\boldsymbol{q}_\mathrm{r}$ the value on the right side. Recall that this implies that $\tilde{\boldsymbol{q}}$ is constant along rays where $\xi = c$ for any fixed number $c \in \mathbb{R}$. So if we look at the ray along the value $c = 0$, then this tells us the solution of the Riemann problem, i. e. $\tilde{\boldsymbol{q}}^n(x_{i-1/2}, t) = \tilde{\boldsymbol{q}}(0; \boldsymbol{Q}^n_{i-1}, \boldsymbol{Q}^n_i)$ for $t \in [t_n, t_{n+1}]$. Hence the integral in (10.6) is actually taken over a constant value and therefore simplifies to

$$\boldsymbol{F}^n_{i-1/2} = \mathcal{F}(\boldsymbol{Q}^n_{i-1}, \boldsymbol{Q}^n_i) = \boldsymbol{f}\big(\tilde{\boldsymbol{q}}(0; \boldsymbol{Q}^n_{i-1}, \boldsymbol{Q}^n_i)\big).$$

Hence, for the application of a Godunov method one needs to be able to compute solutions to Riemann problems (10.4) or more generally at least approximations to it.

11 Approximate Riemann Solvers

By far the most common computation in a simulation using a Godunov method is the solution of a Riemann problem. In theory, this can always be done exactly, although only by an iterative procedure in certain badly-behaved cases. In practice, approximate solutions are usually preferred for two reasons: First, calculating exact solutions can be quite expensive and, second, Godunov's method averages over these results in the end anyway, making attention to detail hard to justify. In this section we will introduce just one type of approximate Riemann solver. We note, however, that a great amount of work

has been dedicated to the creation of different kinds of Riemann solvers. A standard reference which explains many of these in detail is Toro's book [27].

We present here the derivation of the so-called *HLL solver* by Harten, Lax and van Leer which, while remaining relatively simple to implement, is well-suited for the computations in this thesis. Its fundamental idea is to assume that the solution consists of two waves which separate three constant states. This will not cause any problems for our numerical considerations since we only deal with the shallow-water equations in one spatial dimension. However, in more general settings (e. g. the shallow-water equations in two spatial dimensions) it is not always ideal. Its problem is that the assumption of a two-wave configuration is only correct for a hyperbolic system of two equations. Details and methods to circumvent this can also be found in Toro's book.

Let us see how the HLL solver is derived in detail. The setting is as follows. We study the Riemann problem

$$\begin{aligned} \boldsymbol{q}_t + \boldsymbol{f}(\boldsymbol{q})_x &= \boldsymbol{0} && \text{for all } (x,t) \in \mathbb{R} \times \left]\overline{t}, \infty\right[, \\ \boldsymbol{q}(x,\overline{t}) &= \left\{ \begin{array}{ll} \boldsymbol{q}_\ell, & \text{if } x < \overline{x}, \\ \boldsymbol{q}_\mathrm{r}, & \text{if } x > \overline{x} \end{array} \right\} && \text{for all } x \in \mathbb{R} \end{aligned} \tag{11.1}$$

for a system of m (possibly non-linear) conservation laws in one spatial dimension. As usual, $\boldsymbol{q} \in \mathbb{R}^m$ is the vector of to-be-determined conserved quantities and $\boldsymbol{f} : \mathbb{R}^m \to \mathbb{R}^m$ the corresponding known flux function. The values $\boldsymbol{q}_\ell \in \mathbb{R}^m$ and $\boldsymbol{q}_\mathrm{r} \in \mathbb{R}^m$ are assumed to be given. In particular, we have in mind the setting in a subproblem during Godunov's method where $\boldsymbol{q}_\ell = \boldsymbol{Q}_i^n$ and $\boldsymbol{q}_\mathrm{r} = \boldsymbol{Q}_{i+1}^n$ for some $i \in \mathbb{Z}$ and $n \in \mathbb{N}_0$. As usual, $\overline{x} \in \mathbb{R}$ is a given point in space and $\overline{t} \geqslant 0$ a given time. For the sake of simplicity we will assume $\overline{x} = \overline{t} = 0$ throughout this section. Recall from section 3 that the solution of (11.1) is a similarity solution which means that it depends only on $\boldsymbol{q}_\ell$, $\boldsymbol{q}_\mathrm{r}$ and $\xi = x/t$.

The first goal of this section is the determination of an approximation $\boldsymbol{Q} := \boldsymbol{Q}^\mathrm{HLL} \approx \boldsymbol{q}$. In the HLL ansatz we first estimate the smallest and largest signal velocities $s_\ell < s_\mathrm{r}$ in the solution of the Riemann problem (11.1) with a yet-to-be-discussed method. We then approximate the Riemman solution by three constant states given as

$$\boldsymbol{Q}^\mathrm{HLL}(x,t) := \left\{ \begin{array}{ll} \boldsymbol{q}_\ell, & \text{if } \frac{x}{t} < s_\ell, \\ \boldsymbol{q}_\mathrm{m}, & \text{if } s_\ell < \frac{x}{t} < s_\mathrm{r}, \\ \boldsymbol{q}_\mathrm{r}, & \text{if } \frac{x}{t} > s_\mathrm{r} \end{array} \right\} \quad \text{for all } (x,t) \in \mathbb{R} \times \left]0, \infty\right[, \tag{11.2}$$

where $\boldsymbol{q}_\mathrm{m}$ is a constant yet-to-be-determined middle state vector. This means that we only

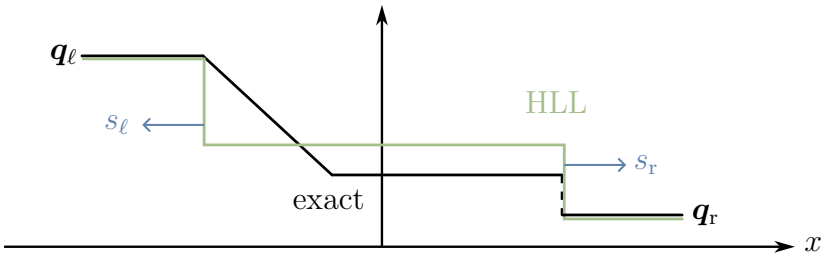

Figure 11.1: Comparison of an exact Riemann solution with its HLL approximation.

view two waves of which the first travels to the left with speed $s_\ell < 0$ and the second travels to the right with speed $s_\mathrm{r} > 0$ (the subsonic case).

To find the concrete value of $\boldsymbol{q}_\mathrm{m}$, we invoke the conservation law over a special control volume $[x_\ell, x_\mathrm{r}] \times [0, T]$ which is chosen in such a way that $x_\ell \leqslant T s_\ell$ and $x_\mathrm{r} \geqslant T s_\mathrm{r}$. Notice that by construction such a volume is designed in a way which contains the exact solution of the Riemann problem inside of it. Notice, too, that $0 \in [x_\ell, x_\mathrm{r}]$ and that

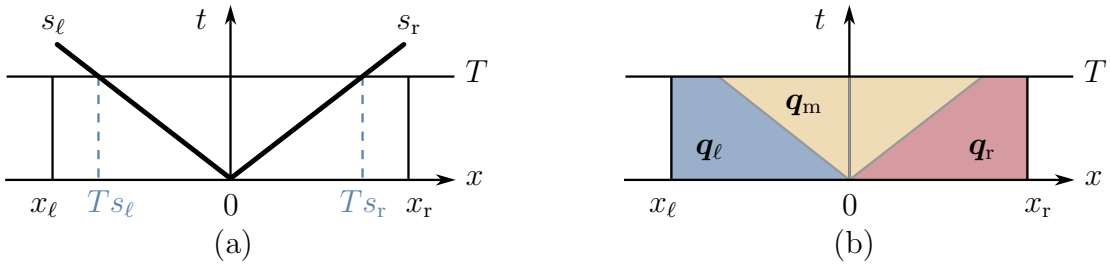

Figure 11.2: Setup of the HLL solver. (a) Speeds. (b) States. Figure adapted from [27, Figure 10.2].

$$\boldsymbol{q}(x_\ell, t) = \boldsymbol{q}_\ell \text{ and } \boldsymbol{q}(x_\mathrm{r}, t) = \boldsymbol{q}_\mathrm{r} \quad \text{for } t \in [0, T], \tag{11.3}$$

cf. figure 11.2. The integral formulation of the conservation law over this domain takes the form (cf. section 3)

$$\int_{x_\ell}^{x_\mathrm{r}} \boldsymbol{q}(x, T)\,\mathrm{d}x = \int_{x_\ell}^{x_\mathrm{r}} \boldsymbol{q}(x, 0)\,\mathrm{d}x + \int_0^T \boldsymbol{f}\big(\boldsymbol{q}(x_\ell, t)\big)\,\mathrm{d}t - \int_0^T \boldsymbol{f}\big(\boldsymbol{q}(x_\mathrm{r}, t)\big)\,\mathrm{d}t. \tag{11.4}$$

The right-hand side of (11.4) can actually be simplified, if we use

$$\int_{x_\ell}^{x_\mathrm{r}} \boldsymbol{q}(x, 0)\,\mathrm{d}x = \int_{x_\ell}^{0} \boldsymbol{q}_\ell\,\mathrm{d}x + \int_0^{x_\mathrm{r}} \boldsymbol{q}_\mathrm{r}\,\mathrm{d}x = x_\mathrm{r}\boldsymbol{q}_\mathrm{r} - x_\ell \boldsymbol{q}_\ell$$

which follows from the initial condition in (11.1) in combination with $\boldsymbol{f}(\boldsymbol{q}(x_\ell, t)) = \boldsymbol{f}(\boldsymbol{q}_\ell)$ and $\boldsymbol{f}(\boldsymbol{q}(x_\mathrm{r}, t)) = \boldsymbol{f}(\boldsymbol{q}_\mathrm{r})$ which, in turn, follow from (11.3). In combination this yields the so-called *consistency condition*

$$\int_{x_\ell}^{x_\mathrm{r}} \boldsymbol{q}(x, T)\,\mathrm{d}x = x_\mathrm{r}\boldsymbol{q}_\mathrm{r} - x_\ell \boldsymbol{q}_\ell + T(\boldsymbol{f}_\ell - \boldsymbol{f}_\mathrm{r}) \tag{11.5}$$

where we set $\boldsymbol{f}_\ell := \boldsymbol{f}(\boldsymbol{q}_\ell)$ and $\boldsymbol{f}_\mathrm{r} := \boldsymbol{f}(\boldsymbol{q}_\mathrm{r})$ as shorthand. Next, we split the left-hand side of (11.4) into the three segments from figure 11.2 (a), namely

$$\begin{aligned} \int_{x_\ell}^{x_\mathrm{r}} \boldsymbol{q}(x, T)\,\mathrm{d}x &= \int_{x_\ell}^{Ts_\ell} \boldsymbol{q}(x, T)\,\mathrm{d}x + \int_{Ts_\ell}^{Ts_\mathrm{r}} \boldsymbol{q}(x, T)\,\mathrm{d}x + \int_{Ts_\mathrm{r}}^{x_\mathrm{r}} \boldsymbol{q}(x, T)\,\mathrm{d}x \\ &= (Ts_\ell - x_\ell)\boldsymbol{q}_\ell + \int_{Ts_\ell}^{Ts_\mathrm{r}} \boldsymbol{q}(x, T)\,\mathrm{d}x + (x_\mathrm{r} - Ts_\mathrm{r})\boldsymbol{q}_\mathrm{r}, \end{aligned} \tag{11.6}$$

where the second equality follows from yet another look at figure 11.2. Since (11.5) is equal to (11.6), we find by comparing terms that

$$\int_{Ts_\ell}^{Ts_\mathrm{r}} \boldsymbol{q}(x, T)\,\mathrm{d}x = T(s_\mathrm{r}\boldsymbol{q}_r - s_\ell \boldsymbol{q}_\ell + \boldsymbol{f}_\ell - \boldsymbol{f}_\mathrm{r}).$$

To obtain the spatial average over the middle region in figure 11.2 we need only divide by its length $Ts_\mathrm{r} - Ts_\ell$ to find

$$\frac{1}{Ts_\mathrm{r} - Ts_\ell} \int_{Ts_\ell}^{Ts_\mathrm{r}} \boldsymbol{q}(x, T)\,\mathrm{d}x = \frac{s_\mathrm{r}\boldsymbol{q}_r - s_\ell \boldsymbol{q}_\ell + \boldsymbol{f}_\ell - \boldsymbol{f}_\mathrm{r}}{s_\mathrm{r} - s_\ell}$$

which suggests that the middle state in (11.2) should be chosen as the constant

$$\boldsymbol{q}_\mathrm{m} = \frac{s_\mathrm{r}\boldsymbol{q}_r - s_\ell \boldsymbol{q}_\ell + \boldsymbol{f}_\ell - \boldsymbol{f}_\mathrm{r}}{s_\mathrm{r} - s_\ell}. \tag{11.7}$$

After inserting (11.7) into (11.2) we can see the HLL solver's approximation to the Riemann problem in its full form. We explicitly point out that all calculations up to this point were exact because they utilized the actual solution of the Riemann problem $\boldsymbol{q}$ instead of the HLL approximation $\boldsymbol{Q}^\mathrm{HLL}$. The only necessary ingredient is that we must know the speeds s_ℓ and s_r.

Let us now turn to the determination of the associated numerical flux. The flux function will take the form

$$\boldsymbol{F} := \begin{cases} \boldsymbol{f}_\ell, & \text{if } s_\ell \geqslant 0, \\ \boldsymbol{f}_\mathrm{m}, & \text{if } s_\ell \leqslant 0 \leqslant s_\mathrm{r}, \\ \boldsymbol{f}_\mathrm{r}, & \text{if } s_\mathrm{r} \leqslant 0 \end{cases} \tag{11.8}$$

with the yet-to-be-determined intermediate output $\boldsymbol{f}_\mathrm{m}$. We warn the reader that we will not set $\boldsymbol{f}_\mathrm{m} := \boldsymbol{f}(\boldsymbol{q}_\mathrm{m})$ as one might expect. To derive the actual value, we begin again with the exact solution $\boldsymbol{q}$ and integrate it over the right half of the rectangle in figure 11.2, i. e. over $[0, x_\mathrm{r}] \times [0, T]$. The conservation law there reads

$$\int_0^{x_\mathrm{r}} \boldsymbol{q}(x, T)\,\mathrm{d}x - \int_0^{x_\mathrm{r}} \boldsymbol{q}(x, 0)\,\mathrm{d}x = \int_0^T \boldsymbol{f}\big(\boldsymbol{q}(0, t)\big)\,\mathrm{d}t - \int_0^T \boldsymbol{f}\big(\boldsymbol{q}(x_\mathrm{r}, t)\big)\,\mathrm{d}t$$

which, by splitting up the relevant integral, can be rewritten as

$$\begin{aligned} \int_0^T \boldsymbol{f}\big(\boldsymbol{q}(0, t)\big)\,\mathrm{d}t = \int_0^{Ts_\mathrm{r}} \boldsymbol{q}(x, T)\,\mathrm{d}x + \int_{Ts_\mathrm{r}}^{x_\mathrm{r}} \boldsymbol{q}(x, T)\,\mathrm{d}x \\ - \int_0^{x_\mathrm{r}} \boldsymbol{q}(x, 0)\,\mathrm{d}x + \int_0^T \boldsymbol{f}\big(\boldsymbol{q}(x_\mathrm{r}, t)\big)\,\mathrm{d}t. \end{aligned}$$

If we evaluate these integrals by looking at figure 11.2 and (11.3), we find, after dividing by T, that

$$\frac{1}{T}\int_0^T \boldsymbol{f}\big(\boldsymbol{q}(0, t)\big)\,\mathrm{d}t = \frac{1}{T}\int_0^{Ts_\mathrm{r}} \boldsymbol{q}(x, T)\,\mathrm{d}x - s_\mathrm{r}\boldsymbol{q}_\mathrm{r} + \boldsymbol{f}(\boldsymbol{q}_\mathrm{r}).$$

The integral term on the left is precisely what we want to approximate, but this would rely on the knowledge of $x \mapsto \boldsymbol{q}(x, T)$ over $[0, Ts_\mathrm{r}]$ which we do not have. This is where the approximation (11.2) comes in. If we replace $\boldsymbol{q}$ with $\boldsymbol{q}_\mathrm{m}$ in the right integral, we find

$$\frac{1}{T}\int_0^T \boldsymbol{f}\big(\boldsymbol{q}(0, t)\big)\,\mathrm{d}t \approx s_\mathrm{r}(\boldsymbol{q}_\mathrm{m} - \boldsymbol{q}_\mathrm{r}) + \boldsymbol{f}(\boldsymbol{q}_\mathrm{r}) =: \boldsymbol{f}_\mathrm{m}. \tag{11.9}$$

By plugging the definition of $\boldsymbol{q}_\mathrm{m}$ from (11.2) into (11.9), we see that

$$\boldsymbol{f}_\mathrm{m} = \frac{s_\mathrm{r}\boldsymbol{f}_\ell - s_\ell \boldsymbol{f}_\mathrm{r} + s_\ell s_\mathrm{r}(\boldsymbol{q}_\mathrm{r} - \boldsymbol{q}_\ell)}{s_\mathrm{r} - s_\ell}. \tag{11.10}$$

Inserting this value into (11.8) gives the HLL numerical flux function.

Thus far, we have not specified how exactly to compute the wave speeds s_ℓ and s_r. And different choices will indeed yield different kinds of HLL solvers. Recall that for the shallow-water equations the speeds can be split up in a form $u \pm c$ where u is the normal velocity component and c the speed of the wave. A very simple method is then given by using the approximation

$$\lambda_{\max} := \max\left\{|u_\ell| + c_\ell, |u_\mathrm{r}| + c_\mathrm{r}\right\} \tag{11.11}$$

for the maximum speed and setting $s_\mathrm{r} = \lambda_{\max}$ and $s_\ell = -\lambda_{\max}$. If we substitute this into the HLL numerical flux (11.10), we get what is typically called the *Rusanov flux function*

$$\mathcal{F}(\boldsymbol{q}_\ell, \boldsymbol{q}_\mathrm{r}) := \boldsymbol{F}^{\mathrm{Rus}} = \tfrac{1}{2}(\boldsymbol{f}_\ell + \boldsymbol{f}_\mathrm{r}) - \tfrac{1}{2}\lambda_{\max}(\boldsymbol{q}_\mathrm{r} - \boldsymbol{q}_\ell). \tag{11.12}$$

This scheme will be used for the numerical computations in section 13.

12 Splitting Methods

All numerical schemes described up to this point assumed a pure conservation law without source terms. This section presents a very simple method for the solution of (generally non-linear) conservation laws with source terms. Its benefit is an easy implementation because the previously-developed algorithms do not need to be changed; its pitfalls will be discussed at the end of this section. Our presentation follows [28].

We will once again study a system of m conservation laws in one spatial dimension

$$\begin{aligned} \boldsymbol{q}_t + \boldsymbol{f}(\boldsymbol{q})_x &= \boldsymbol{\psi}(\boldsymbol{q}) \quad \text{for all } (x,t) \in \mathbb{R} \times \left]\bar{t}, \infty\right[, \\ \boldsymbol{q}(x,\bar{t}) &= \boldsymbol{q}_0(x) \quad \text{for all } x \in \mathbb{R} \end{aligned} \tag{12.1}$$

where $\boldsymbol{q} \in \mathbb{R}^m$ is the vector of conserved quantities, $\boldsymbol{f} : \mathbb{R}^m \to \mathbb{R}^m$ the flux function, $\boldsymbol{\psi}(\boldsymbol{q}) \in \mathbb{R}^m$ the source term, $\bar{t} \geqslant 0$ some point in time and $\boldsymbol{q}_0 : \mathbb{R} \to \mathbb{R}^m$ an initial value. Everything except $\boldsymbol{q}$ is given. Unlike in the previous sections, $\boldsymbol{\psi}$ will not be set to zero.

The fundamental idea of the to-be-described algorithm is essentially contained in the following theoretical result.

Theorem 12.1 *Consider the scalar initial value problem*

$$\begin{aligned} q_t + aq &= \lambda q \qquad \textit{for all } (x,t) \in \mathbb{R} \times \left]\bar{t}, \infty\right[, \\ q(x,\bar{t}) &= q_0(x) \quad \textit{for all } x \in \mathbb{R} \end{aligned} \tag{12.2}$$

with two given constants $a, \lambda \in \mathbb{R}$ and a given smooth function $q_0 : \mathbb{R} \to \mathbb{R}$. Then the exact solution of (12.2) *is also the solution of the ordinary differential equation*

$$s_t = \lambda s \quad \textit{for all } t \in \left]\bar{t}, \infty\right[, \;\; s(\bar{t}) = r(x,t), \tag{12.3}$$

where r is the solution function of the partial differential equation

$$\begin{aligned} r_t + a r_x &= 0 \qquad \textit{for all } (x,t) \in \mathbb{R} \times \left]\bar{t}, \infty\right[, \\ r(x,\bar{t}) &= q_0(x) \quad \textit{for all } x \in \mathbb{R}. \end{aligned} \tag{12.4}$$

Proof: We subdivide the proof into three parts.

Step 1: We begin by showing that the unique solution of (12.3) is given by

$$\tilde{s}(t) := s(\bar{t})\mathrm{e}^{\lambda t}, \quad t \geqslant \bar{t}.$$

To this end, notice that $\tilde{s}$ is certainly a solution of (12.3) because

$$\tilde{s}'(t) = \lambda s(\bar{t})\mathrm{e}^{\lambda t} = \lambda \tilde{s}(t) \tag{12.5}$$

by the chain rule.

Now consider an arbitrary solution $t \mapsto s(t)$ of (12.3). Then we find

$$\begin{aligned}\Big(\frac{s}{\tilde{s}}\Big)'(t) &= \frac{\tilde{s}(t)s'(t) - \tilde{s}'(t)s(t)}{\tilde{s}(t)^2} && \text{(by the quotient rule)}\\ &= \frac{\tilde{s}(t)\lambda s(t) - \lambda\tilde{s}(t)s(t)}{\tilde{s}(t)^2} && \text{(by (12.3) and (12.5))}\\ &= 0.\end{aligned}$$

Therefore the function $s/\tilde{s}$ must be constant, i. e. $s(t)/\tilde{s}(t) = c$ for all $t \geqslant \bar{t}$ with some $c \in \mathbb{R}$. Hence, $s(t) = c\tilde{s}(t) = cs(\bar{t})\mathrm{e}^{\lambda t}$ and this can only hold at $t = \bar{t}$, if $c = 1$.

Step 2: Next, we show that the solution of (12.2) is given by

$$q(x,t) := q_0(x - at)\mathrm{e}^{\lambda t}, \quad (x,t) \in \mathbb{R} \times \left]\bar{t}, \infty\right[.$$

To this end, notice that q is certainly a solution of (12.2) because

$$q_x(x,t) = q_0'(x - at)\mathrm{e}^{\lambda t}, \qquad q_t(x,t) = -aq_0'(x - at)\mathrm{e}^{\lambda t} + \lambda q_0(x - at)\mathrm{e}^{\lambda t}$$

by the chain rule.

Now consider an arbitrary solution $(x,t) \mapsto q(x,t)$ of (12.2). Let us introduce new variables

$$\tau := \tau(x,t) := t \quad \text{and} \quad \xi := \xi(x,t) := x - at$$

and with them a function

$$v : \mathbb{R} \times \left]\bar{t}, \infty\right[\to \mathbb{R}, \quad v(\tau,\xi) := q(at + \xi, \tau)\big(= q(x,t)\big).$$

Applying the chain rule (for functions of two variables) yields

$$q_x(x,t) = v_x(x - at, t) = v_\xi(\xi,\tau)\cdot\xi_x(x,t) + v_\tau(\xi,\tau)\cdot\tau_x(x,t) = v_\xi(\xi,\tau)$$

and analogously

$$q_t(x,t) = v_t(x - at, t) = v_\xi(\xi,\tau)\cdot\xi_t(x,t) + v_\tau(\xi,\tau)\cdot\tau_t(x,t) = -av_\xi(\xi,\tau) + v_\tau(\xi,\tau).$$

This allows us to formulate an ordinary differential equation for v, namely

$$\begin{aligned}v_\tau(\xi,\tau) &= v_\tau(\xi,\tau) - av_\xi(\xi,\tau) + av_\xi(\xi,\tau)\\ &= q_t(x,t) + av_\xi(\xi,\tau) + \lambda q(x,t) - \lambda v(\xi,\tau)\\ &\overset{(12.2)}{=} \lambda v(\xi,\tau).\end{aligned}$$

In combination with the initial value $v(\xi,0) = q(x,0) = q_0(x)$ this is the same type of initial value problem as in step 1. Hence, we find that its solution is $v(\xi,\tau) = v(\xi,0)\mathrm{e}^{\lambda t}$ which is equivalent to

$$q(x,t) = q(x-at,0)\mathrm{e}^{\lambda t} = q_0(x-at)\mathrm{e}^{\lambda t}.$$

Step 3: We can now combine the results of the previous two steps. Let us collect what we know: The solution of (12.2) is $q(x,t) = q_0(x-at)\mathrm{e}^{\lambda t}$. By setting $\lambda = 0$, this also tells us that the solution of (12.4) is $r(x,t) = q_0(x-at)$. Finally, the solution of (12.3) is $s(t) = s(\bar{t})\mathrm{e}^{\lambda t}$. Since we have $s(\bar{t}) = r(x,t) = q_0(x-at)$ this implies $s(t) = q(x,t)$ which was to prove. ■

Notice that (12.4) is just about the simplest conservation law with non-trivial source term which one can think of. The theorem tells us that it can be solved exactly by a two step process in which one first solves the homogeneous conservation law followed by an ordinary differential equation.

So-called *splitting methods* for the more general system (12.1) now use this result as a basis and apply the same procedure of splitting the task into the solution of a homogeneous conservation law and an ordinary differential equation. To formulate this in standard numerical terms, let us consider problem (12.1) where we are given some time grid t_n for $n \in \mathbb{N}_0$ of spacing $\Delta t > 0$ and the initial time is $\bar{t} = t_n$ while the initial data has some form $\boldsymbol{Q}^n$ and we want to determine the next approximation $\boldsymbol{Q}^{n+1}$. To this end, we assume that the spatial domain $\mathbb{R}$ has been discretised into points x_i for $i \in \mathbb{Z}$ of equal spacing $\Delta x > 0$. Recall that $\boldsymbol{Q}^n$ consists of a set of discrete value $\boldsymbol{Q}_i^n$, viewed as the averages over the cell $\mathcal{C}_i = [x_{i-1/2}, x_{i+1/2}]$, at any given time (cf. section 9). We can now give a discrete analogue of theorem 12.1: First, one solves the homogeneous conservation law

$$\begin{aligned} (\boldsymbol{q}^*)_t + \boldsymbol{f}(\boldsymbol{q}^*)_x &= \boldsymbol{0} && \text{for all } (x,t) \in \mathbb{R} \times \left]\bar{t}, \infty\right[\\ \boldsymbol{q}^*(x,\bar{t}) &= \boldsymbol{Q}^n(x) && \text{for all } x \in \mathbb{R}. \end{aligned}$$

followed by the solution of the ordinary differential equation

$$\tfrac{\mathrm{d}}{\mathrm{d}t}\boldsymbol{q}^{n+1} = \boldsymbol{\psi}(\boldsymbol{q}^{n+1}) \quad \text{for all } t \in \left]\bar{t}+\Delta t, \infty\right[, \;\; \boldsymbol{q}^{n+1}(\bar{t}) = \boldsymbol{q}^*(x, \bar{t}+\Delta t). \tag{12.6}$$

It might appear as though we have advanced the solution by two time steps $2\Delta t$ because we have taken two steps of length Δt. Notice, however, that we used only some of the information of the full partial differential equation in each stage. Only in combination do both steps yield a consistent approximation to (12.1) over a single step of length Δt, cf. [20, chapter 17]. The same reference goes into much more detail considering the theoretical underpinnings of this approach.

We note that for the implementation of a splitting method one needs to have both a solver for the homogeneous conservation law (these were discussed in the previous sections) and a solver for ordinary differential equations (cf., for example, the standard reference [12]). For our purposes the *Euler method* will suffice for the solution of the initial value problem (12.6). The full splitting method then consists of the computations

$$\boldsymbol{Q}_i^* = \boldsymbol{Q}_i^n - \frac{\Delta t}{\Delta x}(\boldsymbol{F}_{i+1/2}^n - \boldsymbol{F}_{i-1/2}^n), \tag{12.7}$$

$$\boldsymbol{Q}_i^{n+1} = \boldsymbol{Q}_i^* + \Delta t \boldsymbol{\psi}(\boldsymbol{Q}_i^*). \tag{12.8}$$

We note that, if we were to replace $\boldsymbol{Q}_i^*$ in the source term in (12.8) with the starting data $\boldsymbol{Q}_i^n$, then the resulting scheme could be written in an unsplit form

$$\boldsymbol{Q}_i^{n+1} = \boldsymbol{Q}_i^n - \frac{\Delta t}{\Delta x}(\boldsymbol{F}_{i+1/2}^n - \boldsymbol{F}_{i-1/2}^n) + \Delta t \boldsymbol{\psi}(\boldsymbol{Q}_i^n).$$

Such methods are sometimes preferred by practitioners.

We end this section with a discussion of the problems which are associated with splitting methods. Experience shows that this kind of approach struggles when the exact solution is very close to the *steady-state solution*, i. e. a solution of the conservation law with $\boldsymbol{q}_t(x,t) = 0$ for all $t \geqslant \bar{t}$. Notice that these solutions are naturally time-independent. A solution which is almost a steady-state solution would hence satisfy $\boldsymbol{f}(\boldsymbol{q})_x \approx \boldsymbol{\psi}(\boldsymbol{q}, x)$. The problem then is that the steps (12.7) and (12.8) must nearly undo one another and they must do so with high precision in order to resolve the small deviation which is responsible for the wave. As an example, consider the case of tsunami modeling where the steady state corresponds to the ocean at rest. But a tsunami wave is itself almost the ocean at rest, except for a very small area where there can be deviations with heights of a few meters at most. At the same time the ocean will be about 4 kilometers deep. Resolving this small difference accurately is something that our scheme will not do. An alternative to splitting methods for the solution of the shallow-water equations is discussed in [22].

13 Numerical Experiments

This final section presents some simulations, beginning with the one-dimensional shallow-water system

$$\begin{aligned} h_t + (hu)_x &= 0, \\ (hu)_t + (hu^2 + \tfrac{1}{2}gh^2)_x &= -ghb_x. \end{aligned} \tag{13.1}$$

Once again, $(x,t) \mapsto h(x,t)$ represents the height, $(x,t) \mapsto u(x,t)$ the speed and $x \mapsto b(x)$ the bathymetry. We will set $g := 9.81$ throughout. For simplicity we will omit the units in each case. The simulations will be computed on the basis of the algorithms from the previous sections. The examples that we will look at are dam break and tsunami modeling from section 4.

General Notes on the Implementation

Before any calculation is made one must first specify a spatial domain. The computations in this section will be carried out on a domain D, e. g. $D := [0,2]$. We will discretize this interval with N points x_i for $i = 1, \ldots, N$. For example, if we choose $N := 500$, then the mesh size for $[0,2]$ would then be $\Delta x = \frac{2-0}{N-1} \approx 0.004$. On this domain we introduce initial data

$$h(x,0) = h_0(x), \quad (hu)(x,0) = (hu)_0(x) \qquad \text{for all } x \in D \tag{13.2}$$

described in detail for each numerical test below. Recall that we use the conservation law framework where $\boldsymbol{q} := (q_1, q_2)^{\mathrm{T}} = (h, hu)^{\mathrm{T}}$ are the conserved variables. We will also be given a special bathymetry function $x \mapsto b(x)$ for $x \in D$ in each case. Our numerical algorithms were derived on the basis of piecewise constant functions. Since working with

step functions is typically not as straightforward to do in most programming languages, we will simply assign the value of the step to the cell midpoint x_i ($i = 1, \dots, N$) in each case. The function plotter then links these approximations together with linear splines. The resulting plots are not much different from those which one would obtain with a piecewise constant function because the step size Δx is sufficiently small. To obtain initial data, it is therefore sensible to evaluate the functions from (13.2) at each grid point. The result is a matrix $\boldsymbol{Q}_{\text{initial}} \in \mathbb{R}^{2\times N}$ where the first row corresponds to the initial heights h and the second row to the initial values of hu at each grid point. These values can be seen as good approximations to the average values of the initial data over the respective grid cells. A discrete version of the bathymetry is calculated in the same way, resulting in a vector $\boldsymbol{b}_{\text{data}} \in \mathbb{R}^N$.

The approximate solution will be computed by a Godunov-type method (10.1) where the numerical flux function is obtained through a HLL approximate Riemann solver. Estimates for the maximum and minimum wave speeds will be chosen in accordance with the Rusanov scheme (11.12). When the bathymetry is not flat, a splitting scheme will be used to incorporate the source term. The choice of time step Δt is not free, but rather bounded by the condition

$$C_{\text{Courant}} = \lambda_{\max}\frac{\Delta t}{\Delta x} \leqslant 1$$

where C_{Courant} is the Courant number (cf. (10.5)) and $\lambda_{\max}$ is the maximum wave speed encountered in any of the Riemann problems at a boundary. In our calculations we will choose $C_{\text{Courant}} = 0.9$ throughout. Our goal will be an approximation of the solution function after some fixed final time $t = T$ and to do so, the appropriate time step will be calculated in each iteration until this time target is met.

Before we can implement the algorithms in the way described above, we must first take into account a new problem. In contrast to the previous section, the spatial domain here is finite with boundaries at $x = x_1$ and $x = x_N$. This causes problems in the algorithms because the computation of the numerical flux function relies on information of the surrounding cells. At a boundary point one piece of information is missing: in the case of x_1 that "to the left" of it and in the case of x_N that "to the right" of it. The typical way to handle his issue is by the introduction of so-called *ghost cells* $x_0 := x_1 - \Delta x$ and $x_{N+1} := x_N + \Delta x$ which are fed with the values from the neighboring cells. Using *outflow boundary conditions* means to extrapolate the values from the neighboring cells, i. e. $\boldsymbol{Q}_0 := \boldsymbol{Q}_1$ and $\boldsymbol{Q}_{N+1} := \boldsymbol{Q}_N$. At the same time the bathymetry data $\boldsymbol{b}_{\text{data}} = (b_1, \dots, b_N)^{\mathrm{T}}$ is updated accordingly by $b_0 := b_1$ and $b_{N+1} := b_N$, implying no change at the boundaries. We explicitly note that the addition of ghost cells changes the involved dimensions. We now have $\boldsymbol{Q}_{\text{initial}} = (\boldsymbol{Q}_0, \dots, \boldsymbol{Q}_{N+1}) \in \mathbb{R}^{2\times(N+2)}$ and $\boldsymbol{b}_{\text{data}} \in \mathbb{R}^{N+2}$. After the calculation is done, the ghost cells can be removed again.

Lastly, we must choose an implementation for the derivative of bathymetry b_x in the momentum equation of (13.1). The obvious choice seems to be to simply differentiate the bathymetry function $x \mapsto b(x)$. However, in real-world applications this function might not be given in a closed form, but rather by a series of measurements. To account for this case it is preferable to use a discrete approximation to the derivative, e. g. the centered difference

$$b_x(x) \approx \frac{b(x + \Delta x) - b(x - \Delta x)}{2\Delta x}.$$

Notice that when $x = x_i$ one has $x + \Delta x = x_{i+1}$ and $x - \Delta x = x_{i-1}$ for all $i = 1, \dots, N$.

The implementation for each of the following examples is more or less the same. One starts by introducing the ghost cells as described above. Then one calculates the numerical approximation for as many time steps as needed to reach the final time T. In the end, the ghost cells can be removed again and the result may be plotted. The calculations at some fixed point in time t take the following three steps:

(S. 1) Compute the maximum wave speed $\lambda_{\max}$ that is encountered throughout all the Riemann problems (cf. (11.11)). Calculate the size of the time step

$$\Delta t := \min\left\{T - t, C_{\text{Courant}}\Delta x/\lambda_{\max}\right\}.$$

(S. 2) For each cell compute a Godunov step (cf. (10.1))

$$\boldsymbol{Q}_i^{n+1} = \boldsymbol{Q}_i^n - \frac{\Delta t}{\Delta x}(\boldsymbol{F}_{i+1/2}^n - \boldsymbol{F}_{i-1/2}^n)$$

utilizing the Russanov flux function (cf. (11.12))

$$\mathcal{F}(\boldsymbol{q}_\ell, \boldsymbol{q}_\mathrm{r}) = \tfrac{1}{2}(\boldsymbol{f}_\ell + \boldsymbol{f}_\mathrm{r}) - \tfrac{1}{2}\lambda_{\max}(\boldsymbol{q}_\mathrm{r} - \boldsymbol{q}_\ell).$$

(S. 3) If the bathymetry is not flat, set $\boldsymbol{Q}_i^* := \boldsymbol{Q}_i^{n+1}$ in each cell and perform a splitting step (cf. (12.8))

$$\boldsymbol{Q}_i^{n+1} = \boldsymbol{Q}_i^* + \Delta t\boldsymbol{\psi}(\boldsymbol{Q}_i^*).$$

At the end of an iteration one updates the time to $t + \Delta t$. The iteration ends when $t = T$, i. e., when the desired time is reached. A commented version of the solver's source code may be found in this thesis' appendix. Let us now turn to concrete examples.

Dam Break

We begin by returning to the dam break problem which is given by combining (13.1) with piecewise constant initial data. We set $N := 500$ (i. e. $\Delta x \approx 0.004$) and $C_{\text{Courant}} := 0.9$. In our first example we will use

$$h_0(x) := \left\{ \begin{array}{ll} 2 - b(x), & \text{if } x < 1, \\ 1 - b(x), & \text{if } x \geqslant 1 \end{array} \right\}, \quad (hu)_0(x) := 0 \qquad \text{for all } x \in [0, 2]$$

with constant bathymetry $b(x) := 0.5$ for $x \in [0, 2]$. In a second plot we change the initial data to

$$h_0(x) := \left\{ \begin{array}{ll} 2 - b(x), & \text{if } x < 1, \\ 1.5 - b(x), & \text{if } x \geqslant 1 \end{array} \right\}, \quad (hu)_0(x) := 0 \qquad \text{for all } x \in [0, 2]$$

and use variable bathymetry given by the function $b(x) := 0.2\cos(20x) - 0.4x + 1.5$ for $x \in [0, 2]$. We remind the reader that h refers to the height of the water above the bottom elevation b such that the plot must contain their sum $\eta = b + h$. The results are shown in figure 13.1 and 13.2.

We recall that the dam break problem also corresponds to the standard Riemann problem. This has the added benefit that an exact solution is known. Comparing the numerical results against the theoretical ones of figure 8.1 yields a suitable way to check that the solver

is implemented correctly. In fact, this problem is commonly used as a numerical test problem for exactly this reason. The resulting wave is roughly the same in each case, showing a left-moving rarefaction and a right-moving shock wave. In the case with bathymetry these waves start to smear out due to the changing bottom bathymetry. As we have pointed out before, this is only a model solution. Real-world dam breaks have been observed to have more or less this shape. One characteristic which is missing, however, is a certain type of undulation which occurs towards the ends of the middle segment of the solution wave. These waves can only be explained using a nonhydrostatic theory.

Tsunamis

After we have seen that our solver is configured correctly from the previous examples, we can now turn to the more complex case of a tsunami wave. Again, we will first test a case with flat bathymetry $b(x) := 0.5$ for $x \in [0, 2]$. We set $N := 500$ (i. e. $\Delta x \approx 0.004$) and $C_{\text{Courant}} := 0.9$. A commonly chosen initial height is some form of Gaussian function. In our case we will use

$$h_0(x) := 1.3 \exp\big(-50(x-1)^2\big) + 2 - b(x), \quad (hu)_0(x) := 0 \qquad \text{for all } x \in [0, 2].$$

The resulting wave is plotted in figure 13.3. We can see that the initial disturbance breaks into two pieces of which the first travels off to the left and the second to the right. Just like the initial condition, the resulting wave remains symmetric to $x = 1$. The same can be said about the speed.

To see how such a wave interacts with a steep shelf (e. g. the continental shelf) we also provide figure 13.4 where the initial height is a shallower Gaussian

$$h_0(x) := 0.3 \exp\big(-10(x-0.5)^2\big) + 2 - b(x), \quad (hu)_0(x) := 0 \qquad \text{for all } x \in [0, 2]$$

and the shelf is modeled by a sigmoid function around $x = 1$, namely

$$b(x) := \frac{1.5}{1 + \exp\big(-100(x-1)\big)} + 0.3 \qquad \text{for all } x \in [0, 2].$$

It is worth noting at this point that these simulations are not carried out at realistic scales. They only serve to demonstrate the rough shape of a solution. In a real-world tsunami application one would have a wave with an initial height of less than one meter over a basin of a depth of around four kilometers. This thesis did not focus on a maximally efficient way to calculate the numerical estimations. For our purposes, these imprecissions can simply be balanced out by choosing an appropriately large number of cells N. As we have mentioned before, however, resolving such a small deviation to an otherwise undisturbed steady state would cause problems with our method of implementation.

Radial Dam Break

Lastly we would like to simulate the solution of a two-dimensional shallow-water problem. The most popular test problem in this case is the radial dam break problem

$$\begin{aligned} h_t + (hu)_r &= -\tfrac{hu}{r}, \\ (hu)_t + (hu^2 + \tfrac{1}{2}gh^2)_r &= -\tfrac{hu^2}{r} \end{aligned}$$

which we will view on the finite domain $]0, 2.5]$ discretized with $N := 500$ (i. e. $\Delta x \approx 0.005$) and $C_{\text{Courant}} := 0.9$ with initial conditions

$$h_0(r) := \left\{ \begin{array}{ll} 2 - b(r), & \text{if } r < 0.5, \\ 1 - b(r), & \text{if } r \geqslant 0.5 \end{array} \right\}, \quad (hu)_0(r) := 0 \qquad \text{for all } r \in]0, 2.5]$$

and $b(r) := 0.5$ for all $r \in]0, 2.5]$. Here $(r, t) \mapsto h(r, t)$ represents the height, $(r, t) \mapsto u(r, t)$ the speed and $r \mapsto b(r)$ the bathymetry. Because of its radial symmetry one can actually obtain the solution of the radial dam break problem with a one-dimensional model by rotating the resulting function around the vertical axis (cf. section 8). Figure 13.5 shows both the initial condition as well as two later points in time. Figure 13.6 gives a more traditional plot of the solution functions of height and velocity, namely their one-dimensional origins, for different points in time.

It is clearly visible that the resulting wave consists of an outward-propagating circular shock wave as well as an inward-propagating circular rarefaction. Once this rarefaction wave meets the center, it gets reflected and causes the height of the center column to drop with it. This dip in the center is difficult to resolve numerically. As time passes, the circular shock wave propagates further outward and the inner rarefaction continuously lowers the center's height. One observes the creation of one more circular shock wave which propagates accordingly before the fluid in the center returns to the original elevation of the water and is no longer affected. A more thorough investigation is given in [28]. The same reference also includes the discussion of a more realistic numerical example which models a real-world dam more closely.

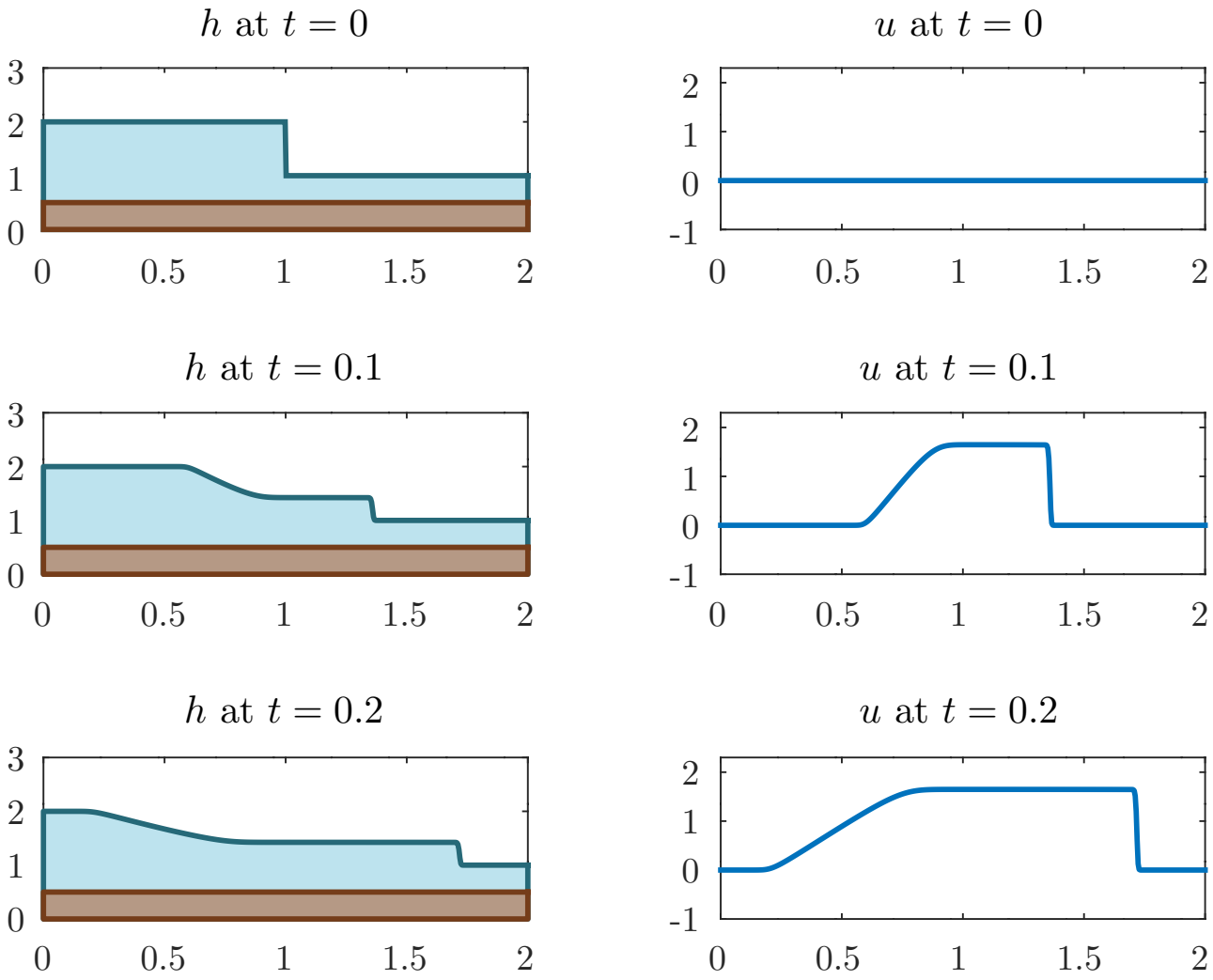

Figure 13.1: Numerical results of the dam break problem with constant bathymetry.

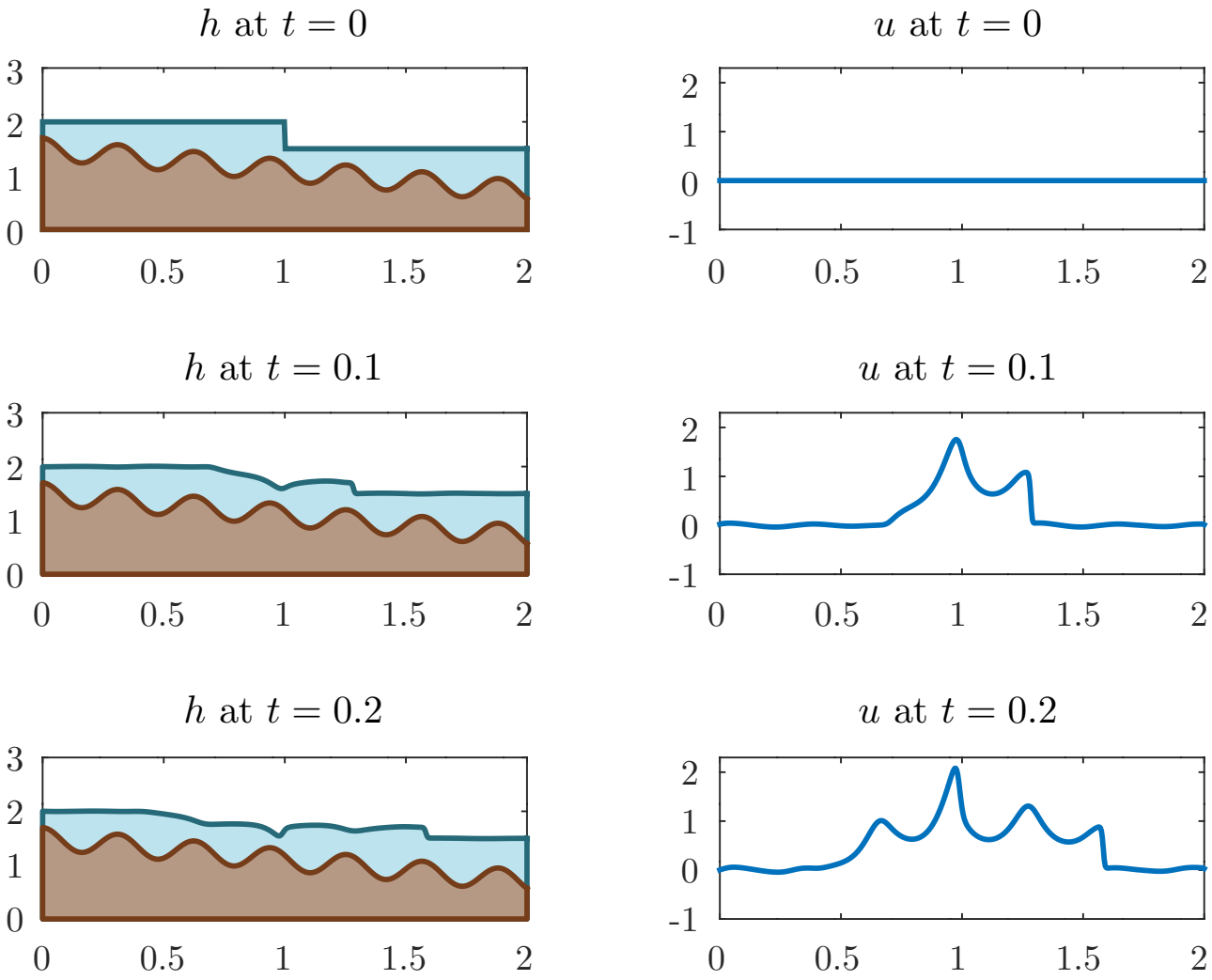

Figure 13.2: Numerical results of the dam break problem with varying bathymetry.

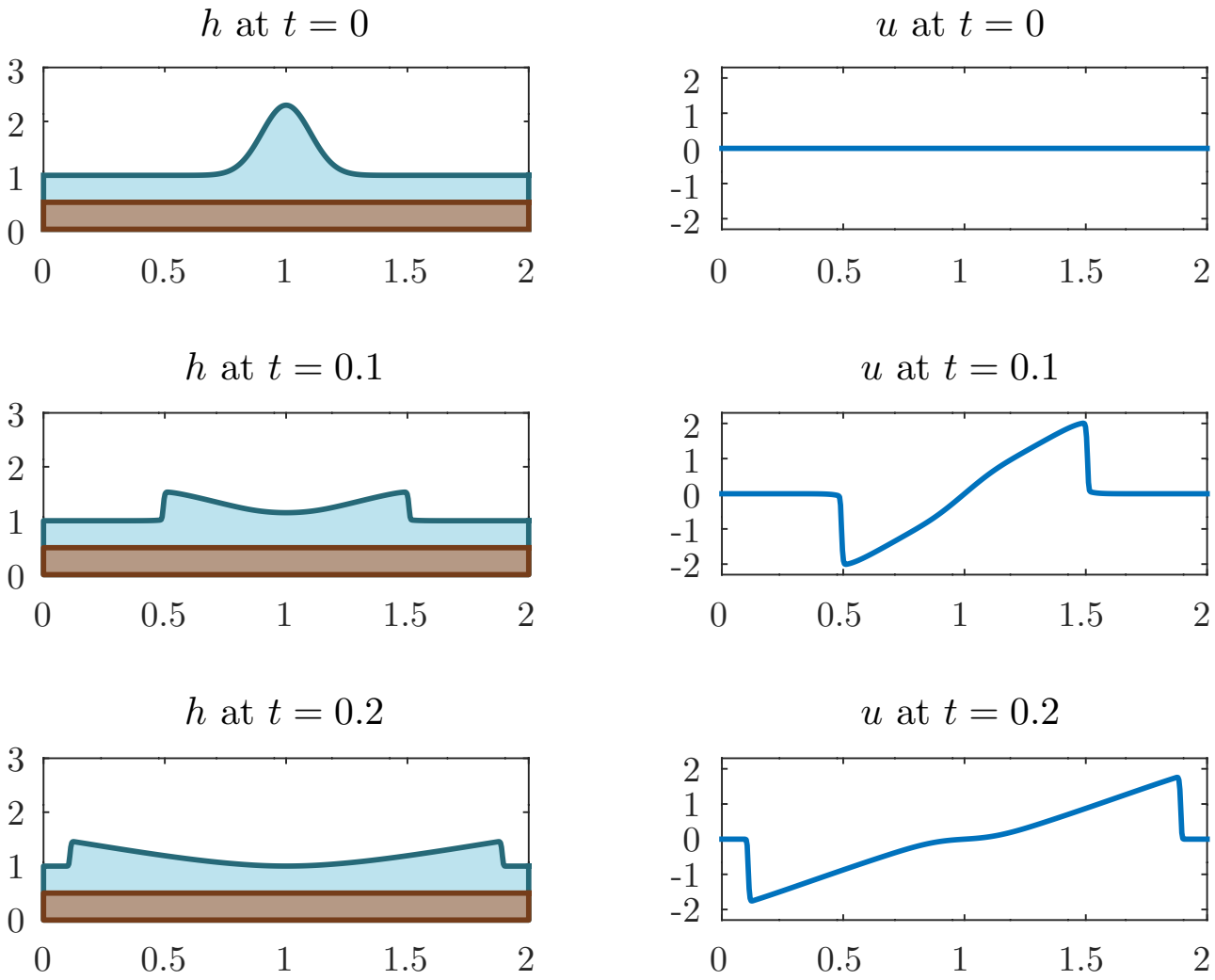

Figure 13.3: Tsunami wave dispersing on open ocean without bathymetry.

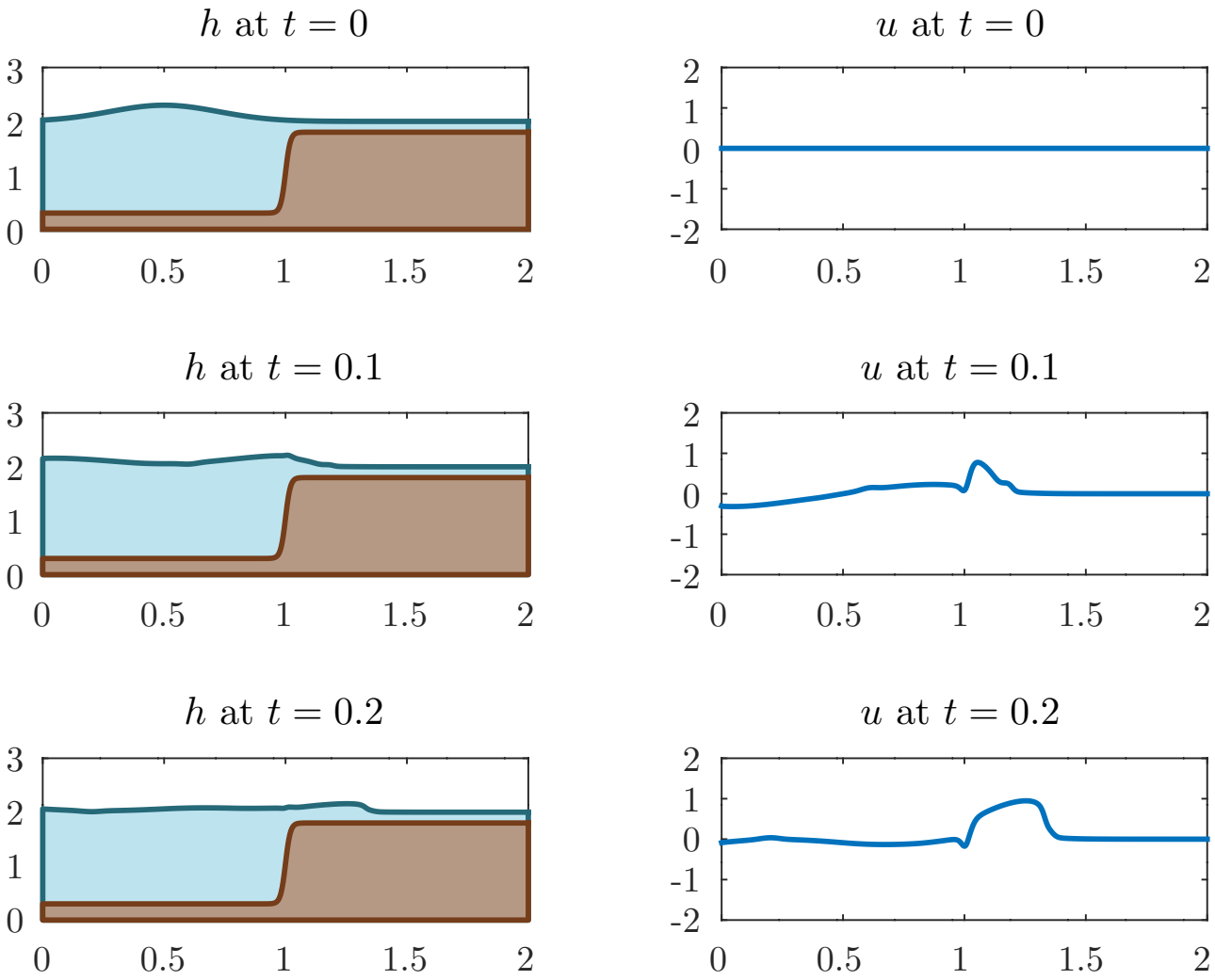

Figure 13.4: Tsunami wave interacting with a steep shelf.

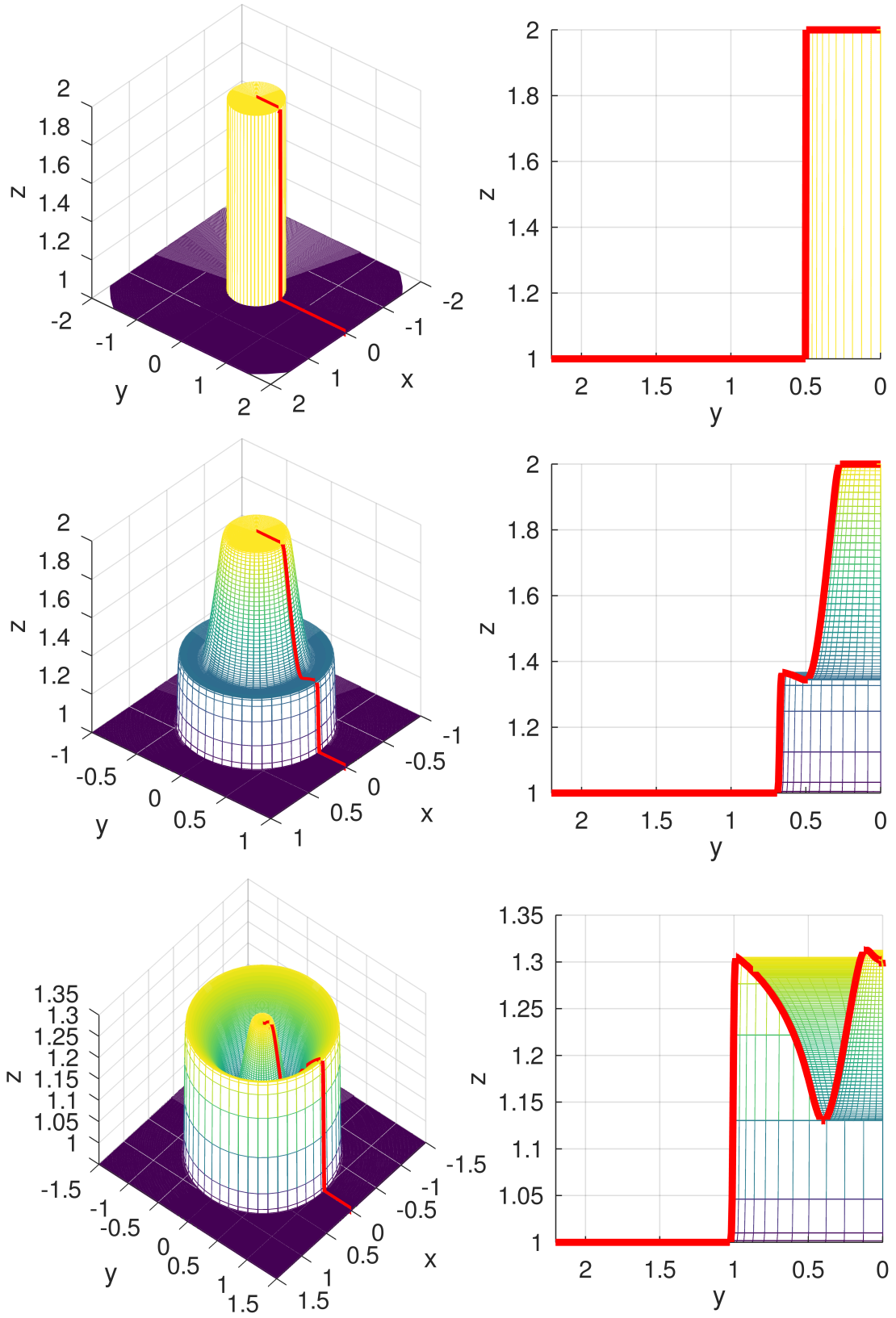

Figure 13.5: Solution of the radial dam break problem after $t = 0$, $t = 0.05$ and $t = 0.15$. The radial solution which is being rotated around the horizontal axis is shown in red.

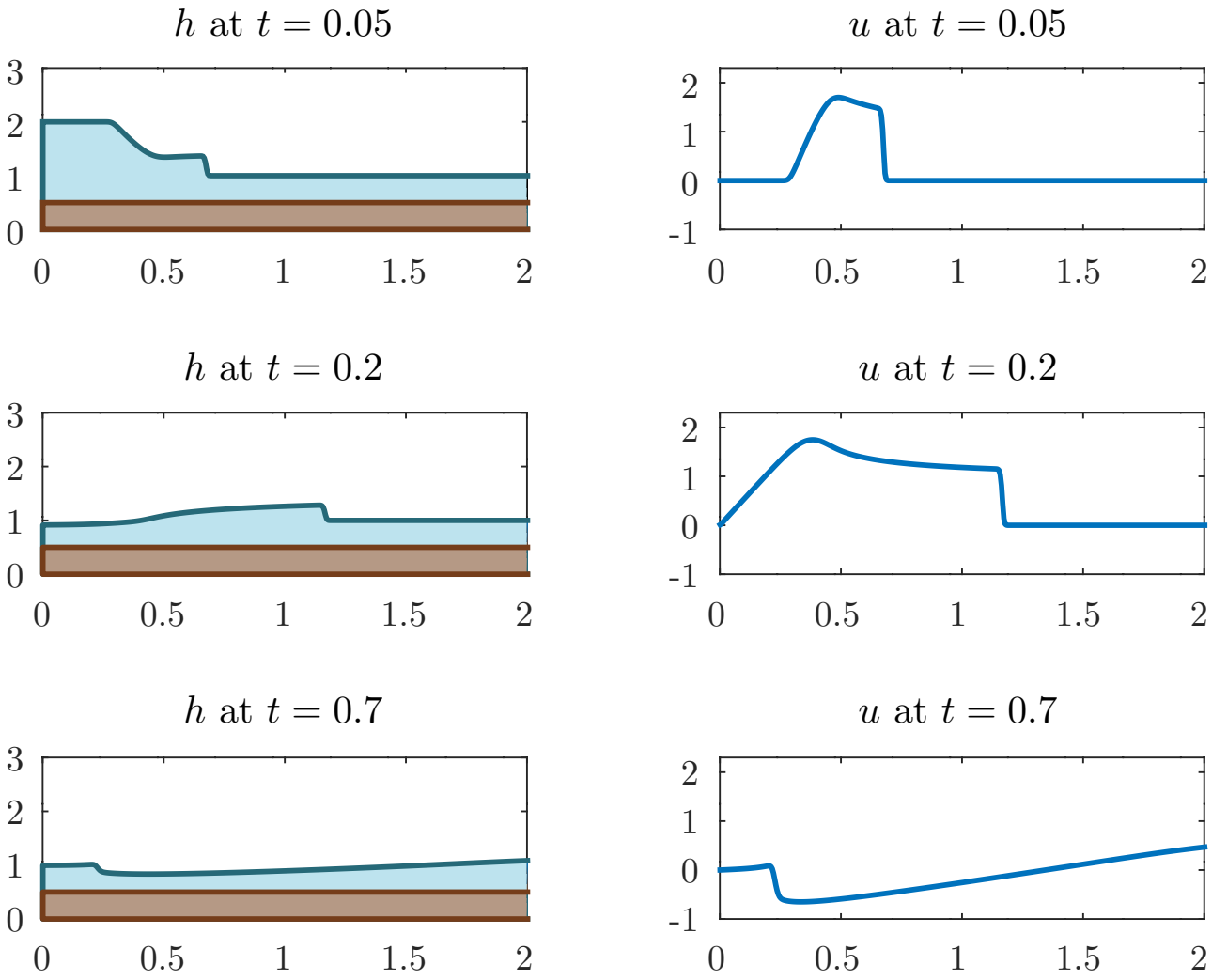

Figure 13.6: Solution of the radial dam break problem after $t = 0.05$, $t = 0.2$ and $t = 0.7$.

Conclusion and Outlook

The goal of this thesis was to give an accessible introduction to the shallow-water model and its numerical solution with finite-volume methods. After collecting some fundamental facts on differential equations, vector analysis and conservation laws in chapter I, chapter II was dedicated to mathematical modeling. It presented a full derivation of the two-dimensional shallow-water system with bathymetry. To this end, the Euler equations were needed and derived from their fluid-dynamical origin. We also discussed several extensions of the shallow-water framework and its theoretical properties. Chapter III gave an introduction to the finite-volume method. It presented Godunov-type schemes and approximate Riemann solvers for the Riemann problems which arise during their solution. We also discussed the treatment of source terms via a splitting approach. Lastly, we computed several solutions of the models from chapter II and studied their behavior.

There are many possible extensions to what this thesis has presented. Although most of these were already mentioned throughout the text, we will collect them here once more to give the reader a better overview. Details can be found in the respective sections.

In chapter I the framework of hyperbolic conservation laws was only formally introduced for the one-dimensional case. Although the shallow-water model was derived in its general two-dimensional form, this was not used for the numerical studies later on. The multi-dimensional case is far more important in real-world applications (e. g. [22]). After all, the "volumes" in our presentation were merely intervals. As it turns out, most of the fundamental ideas behind the algorithms and the theoretical considerations carry over to several dimensions. An extensive general treatment is given in part III of the book [20] by LeVeque. Toro's book [28] treats the two-dimensional shallow-water equations in detail (this includes the solution of the corresponding Riemann problem).

Chapter II dealt with the derivation of the shallow-water equations. In section 8 we hinted at how this model could be extended to fit different types of tsunamis (e. g. those generated by asteroids or by underwater landslides). Of course, one can study fluid dynamics more generally and derive different models which govern not just the flow of water, but also that of gases and ice, to name just two examples. The Navier-Stokes system (see also remark 5.1) comes to mind. It is the most general model that actually describes all of these phenomena. The texts by Vallis [30] and Klinger, Haine [19] use a geophysical approach and derive many different partial differential equations for oceanic and atmospheric flows. The texts [17] and [26] by Johnson and Stoker focus exclusively on water. In [13] one finds more extensions to the shallow-water equations and [15] deals with tsunami modeling more generally.

The last chapter dealt with the numerical solution of the shallow-water equations. We could only give a very sparse introduction here. In particular, the algorithms were not analyzed theoretically and they were not optimized for speed. The text [20] by LeVeque treats all of these issues. The book [27] by Toro develops our algorithms much further.

It also includes an extensive treatment of approximate Riemann solvers. The paper [22] by LeVeque, George and Berger includes a discussion of adaptive mesh refinement for the shallow-water equations which is essential for fast tsunami predictions.

Besides improving the finite-volume method, one could also go down a different route and consider other algorithms for the solution of partial differential equations. The book [15] by Horrillo, Knight and Kowalik focuses on a finite-difference approach for tsunamis. Vreghdenhill's book [31] presents a finite-element ansatz for the shallow-water equations. A question that is of particular interest is, of course, which type of algorithm is best suited for the solution of the shallow-water system.

Appendix: Source Code

In this appendix we list the Octave/MATLAB source code that was used in section 13 to produce the numerical simulations there. We note again that the Godunov method that is implemented below is only of first order. This will not be sufficiently fast for most practical applications for which higher-order methods should be employed.

Code for the Flux Function

```
function fluxQ = numericalFlux(Q_L, Q_R)
  %The numericalFlux function computes the numerical flux between
  %the two states Q_L and Q_R by approximately solving a Riemann
  %problem for the one-dimensional shallow-water equations via the
  %HLL solver. The utilized speed estimates result in the Rusanov
  %flux function.
  %
  %Inputs: Q_L    2x1 vector, initial condition on LEFT boundary,
  %               first component is height=h, second component is
  %               height*speed=h*u
  %        Q_R    2x1 vector, initial condition on RIGHT boundary,
  %               first component is height=h, second component is
  %               height*speed=h*u
  %
  %Output: fluxQ  2x1 vector, \mathcal{F}(Q_L, Q_R)

  %Translating conserved quantities into original values
  h_L = Q_L(1); u_L = Q_L(2)/Q_L(1);
  h_R = Q_R(1); u_R = Q_R(2)/Q_R(1);

  %Flux at the boundaries
  F_L = [Q_L(2); Q_L(2)^2/Q_L(1) + 0.5*9.81*Q_L(1)^2];
  F_R = [Q_R(2); Q_R(2)^2/Q_R(1) + 0.5*9.81*Q_R(1)^2];

  %Maximum wave speed
  lambda_Max = max( abs(u_L) + sqrt(9.81*h_L), ...
               abs(u_R) + sqrt(9.81*h_R) );

  %Rusanov flux
  fluxQ = 0.5*(F_R+F_L) - 0.5*lambda_Max*(Q_R-Q_L);
end
```

Code for the Godunov Method

```
function Q = sweSolver(A, B, Q_initial, T, C_courant, b_data)
  %The sweSolver function computes an approximate solution to the
  %one-dimensional shallow-water equations on the intervall [A,B]
  %with initial data Q_initial after time T with bathymatry b_data.
  %The solver utilizes outflow boundary conditions and a time step
  %chosen in accordance with the Courant number C_courant.
  %
  %Inputs: A          scalar, left boundary of spacial domain
  %        B          scalar, right boundary of spacial domain
  %        Q_initial  2xN matrix, where N is the choosen number of
  %                   discretization points (see main.m); first row
  %                   corresponds to heights=h, second row cor-
  %                   responds to height*speed=h*u
  %        T          scalar, time after which solution is computed
  %        C_courant  scalar<= 1, needed to choose the size of the
  %                   time step dt=\Delta t.
  %        b_data     1xN vector
  %
  %Output: Q          2xN matrix, approximate solution to the cons-
  %                   ervation law after time T

  %Computing spacial step size dx=\Delta x
  N  = size(Q_initial)(2);
  dx = (B-A)/(N-1);

  %Adding ghost cells in spacial domain and initial data
  x      = linspace(A,B,N);
  x      = [ A-dx, x, B+dx];
  Q      = [ Q_initial(:,1), Q_initial, Q_initial(:,N) ];
  b_data = [b_data(1), b_data, b_data(N)];

  %Euler method
  t = 0
  while t < T
    %Computing maximal wave speed over all cells
    lambda_Max = 0;
    for i=2:N+1
      %Choosing indices
      L = i-1;
      R = i;
      %Converting from conserved variables to original variables
      h_L = Q(1,L);
      h_R = Q(1,R);
      u_L = Q(2,L)/Q(1,L);
      u_R = Q(2,R)/Q(1,R);

      lambda_Max = max( lambda_Max, max(abs(u_L)+sqrt(9.81*h_L), ...
                   abs(u_R) + sqrt(9.81*h_R)) );
    end

    %Compute time step dt=\Delta t. In case t+dt>T, we choose the step
    %such that the iteration terminates at the final time T
    dt = min(T-t, C_courant*dx/lambda_Max);

    %One time iteration. Q_new is introduced to prevent overwriting Q
```

```
56      Q_new = Q;
57      for i=2:N+1
58        %Solving the homogenous conservation law
59        Q_new(:,i) = Q(:,i) - dt/dx*(numericalFlux(Q(:,i), Q(:,i+1)) ...
60                     - numericalFlux( Q(:,i-1), Q(:,i) ));
61        %Splitting step
62        Q_new(2,i) = Q_new(2,i)+dt*( -9.81*Q_new(1,i)*...
63                     ( b_data(i+1)-b_data(i-1) )/(2*dx) );
64      end
65      Q = Q_new;
66
67      t = t + dt
68    end
69
70    %Removes the Ghost cells from the computed solution
71    Q = Q(:,2:N+1);
72
73  end
```

Bibliography

[1] H. Altaie. "New Techniques Of Derivations for Shallow Water Equations". In: *International Journal of Advanced Scientific and Technical Research* 3 (May 2016), pp. 131–150.

[2] B. F. Atwater et al. *The orphan tsunami of 1700: Japanese clues to a parent earthquake in North America*. University of Washington Press, 2011.

[3] C. Beffa. *Praktische Lösung der tiefengemittelten Flachwassergleichungen*. German. Mitteilungen der Versuchsanstalt für Wasserbau, Hydrologie und Glaziologie an der Eidgenössischen Technischen Hochschule Zürich. VAW, 1994.

[4] M. Berger. "Asteroid-Generated Tsunamis: A Review". In: *Recent Advances in Industrial and Applied Mathematics* (2022), pp. 3–17.

[5] D. Calhoun. *The Riemann problem shallow water wave systems*. Slides from a school held by the Pan American Advanced Studies Institute titled *The Science of Predicting and Understanding Tsunamis, Storm Surges, and Tidal Phenomena* in Valparaiso, Chile. Link accessed on March 13, 2024. Jan. 2, 2013. URL: https://web.archive.org/web/20240313101838/http://www.forestclaw.org/gh_pages_files/talks/pasi-01-2013.pdf.

[6] A. J. Chorin and J. E. Marsden. *A mathematical introduction to fluid mechanics*. 3. ed. Vol. 4. Texts in Applied Mathematics. New York: Springer-Verlag, 1993.

[7] B. Cushman-Roisin and J.-M. Beckers. *Introduction to geophysical fluid dynamics: physical and numerical aspects*. Academic press, 2011.

[8] K. Endl and W. Luh. *Analysis II*. German. Studien-Text. 4. ed. Wiesbaden: Aula-Verlag, 1978.

[9] L. C. Evans. *Partial differential equations*. 2. ed. Vol. 19. Graduate Studies in Mathematics. Providence: American Mathematical Society (AMS), 2010.

[10] D. L. George. *Finite volume methods and adaptive refinement for tsunami propagation and inundation*. PhD thesis. University of Washington, 2006.

[11] M. Griebel, T. Dornseifer, and T. Neunhoeffer. *Numerische Simulation in der Strömungslehre. Eine praxisorientierte Einführung*. German. Wiesbaden: Vieweg, 1995.

[12] E. Hairer, S. P. Nørsett, and G. Wanner. *Solving ordinary differential equations. I: Nonstiff problems*. 2. rev. ed. Vol. 8. Springer Series in Computational Mathematics. Berlin: Springer-Verlag, 1993.

[13] M. Hilden. *Extensions of Shallow Water Equations*. PhD thesis. Universität Kaiserslautern, 2003.

[14] K. Hokusai. *The Great Wave off Kanagawa*. Published between 1826 and 1833. Link accessed on April 13, 2024. URL: https://commons.wikimedia.org/w/index.php?title=File:Great_Wave_off_Kanagawa2.jpg&oldid=863949836.

[15] J. J. Horrillo, W. R. Knight, and Z. Kowalik. *Numerical Modeling of Tsunami Waves*. Vol. 54. Advanced Series on Ocean Engineering. World Scientific, 2021.

[16] K. Hutter and Y. Wang. *Fluid and thermodynamics. Volume 1. Basic fluid mechanics*. Advances in Geophysical and Environmental Mechanics and Mathematics. Cham: Springer, 2016.

[17] R. S. Johnson. *A modern introduction to the mathematical theory of water waves*. Cambridge Texts in Applied Mathematics. Cambridge: Cambridge University Press, 1997.

[18] D. I. Ketcheson, R. J. LeVeque, and M. J. del Razo. *Riemann problems and Jupyter solutions*. Vol. 16. Fundamentals of Algorithms. Philadelphia: Society for Industrial and Applied Mathematics (SIAM), 2020.

[19] B. A. Klinger and T. W. N. Haine. *Ocean circulation in three dimensions*. Cambridge: Cambridge University Press, 2019.

[20] R. J. LeVeque. *Finite volume methods for hyperbolic problems*. Cambridge Texts in Applied Mathematics. Cambridge: Cambridge University Press, 2002.

[21] R. J. LeVeque. *Numerical methods for conservation laws*. 2. ed. Basel: Birkhäuser, 1992.

[22] R. J. LeVeque, D. L. George, and M. J. Berger. "Tsunami modelling with adaptively refined finite volume methods". In: *Acta Numerica* 20 (2011), pp. 211–289.

[23] J. D. Logan. *An introduction to nonlinear partial differential equations*. 2. ed. New York: John Wiley & Sons, 2008.

[24] R. Malek-Madani. *Physical oceanography: a mathematical introduction with MATLAB*. Crc Press, 2012.

[25] P. J. Olver. *Introduction to partial differential equations*. Undergraduate Texts in Mathematics. Cham: Springer, 2014.

[26] J. J. Stoker. *Water waves: The mathematical theory with applications*. Vol. 36. John Wiley & Sons, 1992.

[27] E. F. Toro. *Riemann solvers and numerical methods for fluid dynamics. A practical introduction*. 3. ed. Berlin: Springer, 2009.

[28] E. F. Toro. *Shock-capturing methods for free-surface shallow flows*. Chichester: Wiley, 2001.

[29] B. Tozer et al. "Global bathymetry and topography at 15 arc seconds: SRTM15+". In: *Earth and Space Science* 6 (Oct. 2019), pp. 1847–1864.

[30] G. K. Vallis. *Essentials of atmospheric and oceanic dynamics*. Cambridge university press, 2019.

[31] C. B. Vreugdenhil. *Numerical methods for shallow-water flow*. Water Science and Technology Library. Springer Science & Business Media, 1994.